Roma Tre

Scienze della Terra

CORSO DI DOTTORATO DI RICERCA IN

XXXVIII

CICLO DEL CORSO DI DOTTORATO

Analysis of macroseismic data of seismic sequences: the case of 1783 Calabria earthquakes

Titolo della tesi

Martina Orlando
Nome e Cognome del dottorando — firma

Prof. Domenico Cosentino
Docente Guida/Tutor: Prof. — firma

Dott. Andrea Tertulliani
Docente Guida/Tutor: Prof. — firma

Dott.ssa Laura Graziani
Docente Guida/Tutor: Prof. — firma

Prof. Valerio Acocella
Coordinatore: Prof. — firma

Ph.D. in Earth Science

38th Cycle

Ph.D. Thesis

Analysis of macroseismic data of seismic sequences: the case of 1783 Calabria earthquakes

Ph.D. candidate: Martina Orlando

Advisers: Prof. Domenico Cosentino

Dott. Andrea Tertulliani

Dott.ssa Laura Graziani

Abstract

The present study focuses on macroseismology and historical seismology and aims to improve the understanding of the 1783 Calabrian seismic sequence, one of the most significant and paradigmatic cases of Italian seismicity.

The Calabrian Arc is one of the most active tectonic systems in the Italian peninsula and has been affected over the last four centuries by numerous high-intensity earthquakes.

Among these, the 1783 seismic sequence is particularly relevant, as it includes three main earthquakes (5 February, 7 February, and 28 March) and at least two other significant events (6 February and 1 March).

This research is based on the collection, cataloguing, and systematic analysis of historical sources, including archival documentation, periodicals, chronicles, and iconographic material.

This analysis has enabled the integration of previously unconsidered information and a more comprehensive reconstruction of the 1783 seismic sequence. The revised dataset comprises 1193 macroseismic data points (MDPs) spanning 562 localities, representing an increase of approximately 33% compared to the reference study [Guidoboni et al., 2007].

Macroseismic intensities are assigned using both the MCS scale, to ensure continuity with the Italian seismological tradition and existing historical earthquake catalogues, and the EMS-98 scale, in accordance with the modern international methodological framework.

To address issues such as cumulative damage and false damage attribution, the chronology of sources was used to isolate the effects of each event, giving greater weight to contemporary accounts to evaluate the reliability and consistency of the evidence.

For the three main earthquakes, macroseismic parameters (epicentral coordinates and macroseismic magnitude) are estimated using the BOXER code (Methods 0 and 1) [Gasperini et al., 1999; 2010]. In addition, the cumulative intensity subtraction approach (CIS) [Graziani et al., 2022] was applied to isolate the contributions attributable to individual events and to exclude localities likely affected by cumulative damage from the parametrisation.

The 5 February earthquake (438 MDPs) is well constrained by the intensity data, with information available from both the epicentral area and the far field. The analysis yields an epicentral intensity of 10 EMS-98 (10–11 MCS), a magnitude of Mw 6.73–6.90, and a relocation of the epicentre approximately 12–17 km north of the CPTI15 epicentre [Rovida et al., 2022]. The estimated source geometry is consistent with the Cittanova Fault, a high-angle W-NW dipping normal fault, in agreement with seismogenetic models proposed in the literature [Jacques et al., 2001; Galli and Bosi, 2002; Cucci, 2022].

The 7 February earthquake (327 MDPs) is characterised by an epicentral intensity of 10 EMS-98 (10–11 MCS). The dataset is strongly influenced by a cumulative damage scenario. Analysis of the full dataset locates the epicentre further south than the CPTI15 solution [Rovida et al., 2022] and yields a magnitude of Mw 6.61–6.91, whereas the application of the CIS procedure results in a relocation of the epicentre approximately 12–24 km to the north-east and a lower magnitude estimate of Mw 6.48–6.70. The estimated source geometry derived from the non-cumulative data is consistent with the southern segment of the Serre Fault, a west-dipping extensional structure, supporting this seismogenetic interpretation [Galli and Bosi, 2002; Galli et al., 2007].

The 28 March earthquake (339 MDPs) shows an epicentral intensity of 10 EMS-98 (10–11 MCS) as well. The macroseismic pattern is strongly conditioned by the cumulative damage scenario. Processing of the full dataset locates the epicentre to the south-west of the CPTI15 epicentre [Rovida et al., 2022], defining a NW–SE oriented source with magnitudes ranging from Mw 6.82 to 6.98. Conversely, the CIS approach allows for the isolation of non-cumulative data, resulting in a lower magnitude estimate of Mw 6.67–6.83 and shifting the epicentre approximately 10 km to the north-east relative to the CPTI15 location. The source derived from this analysis shows an E–W geometry beneath the Catanzaro Basin, appearing consistent with the composite seismogenic structure of the Golfo di Caraffa–Squillace, a south-dipping, subvertical, left-lateral strike-slip fault, proposed by the DISS Working Group [2025].

Finally, for the 6 February (67 MDPs) and 1 March (22 MDPs) earthquakes, the available information did not allow reliable parametrisation in either case. The first is too strongly affected by cumulative damage and could plausibly represent a strong aftershock of the 5 February event, whereas the second is characterised by considerable uncertainty due to the fragmentary nature of the contemporary sources.

A key aspect of the research involves the assessment of the effect of cumulative damage on the estimation of seismic parameters. The findings highlight the limitations of conventional methodologies, demonstrating how cumulative intensities can result in considerable inaccuracies in the estimates of seismic parameters.

The results include a more robust and reliable reinterpretation of the 1783 Calabrian sequence, a refined reconstruction of the chronology of damage effects, the creation of a comprehensive thematic database on macroseismic effects, and a new characterisation of the major earthquakes within their seismotectonic context.

Table of Contents

1. Introduction

The study of earthquakes has a long tradition, evolving over the centuries. Despite the significant acceleration in the progress of seismological research in recent decades due to the development of increasingly sophisticated monitoring networks (seismic networks, GPS networks, InSAR and others), evaluations of seismic hazard, which form the basis for risk estimates and inform planning decisions aimed at reducing the impact of earthquakes, still rely heavily on knowledge of past earthquakes (Fig. 1).

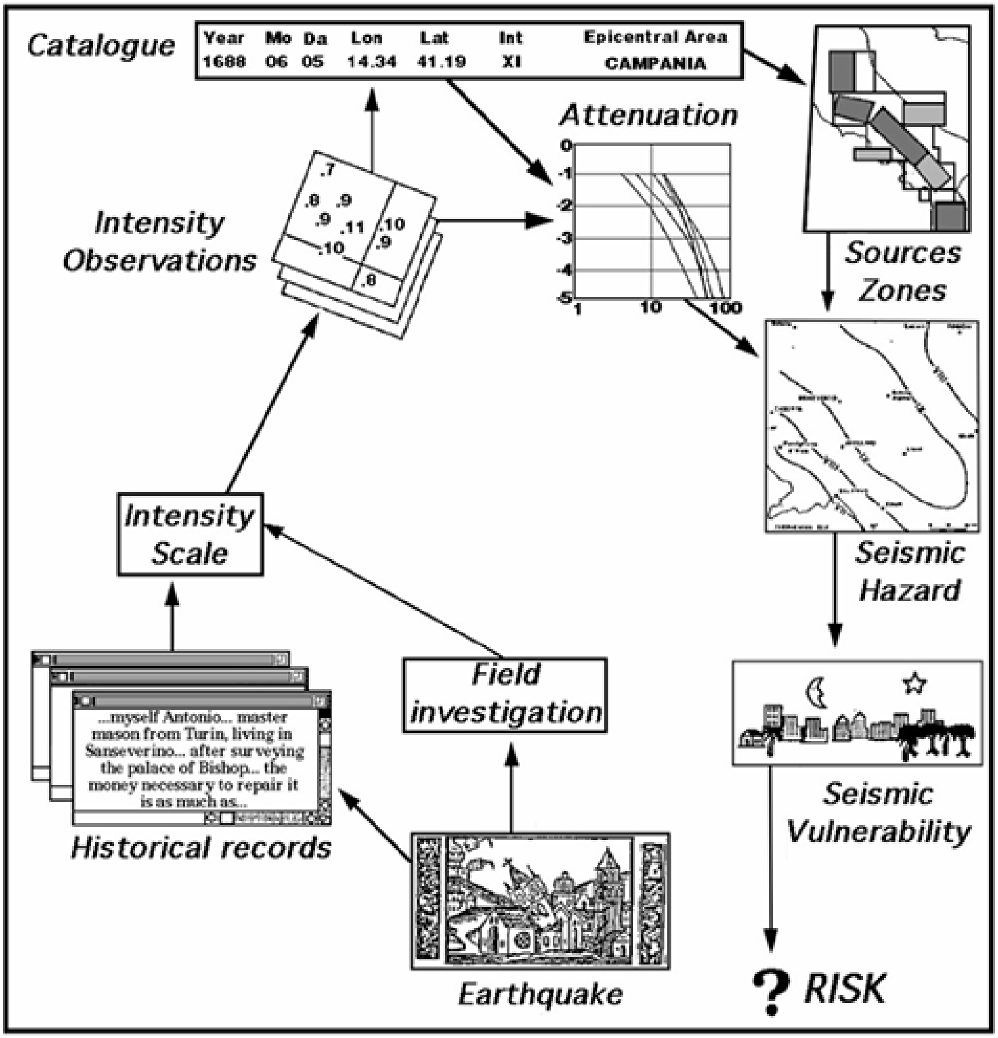

Figure 1. *Scheme for the processing and use of macroseismic data for the assessment of seismic hazard and risk [Stucchi, 1993].*

The collection of information relating to past earthquakes has a long tradition in Italy, as well as in several other European countries. It reached its apogee in the second half of the nineteenth century, when numerous scholars undertook the task of compiling data. Among them, Robert Mallet is credited with producing one of the earliest modern maps of world seismicity. In Italy, the geographer Mario Baratta, in his comprehensive work '*I terremoti d'Italia*' [Baratta, 1901], synthesises the contributions of numerous compilers.

After a long period of declining interest in this research/cataloguing activity, in the 1970s and 1980s, interest in the study of past earthquakes grew again in Europe. It was during this period that historical seismology was born, emerging as a distinct discipline with its own set of rules, procedures, instruments and objectives.

Historical seismology is a field of study that applies the methods of quantitative historical research to investigate the effects of earthquakes of the past. Its principal aim is to document these effects as comprehensively as possible across a wide range of localities. The research process therefore consists of the identification of sources, their critical analysis, and their interpretation in seismological terms through a classification system and ranking of effect scenarios (macroseismic scales). The seismological parameters of each earthquake can be derived from the collected and properly georeferenced data: origin time, epicentral location, epicentral intensity and magnitude.

The first crucial phase of seismological-historical research involves identifying and collecting sources. Evidence of seismic occurrences is indeed to be found in a plethora of documents, which may have been preserved in locations distant from the area of interest. Useful documentary materials for studying earthquakes include narrative sources (chronicles, diaries, memoirs), journalistic sources (handwritten notices, gazettes and newspapers), administrative sources (minutes, registers, technical reports, etc.) and 'scientific' sources (meteorological and seismological registers, bulletins, seismic postcards), in addition to iconographic sources.

The second step involves the seismological interpretation of the information collected and selected through critical analysis. This process converts documentary information into a grade on a macroseismic scale by associating the reconstructed effects scenario for each locality (Macroseismic Data Point, MDP) with the theoretical scenario described by the scale. This procedure should be applied to as many localities as possible, with each locality representing a sample of buildings or individuals. Macroseismic intensity, therefore, functions as an estimator of shaking and cannot be used to assess the effects on individual buildings or people.

Finally, based on the geographical distribution of macroseismic intensities, the epicentral parameters (epicentral location and magnitude) of the earthquake are estimated through an inversion algorithm. The method most widely adopted in Italy, and employed in this study, is the BOXER code [Gasperini et al., 1999; 2010]. This code has been extensively used to estimate the principal parameters of historical earthquakes. The methodology involves the analysis of intensity maps, derived from evaluations of seismic effects on structures, individuals and the environment. The aim of this analysis is to identify the barycentre within the area of maximum intensity, thereby estimating the macroseismic epicentre. The magnitude is then calculated utilising an empirical relationship between the area affected by the seismic effects and the maximum intensity. This approach has been shown to result in a significant enhancement in the precision of intensity estimates and the localisation of effects. The data collected and formulated with regard to intensity serve two principal purposes: the definition of epicentral earthquake parameters and the compilation of seismic site histories. Hazard and risk assessments are based on this data set, which has considerable value, including economic value, for our societies.

Italy has one of the richest seismic catalogues in the world; the centuries-old knowledge of Italian seismicity is organised in highly advanced databases and catalogues. Such resources include the Catalogue of Strong Earthquakes in Italy (CFTI) [Guidoboni et al., 2018], the Italian Archive of Historical Earthquake Data (ASMI) [Rovida et al., 2017], the Parametric Catalogue of Italian Earthquake (CPTI) [Rovida et al., 2022] and the Italian Macroseismic Database (DBMI) [Locati et al., 2022]. However, a significant number of the studies that form the foundation of the parametric reference catalogue are either severely outdated or are still in the preliminary stages of research. It is for this reason that the Italian historical seismological community has long since initiated a process of revising and updating data, as well as undertaking specific research on possible earthquakes that are unknown to seismological tradition [Among the most recent, Azzaro et al., 2020; Tertulliani et al., 2022; Camassi et al., 2023; Galadini and Tertulliani, 2025; Baranello, 2025; Tertulliani et al., 2025; Antonucci et al., 2026.].

The present research is situated within this scientific and methodological framework and focuses on the seismic sequence that struck Calabria in 1783, one of the strongest and complex cases in Italian seismic history. Between February and March 1783, at least five strong earthquakes occurred, three of which had magnitudes close to 7, concentrated within a very short time interval and within a relatively limited geographical area. The occurrence of several strong earthquakes in such a limited time span, particularly those from the pre-instrumental era, poses a significant challenge in distinguishing the individual effects of each event and, consequently, in the accurate chronological reconstruction and interpretation of each earthquake.

Knowledge of cumulative damage evolution provides a more robust basis for understanding its influence on the estimation of earthquake parameters. Accordingly, evaluating cumulative damage is a fundamental methodological requirement to ensure the reliability of the reinterpretation of the 1783 Calabrian sequence. Furthermore, the identification of the causative fault through geological evidence is fundamental to parameterise pre-instrumental earthquakes, as documented, for example, for the 16 June 1638 Sila earthquake [Galli and Bosi, 2003].

The objective of this research is twofold: firstly, to propose a new interpretation of the 1783 seismic sequence through a macroseismic approach that explicitly considers the cumulative effects of damage by means of a rigorous chronological reconstruction of the observed effects; and secondly, to provide a new parametrisation of the individual earthquakes of the sequence and to place them within the seismotectonic framework of Calabria.

The thesis is organised into distinct chapters, each focused on a specific aspect of the investigation. The initial section provides a comprehensive overview of the seismotectonic context of the study area, accompanied by an analysis of its historical and recent seismicity. This is followed by an overview of the current state of knowledge on the 1783 Calabrian seismic sequence, set within its broader historical framework and focusing on its main events.

Furthermore, the methodology employed, the research pathway, the criteria for assigning macroseismic intensity, and the procedures for parameterising earthquakes, are all illustrated.

The first phase of the work entailed the identification, compilation, and critical evaluation of the existing documentary sources, with a particular focus on the impact of the individual earthquakes on the built heritage. Following the acquisition of relevant information, intensity estimates were assigned to the affected localities, and the corresponding macroseismic intensity maps were produced. This activity enabled the creation of a thematic database on the 1783 sequence, including the original documentation.

The second phase of the study involved the parametrisation of the earthquakes with the BOXER algorithm. Through the processing of the reconstructed dataset, new parameters were defined for the principal earthquakes of the Calabrian sequence, and their placement within the regional seismotectonic framework was reassessed.

2. Geodynamic and Structural Setting of Calabria

The Calabrian Arc (CA) constitutes the southernmost sector of the Apennines. It was formed during the Eocene-Tortonian [Amodio Morelli et al., 1976] and represents the emerged portion of a complex accretionary wedge situated at the margin of the European plate, overthrusting the Apulian promontory and the Ionian lithosphere.

The formation of the CA is the result of a complex geodynamic interaction driven by the co-existence of two main processes, the slow NNW–SSE convergence between the African and Eurasian plates, and the SE-ward rollback of the Ionian lithospheric slab subducting beneath the Tyrrhenian lithosphere [Malinverno and Ryan, 1986; Patacca et al., 1990; Faccenna et al., 1996]. From the Neogene to the Quaternary, the rollback of the Ionian plate hinge, initiated about 35–30 Ma ago [Dellong et al., 2020], has been the primary kinematic driver of the region. During its peak activity (ca. 5 Ma ago), this mechanism enabled the Calabrian block to migrate eastwards at speeds of up to 3–4 cm/year [Doglioni, 1991], triggering the thinning of the overlying lithosphere and the opening of the Tyrrhenian back-arc basin. Currently, the region is transitioning toward a regime dominated by Africa-Eurasia plate convergence [Nijholt et al., 2018], with a residual rollback rate of ~2 mm/year [Hollenstein et al., 2003; Devoti et al., 2008] and a convergence rate of 3–5 mm/year [D'Agostino and Selvaggi, 2004], of which approximately 2 mm/year is absorbed within the outer prism [D'Agostino et al., 2011]. The deep structure of this subduction is well evidenced by a Benioff zone reaching 500–600 km [Peterschmitt, 1956; Amato et al., 1993; Chiarabba et al., 2008] and by P-wave tomographic anomalies beneath the southern Tyrrhenian Sea [Piromallo and Morelli, 2003].

From a seismotectonic perspective, starting from the Upper Miocene, the area underwent a transition in its tectonic regime, shifting from one dominated by compression and imbricated thrust faults to a predominantly extensional setting [Tortorici et al., 1995; Moretti & Guerra, 1997]. Subsequently, from the Lower Pliocene onwards, a series of tectonic depressions developed along the Tyrrhenian flank of the range, oriented mainly in a N–S and NE–SW direction (Crati, Mesima, Gioia Tauro and the Strait of Messina). The opening of these basins is governed by an imposing system of high-angle normal faults, which mostly dip towards WNW. These displace the crystalline basement, causing it to step down towards the sea [Ghisetti, 1981; Galli and Bosi, 2002, 2003].

This complex extensional dynamic has generated a significant crustal imbalance between the Tyrrhenian sector, which is undergoing rapid subsidence [Finetti and Morelli, 1973], and the adjacent continental mountain range [Ghisetti and Vezzani, 1982]. The latter, from the

Pleistocene epoch onwards, exhibited a notable regional uplift, with average rates ranging from 0.6 to 1.3 mm/year and local peaks of 1.67 mm/year [Westaway, 1993; Dumas and Raffy, 2004], which contrasts with the local subsidence within the tectonic troughs [Monaco et al., 1996; Faccenna et al., 2011].

The origin of this regional uplift is attributed to deep-seated geodynamic processes, such as the underplating of Ionian sediments [Minelli and Faccenna, 2010] or the detachment of the Ionian slab [Monaco et al., 1996; Neri et al., 2009, 2012]. This phenomenon is evidenced by relict palaeosurfaces that flatten the summits of the crystalline massifs (Sila, Serre, Aspromonte) and by the imposing sequences of Quaternary marine terraces outcropping along the coasts[Bordoni and Valensise, 1998; Cucci, 2004].

From a structural point of view, the CA is characterised by fault systems that can be grouped into two main orientations: longitudinal faults, broadly parallel to the arc axis and generally striking NNE-SSW to N-S, with predominantly normal kinematics, and transverse to oblique faults, trending WNW-ESE to NW-SE, commonly associated with strike-slip or transtensional kinematics (Fig.2) [Galli e Bosi, 2003; Galli e Scionti, 2006; Pirrotta et al., 2021].

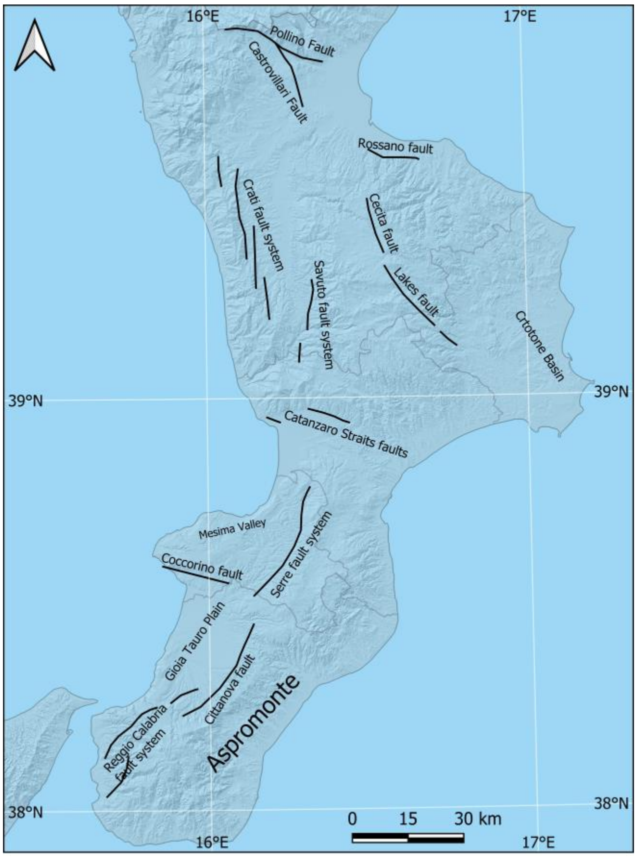

***Figure 2**. Simplified primary seismogenic faults of Calabria. The Cittanova Fault, the Serre fault system, and the Lakes fault are well-established seismogenic structures on which paleoseismological analyses have been carried out.[modified from Galli et al., 2007].*

This structural framework reflects the complexity of the active deformation field and strongly controls both the morphological segmentation of the region and the distribution of historical and recent seismicity.

In northern and central Calabria, extensional deformation is accommodated by major longitudinal and transverse fault systems.

In the northernmost sector, the Pollino fault, approximately 18 km long, trends predominantly WNW-ESE. It currently displays extensional kinematics, which succeeded an original left-lateral strike-slip activity during the Early Pleistocene. This structure is still considered seismogenic and, based on paleoseismological evidence [Michetti et al., 1997], has been interpreted as the source of two strong pre-instrumental earthquakes (Mw 6.5–7.0) that occurred between the 6th–12th centuries and the 13th–15th centuries AD, respectively, which are currently missing from official catalogues. To the southwest lies the Castrovillari fault, a major normal fault predominantly trending NNW-SSE. Its surface expression features a 1–2 km wide zone of SW-dipping, step-like fault scarps exposed for 10–13 km, though its total length may reach 25 km. Paleoseismological analyses [Cinti et al., 1997; Cucci and Cinti, 1998] associate this structure with at least four strong earthquakes over the last 30,000 years. The most recent event (post-760 AD) is missing from local seismic catalogues, likely mislocated due to the low historical population density, which prevented an accurate macroseismic reconstruction.

Farther south, the Crati Valley fault system consists of a set of N-S-trending normal faults extending for about 40 km, which bound the eastern margin of the coastal chain and define the Crati semigraben. These structures are associated with moderate-to-high historical seismicity, interpreted as the expression of a southward migration of deformation between 1767 and 1870 [Galli and Bosi, 2003; Galli et al., 2007].

The Sila Massif is also affected by major active faults. Among these, the Lakes fault is one of the main tectonic structures in the area: it is approximately 33 km long, trends NW-SE and displays transtensional kinematics, with both normal and left-lateral strike-slip components. This structure has been interpreted as the source of the 9 June 1638 earthquake [Galli et al., 2007]. In the same sector, the Lago Cecita Fault, oriented NNW-SSW, has also been identified, although no unequivocal historical activation has yet been documented. Along the Ionian margin of the Sila, the Rossano Fault, oriented E-W to NW-SE and approximately 12 km long, downthrows the Paleozoic rocks of the massif beneath the deposits of the Ionian coastal plain and is generally associated with the strong 25 April 1836 earthquake [Galli et al., 2007; Galli et al., 2010].

A major structural role is played by the Catanzaro Straits, a transverse depression across the CA that acts as an accommodation zone between the Sila and Serre domains. In this sector, lateral crustal movements interact with local extensional components, producing a complex tectonic framework. The main structural element is the Lamezia-Catanzaro fault system, which bounds the depression to the north and extends for about 35 km, with WNW-ESE and WSW-ENE trends. Geomorphological and structural evidence indicates oblique-normal faulting associated with left-lateral strike-slip kinematics. This system is considered capable of generating earthquakes up to about magnitude 7 and has been proposed as a possible source, among others, of the 28 March 1783 earthquake [Pirrotta et al., 2021]. Recent paleoseismological analyses across its westernmost sector have documented Holocene activity along the ENE-WSW-trending Sant'Eufemia Fault and suggested that it may represent the source of the 28 March 1638 earthquake [Galli et al., 2025]. Three mainshocks occurred in 1638, one on 27 March in the upper Savuto Valley, one on 28 March in the Lamezia area, and one on 8–9 June in the inner Sila massif. Along the southern margin of the trough, smaller structures crop out, such as the Maida and Stalettì faults, which are now mainly recognisable as deeply eroded and exhumed scarps [Galli et al., 2007].

Southern Calabria is dominated by high-angle normal faults, mostly dipping westward, that bound the Serre and Aspromonte massifs. The Serre Fault is one of the principal structures in this sector: approximately 35 km long, it bounds the western edge of the Serre and the Mesima Graben. The presence of scarps several tens of metres high, together with paleoseismological trench data, has allowed its identification as the source of the 7 February 1783 earthquake [Galli et al., 2007].

Farther south, the Cittanova Fault, also referred to as the Aspromonte Fault, represents the structural continuation of the Serre Fault. It is approximately 30 km long, oriented NE-SW, and dipping toward NW, separating the crystalline basement of the Aspromonte from the sediments of the Gioia Tauro Plain. It shows an estimated vertical slip rate of about 0.6-0.7 mm/year and a cumulative vertical offset exceeding 1000 m [Galli e Bosi 2002; Galli and Peronace 2015]. The literature identifies it as the source of the 5 February 1783 earthquake, while paleoseismological evidence also indicates repeated reactivation during the Holocene, with recurrence intervals on the order of 3 millennia.

Along the Tyrrhenian margin and in the Messina Straits area, additional extensional systems occur both onshore and offshore. Among these, the Scilla Fault controls the prominent coastal escarpment of the Palmi sector and is generally regarded as responsible for the 6 February 1783 earthquake [Jacques et al., 2001]. Farther south, the Reggio Calabria-Armo fault system, together with possible blind structures within the Strait, is commonly considered among the debated candidates for the source of the 1908 earthquake [Minelli et al., 2016; Tiberti et al., 2017].

In the Capo Vaticano area, the E-W-trending Coccorino fault represents the seismogenic source of the 1905 earthquake. Modelled as a deeply buried pure normal fault [Cucci and Tertulliani, 2010], it displaces the marine terraces of the Gioia Tauro Basin and acts as a crucial regional transverse structure transferring extensional deformation from the northern offshore domains to the onshore faults south of Capo Vaticano. Further south, this transverse system is characterized by WNW-ESE-trending structures, such as the Palmi-Locri and Bagnara-Bovalino shear zones. These segment the arc into distinct blocks and act as strike-slip structures accommodating differential uplift and deformation among the various sectors of the chain [Tripodi et al., 2022].

3. Seismicity

Calabria is one of the regions with the highest seismic hazard in Italy and, more generally, in the entire Mediterranean basin.

Seismic hazard is defined as the probability of a certain level of ground shaking occurring in a given area over a defined time period. Based on geological, historical, and seismological data, it is evaluated through advanced scientific studies and summarised in hazard models and curves that synthesise current knowledge and support hazard assessment. These results underpin hazard maps, which are essential tools for urban planning, infrastructure design, and seismic risk mitigation.

The seismic hazard map MPS04 (http://zonesismiche.mi.ingv.it), published in 2004 by the INGV [MPS Working Group, 2004; Stucchi et al., 2011], expresses hazard in terms of peak ground acceleration (PGA) with a 10% probability of exceedance over 50 years, corresponding to a return period of approximately 475 years, and based on standard conditions of rigid soil.

According to this model, Calabria and eastern Sicily have the highest PGA values expected in Italy. In particular, within the Calabria region, the highest values are concentrated in the northern sector, especially in the province of Cosenza, where the expected acceleration exceeds 0.275 g; however, conditions of high hazard are widespread across much of the region, including the Tyrrhenian sectors and the Strait of Messina area (Fig. 3a).

Instead, seismic risk is defined as the potential impact of seismic occurrence on the exposed community, including population, buildings, and infrastructure. Seismic risk is defined as the product of three distinct factors: hazard, exposure (or exposed value), and vulnerability. It can be expressed in terms of loss of life, damage to buildings, and economic losses. As mentioned before, hazard expresses the probability that a given level of ground shaking will be reached in a given area within a given time interval. Exposed value is defined as the population, buildings, infrastructures, services, and productive and economic activities that could potentially be damaged by an earthquake. Vulnerability is defined as the propensity of a building to sustain damage during an earthquake, and is significantly influenced by the quality of construction materials and techniques employed. In contrast to hazard, which is contingent on natural factors such as earthquake type and site effects, exposure and vulnerability represent factors that are amenable to intervention in order to mitigate seismic risk.

According to the current seismic classification (OPCM 3274/2003, OPCM 3519/2006 and the subsequent Technical Standards for Construction NTC08 and NTC18), Calabria is almost entirely classified within the highest hazard classes: out of 404 municipalities, as many as 257 (64% of the municipalities) are classified within seismic zone 1, where the probability of strong earthquakes is high, characterised by acceleration values between 0.25 g and 0.35 g, whilst the remaining 147 (36% of the municipalities) are classified within seismic zone 2, where, although the values are lower, the possibility of intense seismic events still remains significant, albeit less frequent (Fig. 3b).

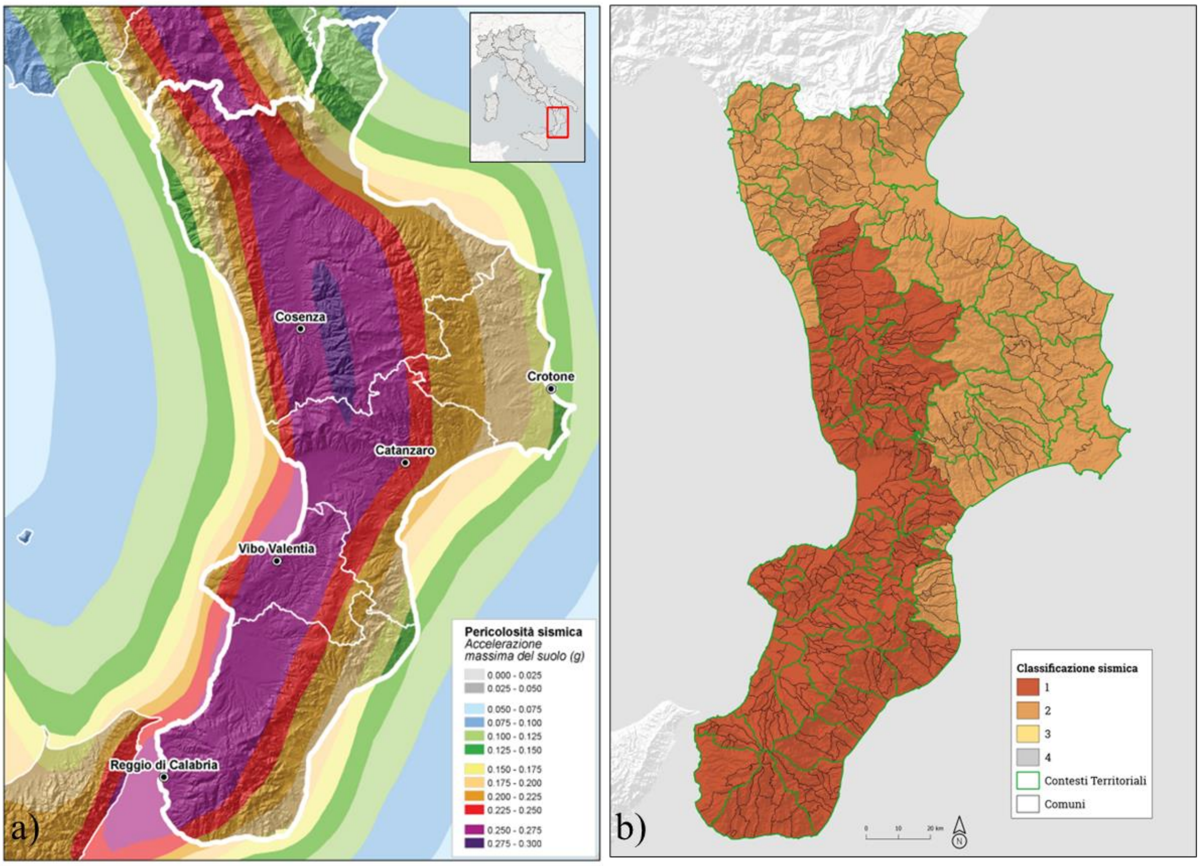

Figure 3. *(a) Seismic hazard map of Calabria [MPS Working Group, 2004]; (b) Seismic classification map of the municipalities of Calabria, taken from the CNR GOVRISV portal (https://govrisv.cnr.it/regioni/regione-calabria/).*

3.1 Historical Seismicity

The reconstruction of seismic activity in the pre-instrumental era is based on the Parametric Catalogue of Italian Earthquakes (CPTI15) [Rovida et al., 2022], which provides homogeneous macroseismic and instrumental data and parameters for Italian earthquakes with maximum intensity ≥ 5 or magnitude ≥ 4.0 in the period 1000-2020.

Within this framework, for the study area, the catalogue documents numerous high-intensity and often destructive earthquakes. (Fig. 4).

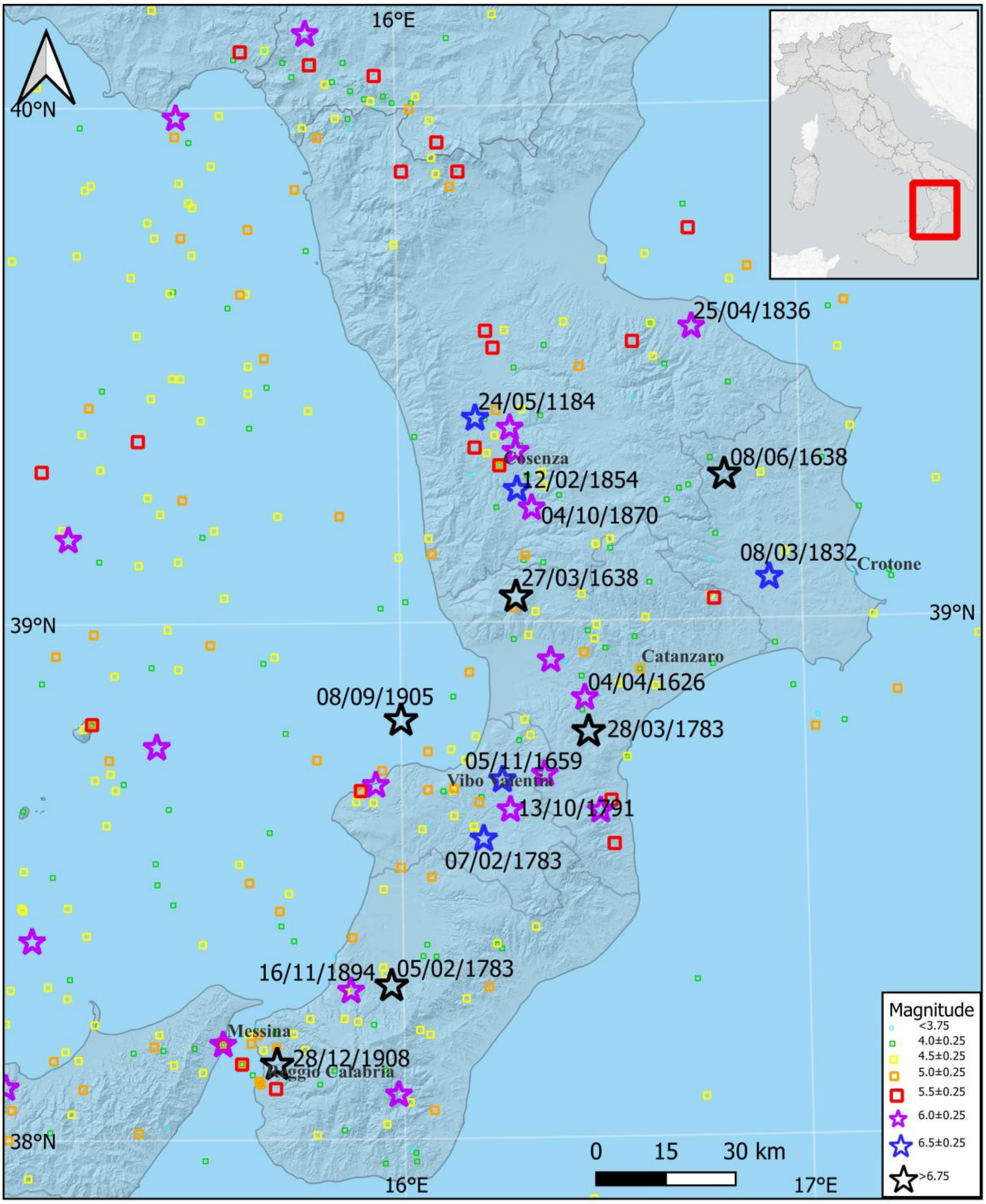

Figure 4. *Map of the seismicity of Calabria in the period 1000–2020 from CPTI15[Rovida et al., 2022].*

Along the approximately 180 km between the Messina Straits and the Crati Valley, 16 earthquakes (Table 1) with a magnitude Mw ≥ 6 occurred.

Date	Epicentral Area	Latitude	Longitude	Io (MCS)	Mw
24/05/1184	Crati Valley	39.395	16.193	9	6.75
04/04/1626	Central Calabria	38.851	16.456	9	6.07
27/03/1638	Central Calabria	39.048	16.289	11	7.09
08/06/1638	Crotone area	39.279	16.812	10	6.76
05/11/1659	Central Calabria	38.694	16.249	10	6.57
05/02/1783	Southern Calabria	38.297	15.97	11	7.1
07/02/1783	Central Calabria	38.58	16.201	10-11	6.74
28/03/1783	Central Calabria	38.785	16.464	11	7.03
13/10/1791	Central Calabria	38.636	16.268	9	6.14
08/03/1832	Crotone area	39.079	16.919	10	6.65
25/04/1836	Northern Calabria	39.567	16.737	9	6.18
12/02/1854	Cosenza area	39.256	16.295	10	6.34
04/10/1870	Cosenza area	39.22	16.331	9-10	6.24
16/11/1894	Southern Calabria	38.288	15.87	9	6.12
08/09/1905	Central Calabria	38.811	16	10-11	6.95
28/12/1908	Strait of Messina	38.146	15.687	11	7.1

Table 1. *Earthquakes with Mw > 6 in Calabria [CPTI15; Rovida et al., 2022]. The table reports date, epicentral area, epicentral coordinates (latitude and longitude), epicentral macroseismic intensity (Io), and moment magnitude (Mw). Intensity is expressed according to the Mercalli-Cancani-Sieberg (MCS) scale.*

Information about seismic activity in Calabria can also be extended to period prior to the year 1000, as the Catalogue of Strong Earthquakes in Italy and the Mediterranean Area (CFTI5Med) [Guidoboni et al., 2018] documents earthquakes dating back to 91 BC and subsequently in the years 17, 361, 853 and 951 AD.

The temporal distribution of seismic events demonstrates a notable concentration within a period of less than three centuries, between 1638 and 1908 [e.g., Scionti et al., 2006], frequently occurring in close succession (as in the seismic sequences of 1638, 1783 and the period 1905–1908). Furthermore, with the exception of the events of 1638, those of greater magnitude are predominantly located in the southern sector, between the Messina Straits and Catanzaro area.

From a spatial perspective, and according to the current knowledge, the majority of seismic activity is concentrated along the Tyrrhenian coast. In particular, northern Calabria, and especially the middle Crati Valley (province of Cosenza), was affected by a series of earthquakes with magnitudes close to 6 between the late 18th and 19th centuries (1767, 1835, 1854, 1870), preceded by the catastrophic earthquake of 27 March 1638 (Mw 7.09; Io 11 MCS) and by an earlier event, dated to 1184 (Mw 6.75; Io 9 MCS). Another significant seismic zone extends in a NW–SE direction into the Crotone area, where major earthquakes have occurred, including those of 8 June 1638 (Mw 6.76; Io 10 MCS), 1744 (Mw 5.74; Io 8 MCS) and 1832 (Mw 6.65; Io 10 MCS).

The Strait of Catanzaro is an area of particularly high seismic activity, which culminated in the earthquakes of 27 March 1638 (Mw 7.09; Io 11 MCS) and 28 March 1783 (Mw 7.03; Io 11 MCS). These events were preceded by a series of earthquakes with magnitudes exceeding 5.5 between the late 16th and early 17th centuries (1599, 1609, 1626), marking the start of the major seismic phase that led to the 1905 earthquake [Scionti et al., 2006].
Southern Calabria is marked by a high level of seismic activity, particularly along the Tyrrhenian coast, where notable events include those of 1659 (Mw = 6.57; Io = X MCS), 1743 (Mw 5.88; Io 8-9 MCS) and 7 February 1783 (Mw 6.74; Io 10-11 MCS). The Aspromonte massif also exhibits significant seismic activity, with the most destructive earthquake of the 1783 sequence occurring on 5 February (Mw 7.1; Io 11 MCS). Furthermore, the area has been impacted by two of the most significant seismic events documented in the history of peninsular Italy: the earthquakes of 1905 (Mw 6.95; Io 10-11 MCS) and 1908 (Mw 7.1; Io 11 MCS).

3.2 Recent Seismicity

The recent seismic activity, as determined by instrumental seismic data, exhibits a significant discrepancy compared with that reconstructed from historical sources.
Since 1985, the National Seismic Network (RSN) of the INGV, which now comprises around 500 stations spread across the country, has been monitoring seismic activity in Italy in real time. The data collected is entered into the Italian Seismological Instrumental and Parametric Data-Base (ISIDe), which compiles all events located by the INGV's seismic monitoring centre in Rome and subsequently reviewed for the compilation of the Italian Seismic Bulletin (BSI).
In the Calabrian region, instrumental seismic data show that approximately 30000 earthquakes have been recorded to date, with magnitudes ranging from 2.0 to 6.1 and hypocentral depths varying from a few kilometres to approximately 460 km (Fig. 5).

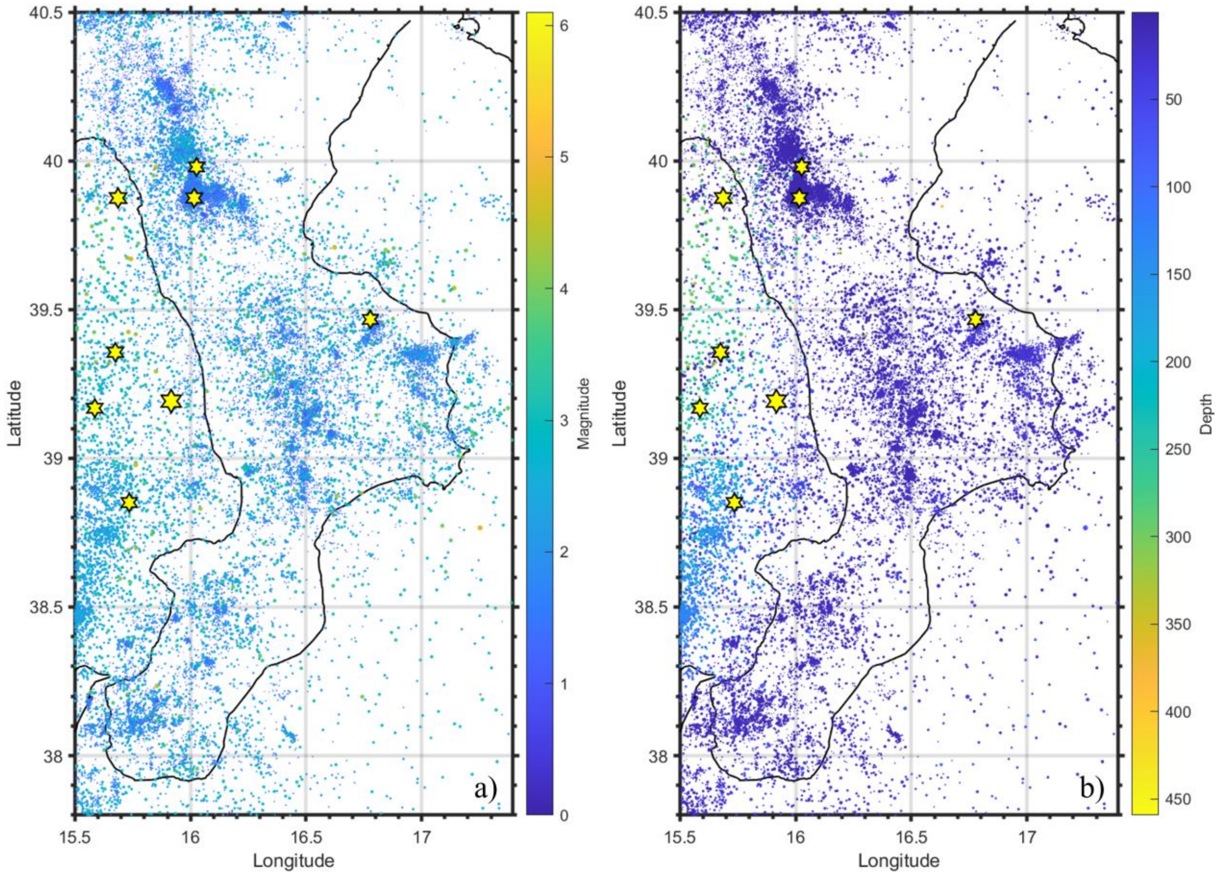

Figure 5. Seismicity map of Calabria for the period 1985-June 2026, based on ISIDe data (https://terremoti.ingv.it/search). Yellow stars represent earthquakes with magnitude ≥ 5.

Within this time interval, only eight earthquakes have reached or exceeded magnitude 5 (Table 2). Except for the 2 June 2026 earthquake (Mw 6.1), instrumental seismicity in Calabria has been characterised predominantly by low- to moderate-magnitude events.

Date	Epicentral Area	Latitude	Longitude	Magnitude	Depth (Km)
1998-09-09	3 km NW of Rotonda (PZ)	39.979	16.026	Md 5.0	7.4
2001-05-17	Southwestern Calabrian Coast	38.851	15.735	ML 5.1	258
2008-12-17	Southern Tyrrhenian Sea	39.168	15.586	ML 5.1	269.4
2012-10-25	3 km SE of Mormanno (CS)	39.8747	16.0158	Mw 5.2	9.7
2022-10-31	Gulf of Policastro	39.8747	15.6865	Mw 5.4	287.1
2023-05-01	Northwestern Calabrian Coast	39.3562	15.6747	Mw 5.2	268.9
2024-08-01	4 km SW of Pietrapaola (CS)	39.4667	16.7777	Mw 5.0	24.3
2026-06-02	Northwestern coast of Calabria (Cosenza)	39.1918	15.9163	Mw 6.1	259

Table 2. Earthquakes with Mw ≥ 5 in Calabria from ISIDe (https://terremoti.ingv.it/search).

The strongest and most recent recorded event is the 2 June 2026 earthquake (Mw 6.1), which occurred offshore along the northwestern coast of Calabria, approximately 32 km from Cosenza, at a depth of 259 km. Other significant events include the 31 October 2022 earthquake (Mw 5.4) in the Gulf of Policastro, located offshore along the Tyrrhenian margin at a depth of about 287 km; the 25 October 2012 Mormanno earthquake (Mw 5.2), a shallow crustal event (depth ~10 km) related to extensional tectonics in the Pollino area; and the 1 May 2023 (Mw 5.2) and 17 December 2008 (Mw 5.1) earthquakes, both occurring at intermediate to deep depths (>250 km) beneath the Tyrrhenian Sea. Furthermore, the 1 August 2024 event near Pietrapaola (Mw 5.0; depth ~24 km) represents a typical shallow crustal earthquake within the Calabrian domain.

The epicentral distribution (Fig. 5) highlights the presence of well-defined clusters of moderate seismicity, mainly concentrated in the Pollino area, in relation to the extensional tectonics of the southern Apennines, and along offshore alignments parallel to the Tyrrhenian margin, where seismicity is often associated with deeper geodynamic processes.

A relevant feature, however, emerges from the analysis of hypocentral depths. Shallow seismicity (0–50 km) is predominantly located beneath the Calabrian peninsula and along the Ionian margin, reflecting active crustal deformation.

Conversely, moving northwestward beneath the Tyrrhenian basin, earthquake hypocentres define a well-organised, dipping alignment extending down to depths over 400 km (Fig. 5b). This distribution indicates the active subduction of the Ionian lithosphere beneath the CA.

4. The 1783 Calabria Earthquake Sequence

4.1 Historical Framework

Among the natural disasters that occurred in Europe in the modern era, the 1783 seismic sequence in Calabria is one of the best known and most extensively studied. As in the case of the 1755 Lisbon earthquake, news of the disaster rapidly spread across the major European cities, sparking debates, reflections and analyses of various kinds [Cecere, 2017]. This interest derived from the wide international resonance of the seismic events as well as the extraordinary volume of documents produced and the complexity of the ambitious reconstruction plan implemented by the Kingdom of Naples.

In 1783, Calabria was under the rule of the Bourbon dynasty of Ferdinand IV and was one of the most remote regions of the Kingdom of Naples. The territory was divided into the two provinces of Calabria Citeriore and Calabria Ulteriore (Fig. 6), formally administered by royal officials but strongly influenced by the feudal power of the local nobility and the control of ecclesiastical institutions. Communication with Naples relied primarily on the maritime route along the Tyrrhenian coast, whereas the mountainous interior was served by a fragmented road network that was often impassable during the winter season.

__Figure 6.__ Map of Calabria Citeriore on the left and Calabria Ulteriore on the right in the atlas by Zatta et al., [1782]. David Rumsey Historical Map Collection [https://www.davidrumsey.com].

The Calabrian seismic sequence of 1783 was preceded by minor seismic activity, which began as early as 1780 (Roscitano, 1783; De Leone, 1783; Baratta, 1901). From 5 February 1783 onwards, the region was hit by a succession of exceptionally intense earthquakes over a period of less than three months.

According to contemporary sources [Sarconi, 1784; Vivenzio, 1788], the death toll is estimated to be between 30,000 and 50,000. 182 settlements out of 384 were completely destroyed, and over a hundred were severely damaged. Secondary effects, including landslides, river course changes, the formation of dammed lakes, and tsunamis, profoundly altered the region's topography and hydrography.

Initial reports of the disaster reached Naples between 7 and 14 February 1783. The response of the Neapolitan government was both rapid and wide-ranging, resulting in a relief and reconstruction plan of considerable scope. On 15 February, Ferdinand IV appointed Francesco Pignatelli, Marquis of Laino, as Vicar General of Calabria, granting him extraordinary powers [Grimaldi, 1784; Minasi, 1785]. Upon arriving in Monteleone (today Vibo Valentia) on 22 February, Pignatelli coordinated the initial relief operations and ordered the immediate deployment of officers and engineers to conduct field surveys in the affected areas.

Alongside these administrative measures, an intensive programme of observation and documentation was initiated. On 5 April 1783, a scientific expedition promoted by the Royal Academy of Sciences and Letters of Naples was approved. At the same time, between April and June, numerous commissioners, scholars, and military engineers operated in the field, including Antonio Winspeare and Francesco La Vega. The extensive body of data collected during these missions was incorporated into the work of the Supreme Council for the Restoration of Calabria, providing the essential knowledge base for the subsequent reconstruction plans. This process resulted in innovative measures for the time, such as relocating settlements on unstable sites, planning new orthogonal urban layouts and adopting building criteria to mitigate seismic risk. These measures were later formalised in the Royal Instructions of 20 March 1784.

In this context, ordinary administrative activity also underwent profound disruption. To provide financial support for the extensive reconstruction programme, the Giunta della Cassa Sacra and the Giunta di Corrispondenza della Cassa Sacra were established in Naples in 1784. They were responsible for administering expropriated ecclesiastical property and managing the procedures related to its sale and allocation. The establishment of the Cassa Sacra was an extraordinary financial, political and administrative intervention intended to raise funds for public works and, in principle at least, to promote a broader redistribution of landed property. In practice, however, this project failed to achieve its expected social effects, as the peasantry lacked the capital to participate in the sales. Consequently, a substantial proportion of the property ended up in the hands of the nobility and the emerging provincial bourgeoisie, thereby reinforcing rather than reducing the inequalities associated with the latifundium system.

4.2 Overview of the Seismic Sequence

The seismic sequence of 1783, which occurred between 5 February and 28 March, was characterised by three main earthquakes, which took place on 5 and 7 February, and 28 March, as well as two smaller events on 6 February and 1 March. The sequence was followed by hundreds of aftershocks. On the whole, this seismic sequence lasted until at least 1793 [Baratta, 1901]. The distribution of epicentres, as estimated by CPTI15, indicates a progressive migration towards the northeast, originating from southern Calabria, specifically the Aspromonte area, the Gioia Tauro Plain, and the Messina Straits, and extending to the sector between the Gulf of Sant'Eufemia and the Gulf of Squillace, corresponding to the Catanzaro Isthmus.

The effects on the region were extensive and diversified, and caused a radical change to the local physiography of the landscape, owing to hundreds of landslides, liquefaction phenomena, subsidence, rockslides, sand cones and craterlets, and damming more than 200 lakes, as well as surface faulting effects [Hamilton, 1783; De Dolomieu, 1784; Vivenzio, 1788]. Figure 7 shows some representations of these phenomena.

Furthermore, tsunamis occurred on 5 and 6 February: the first hit the coast between Messina and Torre Faro and between Scilla and Cenidio; the second, which was originated by a seismic induced landslide, hit the Strait of Messina and killed a thousand people during the night along the shore at Scilla [Sarconi, 1784; Vivenzio, 1788; Graziani et al., 2006].

Overall, more than 180 localities were destroyed or severely affected, and the death toll may have been higher than generally estimated, also considering the mortality that occurred in the following months as a result of epidemics directly connected to the seismic crisis [Grimaldi, 1784; De Stefano, 1987].

Figure 7. *Example of effects induced by the 1783 seismic sequence on the environment: a) Oppido Mamertina: landslides and pond formation in the Cumi River valley; drawing by Pompeo Schiantarelli, in Sarconi [1784], atlas, pl. XLV. b) Polistena, Teresa Luciani's estate: deep ground fissures visible across the property, crossed by a branch of the aqueduct damaged by the earthquake; drawing by Pompeo Schiantarelli, in Sarconi , atlas, pl. XXVII. c) View of the coast near Capo Pacì, south of Scilla, showing the Campallà slope as it appeared after the large landslide triggered by the earthquake of 6 February 1783; in the central part of the drawing the main landslide is shown, with its upper margin indicated by number 1; in the lower left, numbers 7, 8 and 9 mark smaller landslides caused by the earthquake of 5 February 1783; number 4 indicates a huge boulder fallen from above, while numbers 5 and 6 indicate the new shoreline that covered the Formica rock; in the background, the Sicilian coast and smoking Mount Etna are visible; Antonio Minasi, Vedute di varie frane sulla costa calabrese nei dintorni di Scilla avvenute nel 1783 e nel 1790, in Raccolta Calabra di Natale Zerbi. d) Imaginary view of the Strait of Messina during the tsunami of 5 February 1783, in a hand-coloured etching by an anonymous German author; the tsunami is represented as a swirling motion of the waters of the Strait, with ships dragged into the vortex, collapsing coastal cliffs and lighthouses in the foreground, and smoking Mount Etna in the background; British Museum, View of the Strait of Messina during the earthquake of 5th February 1783; rocks falling from the cliff known as Scylla, the lighthouses in the process of falling down and ships hurtling towards the whirlpool, Charybdis, asset no. 1377357001. digital images via CFTIvisual [Bianchi et al.,2022].*

Despite the rescue operations and subsequent reconstruction projects enacted by the Bourbon government, the far-reaching consequences of the *"grande flagello"* (*"the great scourge",* as defined by 18th-century authors) persisted, exerting a profound influence on the region's economic development and growth until the 20th century.

From a macroseismic perspective, the current knowledge of the 1783 seismic sequence is based on the studies by Carrozzo et al., [1975], Cosentino et al. [1982] and on investigations carried out by ENEL [1985]. The latter were later improved by the work of Boschi et al. [1997](Table 3).

From 2007 onwards, the framework was further updated thanks to the revision of the dataset proposed by Guidoboni et al. [2007], which was included in the Catalogo dei Forti Terremoti in Italia (461 a.C.–1997) and for the Mediterranean area. The most recent version of this catalogue [Guidoboni et al., 2018] once again updates the macroseismic dataset; however, the new MDPs concern only environmental effects and are not associated with an intensity value.

Therefore, the reference study for the 1783 Calabrian seismic sequence that was adopted by the Italian Macroseismic Database [DBMI15, Locati et al., 2022] and by the Parametric Catalogue of Italian Earthquakes [CPTI15, Rovida et al., 2022] still remains the study by Guidoboni et al., [2007].

Parametric catalogue	**Reference Study**	**5 February**	**6 February**	**7 February**	**1 March**	**28 March**
Postpischl, 1985	Carrozzo et al., 1975 Cosentino et al., 1982	I_0 11 MM 7.10 MDP --	I_0 10 MM 6.10 MDP --	I_0 11 MM 6.70 MDP --	I_0 9 MM 5.60 MDP --	I_0 10 MM 6.70 MDP --
NT4.1 [Camassi and Stucchi, 1997]	ENEL, 1985	I_0 11 Ms 7.30 MDP 352	not present	I_0 10-11 Ms 7.00 MDP 191	I_0 8-9 Ms 5.90 MDP 19	I_0 10 Ms 6.70 MDP 323
CPTI99 [Boschi et al., 1999]	Boschi et al., 1997	I_0 11 Ms 6.91 MDP 356	I_0 8-9 Ms 5.94 MDP 8	I_0 10-11 Ms 6.59 MDP 192	I_0 9 Ms 5.92 MDP 18	I_0 10 Ms 6.94 MDP 323
CPTI04 [CPTI Working Group, 2004]	Boschi et al., 1997	I_0 11 Mw 6.91 MDP 357	I_0 8-9 Mw 6.34 MDP 8	I_0 10-11 Mw 6.59 MDP 192	I_0 9 Mw 5.92 MDP 18	I_0 10 Mw 6.98 MDP 323
CPTI11 [Rovida et al., 2011]	Guidoboni et al., 2007	I_0 11 Mw 7.02 MDP 356	I_0 -- Mw -- MDP 8	I_0 10-11 Mw 6.62 MDP 191	I_0 -- Mw 5.90 MDP 18	I_0 11 Mw 6.98 MDP 323
CPTI15 [Rovida et al., 2022]	Guidoboni et al., 2007	I_0 11 Mw 7.10 MDP 356	non-parameterised MDP 8	I_0 10-11 Mw 6.74 MDP 191	I_0 -- Mw -- MDP 18	I_0 11 Mw 7.03 MDP 323

Table 3. *Chronological table of the main Italian parametric earthquake catalogues with the reference studies on the five mainshocks of the 1783 sequence. MDP stands for Macroseismic Data Point, whereas Io refers to epicentral intensity.*

As illustrated in Table 3, which displays the chronological development of the parameters contained within the various catalogues, it is observed that the datasets remain largely unaltered.

However, the values that change over time are the magnitudes, which are recalculated using updated regression coefficients for the Intensity–Magnitude relations adopted in each revision [Rovida et al., 2022].

It is also noteworthy that the NT4.1 catalogue does not report the 6 February earthquake, classifying it as an aftershock. Conversely, the CPTI11 and CPTI15 catalogues provide the number of MDPs for the events of 6 February (MDP 8) and 1 March (MDP 18), though they do not include the magnitude or I_0 values (with the exception of the 1 March earthquake, for which only the magnitude is provided).

For completeness, it is also worth mentioning the recent work by Andrenacci et al., [2023] which provides macroseismic fields for the localities affected by the 1783 sequence, as well as for two other destructive events in the same area (the 1791 and 1894 earthquakes, both Mw 6.1) and for the 1908 Messina Strait earthquake (Mw 7.1).

All the aforementioned studies are included in the Italian Historical Macroseismic Archive (ASMI) [Rovida et al., 2017].

4.2.1 The 5 February 1783 Earthquake

The first strong earthquake in the 1783 seismic sequence occurred on 5 February 1783 at 12:00. CPTI15 [Rovida et al., 2022] locates the epicentre between the Gioia Tauro Plain and the Aspromonte Massif, at 38.297 latitude and 15.970 longitude. The earthquake parameters, derived from 356 macroseismic observations, indicate a magnitude of 7.10 and an epicentral and maximum intensity of 11 on the MCS scale (Fig. 8).

The area that exhibited the most severe damage extends across the entire southern Calabria, from Vibo Valentia to the Messina Straits, with the most severe effects occurring in the Gioia Tauro Plain. The shock was felt over a very extensive region, encompassing the whole of Sicily and much of southern Italy, as far as the Amalfi Coast and Salento.

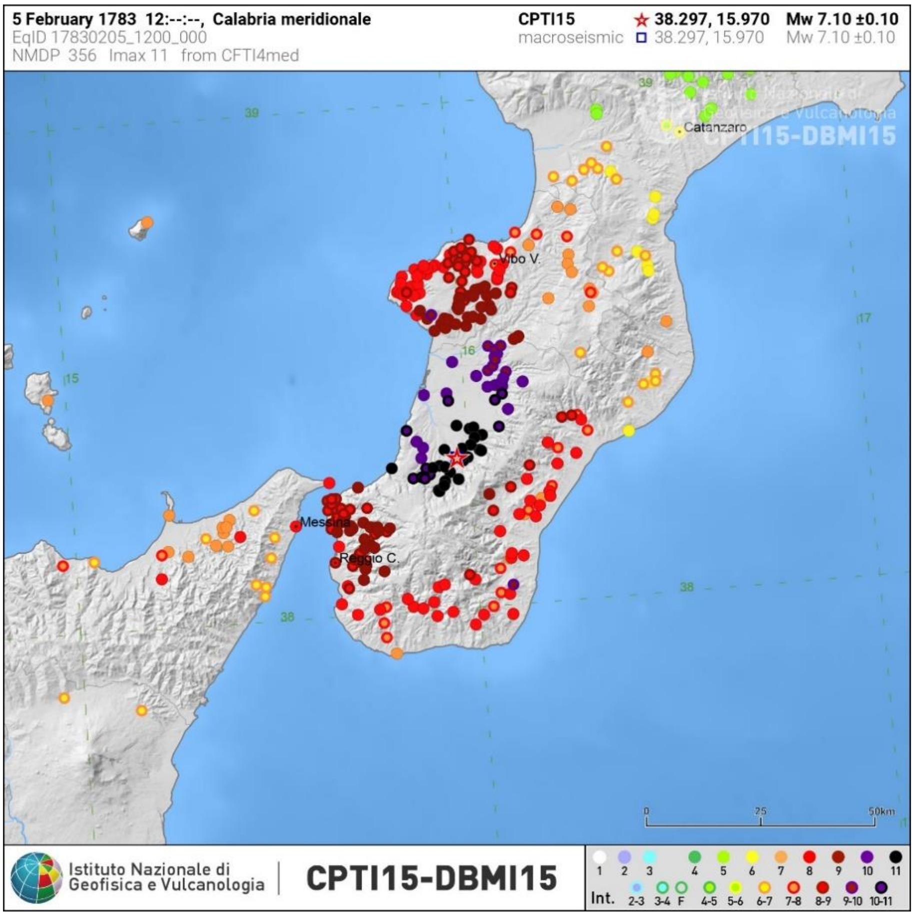

Figure 8. *Map of the intensity distribution of 5 February 1783 [CPTI15, Rovida et al., 2022; DBMI15, Locati et al., 2022]. MDPs from CFTI4med [Guidoboni et al., 2007].*

The attribution of the fault responsible for the 5 February 1783 earthquake remains controversial, with two main interpretative models in clear disagreement with each other.

The first, which has been extensively documented, associates the event with a system of high-angle normal faults dipping towards the W-NW, including the Cittanova fault (also known as the Aspromonte fault). The structure is located at the boundary between the crystalline basement of the Aspromonte and the sedimentary basins of the Gioia Tauro Plain. It is supported by multiple geomorphological, structural and paleoseismological evidence, which have been documented by several researchers, including Cotecchia et al., [1969], Tortorici et al., [1995], Jacques et al., [2001], Bosi and Galli [2002], Galli et al., [2007] and Galli and Peronace [2015].

From a historical perspective, the account by De Dolomieu [1784] provides a detailed description of a 25 km long fracture located at the foot of the Aspromonte hill slope, between the villages of Santa Cristina and Cinquefrondi. This fracture is interpreted as the direct surface expression of coseismic rupture along the Cittanova fault, and of the consequent downthrow of the Gioia Tauro Plain [Galli and Bosi, 2002]. Paleoseismological investigations have identified the rupture plane associated with the February 5 earthquake, along with evidence for at least four or five Holocene and Late Pleistocene paleoearthquakes of comparable magnitude. Furthermore, these studies have inferred slip rates of approximately 0.44–0.60 mm/year and recurrence intervals of approximately 1350–3200 years [Galli and Bosi, 2002].

Additional evidence for this hypothesis is provided by recent aeromagnetic investigations [Minelli et al., 2016], which revealed a continuous structure approximately 40 km long, referred to as the Cittanova–Aspromonte fault. This structure dips to the NW and is consistent with the reconstructed structural setting and with the generation of a large magnitude earthquake.

Finally, a recent study by Cucci [2022] demonstrates that the spatial distribution of coseismic hydrological anomalies reported in historical sources is consistent with the volumetric deformation field predicted for a high-angle, NW-dipping normal fault. This result also raises the possibility that the February 5 rupture may have involved, in a complex manner, adjacent segments such as the Sant'Eufemia and Galatro faults, for a total rupture length estimated at approximately 45–60 km, as previously proposed by Jacques [2001].

In contrast, the second hypothesis attributes the seismic event to a low-angle blind normal fault, the Gioia Tauro Fault, which dips towards the SE. Following the initial stratigraphic indications provided by Ricchetti and Ricchetti [1991], Valensise and D'Addezio [1994] advanced a conceptual model of this low-angle structure, derived from the intricate geometry of the sediments in the Gioia Tauro Plain and distinguished by robust kinematic analogies with the fault responsible for the 1908 Messina Strait earthquake. In this interpretation, which was later adopted by the DISS Working Group [2025], the Gioia Tauro Plain is deformed as a syncline by a buried, deep fault similar in style and geometry to the Messina structure. This suggests that regional deformation would not result from a high-angle, surface-breaking fault, but from a blind fault capable of producing broad crustal flexure.

According to DISS Working Group [2025], the hypothesis is supported by evidence from geomorphological and sedimentary studies conducted over an extended time period. The tilt of the Pleistocene marine terraces, the configuration of the drainage network and the distribution of Quaternary deposits are considered to be difficult to reconcile with rigid uplift associated with a high-angle normal fault. Instead, these features are more consistent with gentle, broad-wavelength deformation produced by a low-angle buried fault. In this framework, the large morphological scarp that bounds the western margin of the Aspromonte massif is interpreted as a relict scarp, shaped by gravitational and erosional processes and by the cumulative effects of seismic shaking, rather than as the direct surface expression of the seismogenic fault.

The validity of this scenario is further substantiated by geochemical evidence. Studies on groundwater and degassing anomalies [Pizzino et al., 2004] have identified, in the Rosarno area along the Nicotera–Gioiosa Ionica lineament, an alignment of geochemical signals consistent with the upper margin of the inferred Gioia Tauro blind fault, whereas such anomalies are largely absent along the Cittanova system. Further constraints were provided by Tiberti et al. [2017], who, based on the analysis of morphology and sedimentary architecture, highlighted the lack of clear geological evidence for post-early-Pleistocene activity along the NW-dipping faults associated with the Cittanova system.

4.2.2 The 6 February 1783 Earthquake

On 6 February 1783, at 00:20, a strong aftershock likely affected the coastal region between Scilla and Palmi. For this earthquake, the CPTI15 does not provide the epicentral coordinates or epicentral intensity, due to the minimal number of macroseismic observations available (only eight). This number is insufficient for the robust estimation of the parameters. The paucity of specific testimonies for the 6 February event is indicative of the overlap between these accounts and those referring to the 5 February earthquake, as evidenced by the chronicles. Based on the available damage descriptions, the maximum intensity is estimated in CPTI15 to be in the range of 9-10 MCS (Fig. 9).

By way of contrast, CFTI5Med estimates the earthquake's magnitude to be Mw 6.3, with the epicentre situated at 38.183° N, 15.638° E.

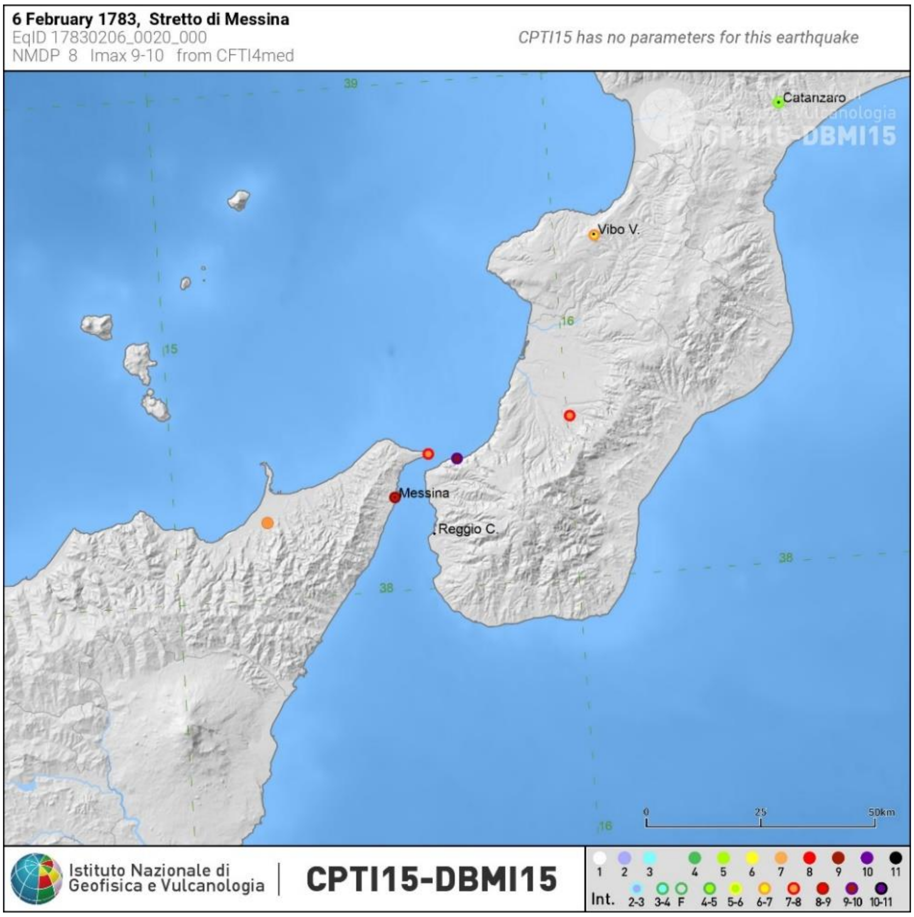

Figure 9. *Map of the intensity distribution of 6 February 1783 [CPTI15, Rovida et al., 2022; DBMI15, Locati et al., 2022]. MDPs from CFTI4med [Guidoboni et al., 2007].*

The earthquake triggered a substantial rockfall along the cliff west of Scilla. Approximately 30 minutes later, the rock mass collapsed into the sea, generating a tsunami [Minasi, 1785; De Lorenzo, 1895; Graziani et al., 2006]. According to historical sources [Minasi, 1785; De Lorenzo, 1895], the landslide front ranged from approximately 450 m to 2 km, with an offshore extent of about 100–110 m. The tsunami severely affected Scilla, where three major inundation waves devastated the Marina Grande district, reaching the rooftops of buildings and causing more than 1,500 fatalities [Hamilton, 1783; Sarconi, 1784; Minasi, 1785; Vivenzio, 1788; De Leone, 1783; Torcia, 1783; De Lorenzo, 1877]. The tsunami was also observed throughout the Strait of Messina, affecting Nicotera, Bagnara, Cannitello, Reggio Calabria, Messina, Torre del Faro, Capo Peloro, and Punta del Pezzo, where coastal inundation, damage to buildings and boats, and significant run-up heights were documented [Sarconi, 1784; Minasi, 1785; De Leone, 1783; Torcia, 1783; Augusti, 1783; Gallo, 1784; Graziani et al., 2006].

Jacques et al. [2001] propose that the 6 February earthquake was generated by the reactivation of the Scilla Fault, a west-dipping normal fault, triggered by the stress increase induced by the rupture of the Galatro–Cittanova–Sant'Eufemia system during the 5 February event. Meanwhile, according to the DISS Working Group [2025], in this sector of the Tyrrhenian margin of the Aspromonte there is also a small intermediate source ("Aspromonte Northwest"), located between the main Gioia Tauro and Scilla offshore sources. This source has been proposed as potentially activated during the 1783 sequence, in particular in connection with the 6 February earthquake. However, both interpretations remain hypothetical, as no direct geological or paleoseismological evidence of Holocene activity has yet been documented for the proposed fault structures.

4.3.2 The 7 February 1783 Earthquake

The second mainshock of the sequence occurred on 7 February at 13:10. The available macroseismic observations for this event are 191, with a maximum intensity of 10-11 MCS. According to the CPTI15, the earthquake was located at epicentral coordinates 38.580° N, 16.201° E and had a magnitude Mw 6.74.

The highest intensities are observed southeast of Vibo Valentia, near Soriano, Sorianello, Gerocarne and Pizzoni, located at the western foot of the Serre Mountains, about 40 km northeast of the epicentral area of the catastrophic 5 February event (Fig. 10).

The damage caused by this earthquake partially overlapped that produced by the 5 February event, although the epicentral area affected a more northern sector than those of the previous earthquakes, extending towards the Mesima and Marepotamo valleys on the Tyrrhenian side of the Serre range.

De Dolomieu [1784] further describes that this event significantly increased the damage in localities such as San Giorgio Morgeto, in the north-eastern part of the epicentral area of the 5 February earthquake, in a manner similar to the 6 February shock, which worsened the damage in the south-western portion of the same area, close to the Tyrrhenian coast. The most widely accepted interpretation identifies the Serre fault, and in particular its southern segment, as the seismogenic source of the 7 February 1783 earthquake. The NNE-striking, NW-dipping Serre normal fault separates the crystalline basement of the Serre range from the Plio–Pleistocene clastic deposits of the Mesima valley [Tortorici et al., 1995; Jacques et al., 2001; Galli et al., 2007].

Stress-transfer modelling demonstrates that the coseismic displacement produced by the 5 February earthquake increased Coulomb stress along the Serre fault to values sufficient to trigger the 7 February event, within an extensional system that was activated in sequence during the 1783 crisis [Jacques et al., 2001]. Paleoseismological investigations [Galli et al., 2007] at Soriano Calabro further document repeated Holocene surface ruptures along this segment, with at least one event younger than the seventeenth century, thereby confirming the recent activity of the fault and its chronostratigraphic compatibility with the 7 February earthquake. This body of evidence, when considered in conjunction with historical descriptions of surface ruptures along the scarp, lend support to the interpretation of the south-Serre fault as the seismogenic source of the 7 February 1783 earthquake [Galli et al., 2007].

Conversely, the DISS Working Group [2025] associates this occurrence with the "Upper Mesima Basin" source, which delineates the eastern margin of the Upper Mesima Valley, constrained to the south by the Nicotera–Gioiosa Ionica line and to the north by the Catanzaro Strait.

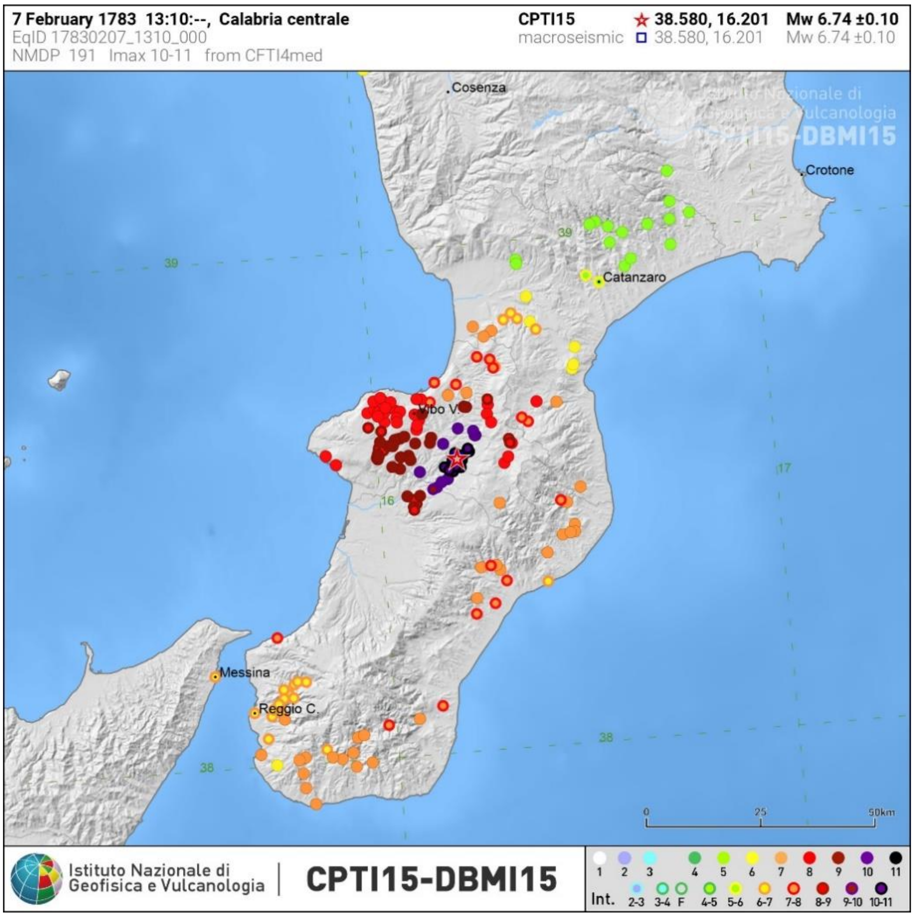

Figure 10. *Map of the intensity distribution of 7 February 1783 [CPTI15, Rovida et al., 2022; DBMI15, Locati et al., 2022. MDPs from CFTI4Med [Guidoboni et al., 2007].*

4.3.3 The 1 March 1783 Earthquake

On 1 March 1783, at 01:40, a moderate aftershock occurred. Similarly to the 6 February event, CPTI15 does not provide either the epicentral coordinates or the epicentral intensity, owing to the very limited number of available macroseismic observations, which for this earthquake amounts to only 18. The estimated maximum intensity is 9–10 MCS. By contrast, CFTI5Med assigns this earthquake a magnitude of Mw 5.9 and places the epicentre at 38.765° N, 16.300° E, approximately 20 km north of that of the 7 February earthquake.

The highest intensity values are concentrated in the Vibo Valentia area and along the western margin of the Serre range, within a more restricted sector located at the western foot of the mountains (Fig. 11).

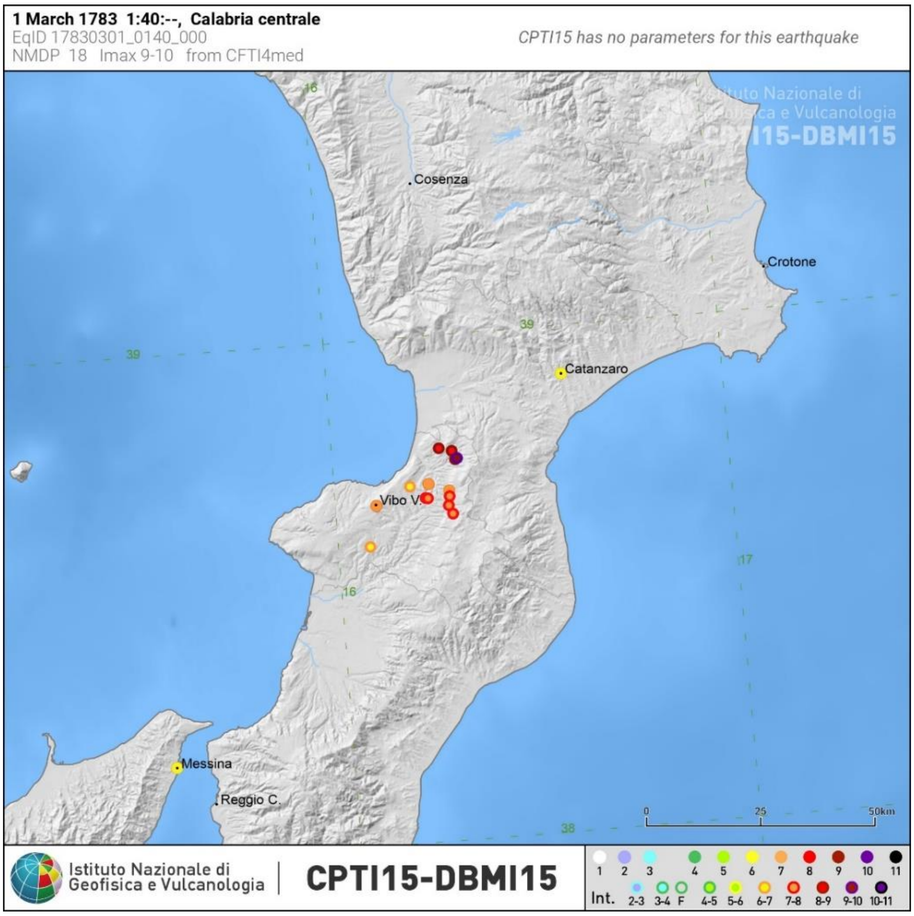

Figure 11. *Map of the intensity distribution of 1 March 1783 [CPTI15, Rovida et al., 2022; DBMI15, Locati et al., 2022].MDPs from CFTI4Med [Guidoboni et al., 2007].*

In the literature, this earthquake is associated with the rupture of the north-eastern segment of the Serre Fault, with an epicentre in the Polia area. The segmentation of the rupture and the temporal delay of about three weeks with respect to the 7 February event have been interpreted as the effect of a stress gap, formed as a consequence of a local release of energy that had occurred more than a century earlier, during the November 1659 earthquake [Jacques et al., 2001].

4.3.4 The 28 March Earthquake

The third mainshock of the sequence occurred on 28 March 1783 at 18:55. For this event, the macroseismic observations used by CPTI15 for parameterisation amount to 323, and the maximum intensity reached degree 11 MCS. CPTI15 locates the epicentre at 38.785° N and 16.64° E and estimates a magnitude of Mw 7.03 for the earthquake, ranking it as the second strongest event of the entire sequence.

The highest intensity values are clustered between Vibo Valentia and Catanzaro, particularly along the Ionian side of the Serre area, confirming the progressive northeastward migration of the seismic sequence (Fig. 12).

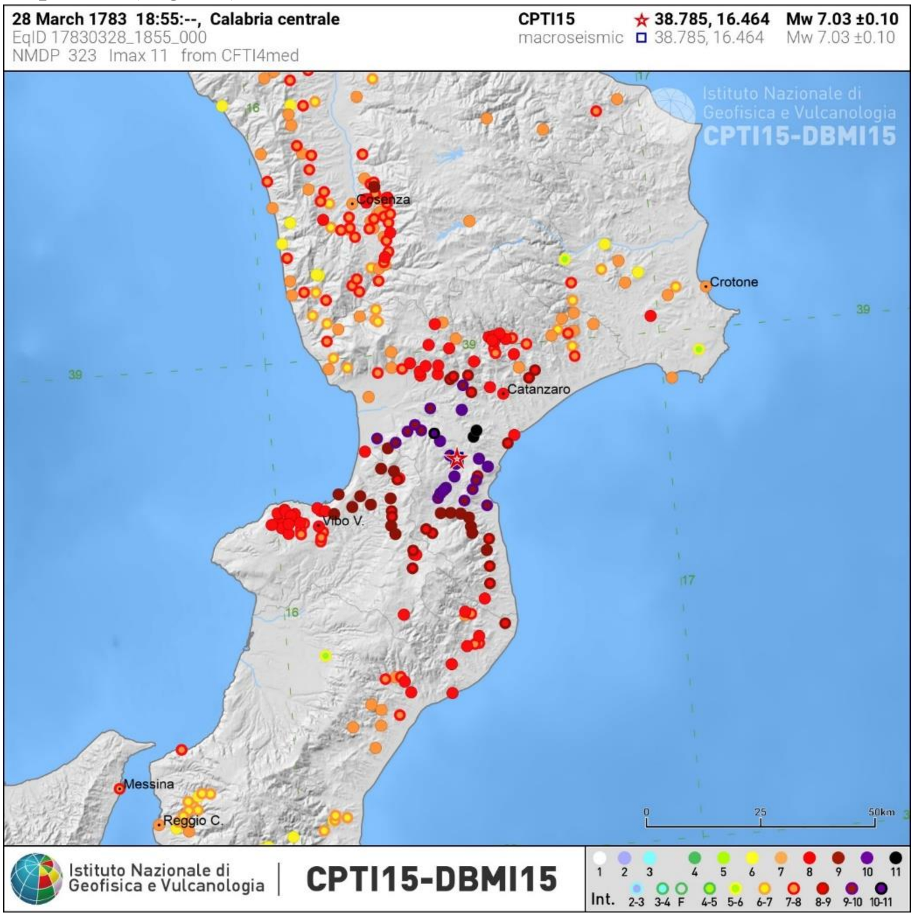

Figure 12. Map of the intensity distribution of 28 March 1783 [CPTI15, Rovida et al., 2022; DBMI15, Locati et al., 2022]. MDPs from CFTI4Med [Guidoboni et al., 2007].

The identification of the seismogenic source responsible for the 28 March earthquake remains most enigmatic. The effects were documented as far as the Catanzaro Basin, close to the Ionian side; however, though its origin is generally placed within the framework of the normal and transtensional faults of the Lamezia area, such as the Sant'Eufemia–Feroleto Fault [Moretti, 2000] or the Lamezia–Catanzaro Fault System [Pirrotta et al., 2021], unequivocal evidence of coeval surface faulting is lacking. Moreover, the anomalies observed in the attenuation of macroseismic intensity suggest a nucleation source located at greater depth than those of the other events in the sequence [Jacques et al., 2001]. To address these macroseismic inconsistencies, the integration of instrumental seismicity and geodetic deformation data has recently led to the hypothesis of the activation of a blind seismogenic source, trending approximately N-S, located in the central-eastern sector of the Catanzaro Isthmus and consistent with the regional WNW-ESE extensional regime [Pirrotta et al., 2021].

By contrast, DISS Working Group [2025] identifies the Caraffa–Squillace Gulf Composite Source as the responsible structure, interpreting it as a south-dipping, subvertical left-lateral strike-slip fault belonging to the strike-slip system that dissects and translates the central and southern Calabrian Arc towards the southeast. Within this framework, this source would also include the fault segment responsible for the 28 March earthquake.

5. Methodology

5.1 Historical Seismological Research

Historical seismology is the branch of seismology concerned with the reconstruction of the effects of earthquakes that occurred prior to the advent of recording instruments. In the absence of instrumental data, the effects of these events are reconstructed on the basis of written accounts describing the consequences for settlements and the natural environment. The nature, completeness and availability of such accounts vary depending on the historical period and the geographical area in which the earthquake occurred, reflecting the political, economic, social and cultural circumstances of each era [for a more comprehensive view of the methodology refer to Guidoboni and Ebel, 2009].

Among the most readily available sources, the following main types can be identified.

- Documentary sources are among the most useful and widely used sources of information in this type of study. They consist of documents of various kinds, both public, i.e. everything relating to the administrative system, including tax exemptions, censuses and fiscal records, parliamentary acts, etc., and private records including notarial deeds, wills, contracts, private letters and correspondence, and so on. To these must be added ecclesiastical records, which include pastoral visitations, ad limina reports, parish registers, and other church-related documents. Italy's documentary heritage is among the oldest and most extensive in the world, making the country an ideal setting for this type of research.
- Seismological compilations are a type of source that emerged in the second half of the nineteenth century and gathered information from various historical sources, including direct and indirect testimonies, journalistic and memoir sources, and local historiography. These works represent a fundamental resource for the reconstruction of Italian seismic history and still constitute one of the main documentary bases of historical seismology [Molin et al., 2008]. Among these, the work of Mario Baratta [1901] is particularly noteworthy, as it is considered the progenitor of that season of research and the main reference work for pre-twentieth-century earthquakes. Also, the annual compilations produced by Alexis Perrey [1848] amassed a substantial body of material on Italian earthquakes, now preserved in the Library of the Neapolitan Society of Local History in Naples (Perrey Fund).
- Seismic postcards and bulletins represent a major turning point in the monitoring and study of the effects of Italian earthquakes between the late nineteenth and early twentieth centuries. Their widespread adoption was closely connected to the development of the

network of the Italian Seismological Society from the 1870s onward, promoted by Michele Stefano De Rossi through the publication of the Bullettino del Vulcanismo Italiano [1895]. The objective of this network was to systematically organise the collection of information on the effects of earthquakes observed across the country. Seismic postcards were standardised questionnaires sent to the various municipalities, post offices, observatories, thermo-udometric stations, etc., to collect information on the macroseismic effects observed in that particular locality. This type of source is mentioned here for the sake of completeness within the documentary framework. However, it was not used in the present study.

- Journalistic sources are of particular importance for the study of historical earthquakes. Modern journalism originated in the 16th century with handwritten "notices" (a modern newsletter), distributed weekly to a limited audience [Infelise, 2002]. Gazettes, which became widespread during the first half of the seventeenth century, represent one of the most valuable journalistic sources for historical seismology. Published periodically and intended for a broad readership, they covered long time spans and relied on a network of correspondents distributed across the main European capitals, allowing for the rapid circulation of information [Camassi et al., 2011]. Their importance lies in the fact that they often preserve reports of earthquake effects, particularly for periods preceding the development of the modern press. However, their documentary value varies according to the historical context. Around the turn of the nineteenth century, for instance, the French Revolution and the Napoleonic Wars caused political and military news to dominate the press, significantly reducing the coverage of natural events [Camassi et al., 2011]. Despite these limitations, gazettes still constitute a fundamental source for integrating and verifying information derived from other documentary materials.
- Iconographic sources — including engravings, drawings, paintings, and photographs — provide visual documentation of the effects on the built environment and the landscape, supplementing written descriptions. Their seismological value lies in their ability to offer an immediate representation of building damage and landscape transformations.

The 1783 seismic sequence is exceptionally well documented and has been extensively studied by contemporary scholars and naturalists, as well as by recent historiography. The result has been the production of a substantial body of sources, unparalleled for any pre-instrumental earthquake in Italy, resulting from the convergence of distinct factors: the intensity of the catastrophe, the cultural context of the Enlightenment, and the political and administrative response of the Bourbon monarchy.

In this research, a systematic examination of the documentary corpus has been carried out, integrating existing bibliographical contributions with new archival research. A considerable number of the analysed texts were retrieved through the CFTI5Med database [Guidoboni et al., 2018], which provides numerous original documents and their corresponding transcriptions.

The sources were initially ordered chronologically and then subjected to critical interpretation, with the objective of reconstructing the evolution of the seismic sequence and its impact on the affected localities. A summary of the main sources examined is presented below.

Among the documentary sources used in this study are documents consulted in archives and libraries, listed in Table 4. Archival research was conducted directly at the Vatican Apostolic Archive in Rome and the State Archive of Naples, while documentation from the other institutions was examined through the CFTI5Med [Guidoboni et al., 2018] database and online.

Archives and libraries sources	
Ecclesiastical Administration	Vatican Apostolic Archive (Rome)
	Archpriest's Archive of S. Maria del Colle di Mormanno (CS)
Lay administration	Municipal Archive of Santa Cristina d'Aspromonte (RC)
	State Archive of Cosenza
	State Archive of Naples (ASNa)
	State Archive of Palermo
	State Archive of Venezia
	General Archive of Simancas (Spain)
	"Mozzi-Borgetti" Municipal Library, Macerata
	Bertoliana Civic Library, Vicenza
	Civic Library of Cosenza
	"Vittorio Emanuele III" National Library, Naples
	Regional Library of Messina

Table 4. *Documentary sources consulted in this study. Among these, on-site archival research was carried out at the Vatican Apostolic Archive and the State Archive of Naples, while documents from the other repositories were consulted online.*

Among institutional sources, the largest share of documentation comes from the State Archives of Naples and the National Library "Vittorio Emanuele III". Of particular importance are the reports of the royal officials sent to Calabria by the Bourbon court, and above all the report by the vicar general Francesco Pignatelli, drafted at the end of March 1783 and preserved at the National Library of Naples. This text, regarded as one of the principal contemporary references, provides the first comprehensive overview of the damage caused by the February shocks in each locality and has formed the basis for numerous subsequent studies. In addition, the correspondence of foreign ambassadors with their respective governments, the letters exchanged between the Marquis of Sambuca and the consul Stefano Rati, published in the

"Avvisi di Genova", and the letters of local ecclesiastics addressed to the Papal Secretary of State (Vatican Apostolic Archives) are of particular interest. These sources offer an external or peripheral, yet often highly detailed, perspective on the spread of news about the earthquakes, the development of the sequence, and the perception of governmental interventions.
The collections of the Suprema Giunta di Corrispondenza di Cassa Sacra, preserved at the State Archives of Naples and partly consulted on site, play a crucial role in this regard. The documentarians meticulously record the reconstruction undertaken by the Bourbon government through the expropriation and redistribution of ecclesiastical property, as well as the widespread conflicts that these measures provoked among local communities, religious institutions, and central authorities. This documentation includes directives addressed to the vicar general, engineering reports on religious buildings drawn up in the years following the earthquake (1787–1792), and surveys on the condition of Calabrian localities. As a whole, these documents provide an administrative and technical framework for the reconstruction that complements the more immediate descriptions of damage.
Within the same institutional sphere are the 27 letters written by the military engineers Antonio Winspeare and Francesco La Vega, preserved at the National Library of Naples and addressed to the prime minister, the Marquis of Sambuca, the Minister of War and Navy John Acton, and the vicar general. These letters, which were written with the intention of selecting sites for the reconstruction of destroyed settlements and to oversee the profound hydrogeological changes induced by the earthquake, frequently take the form of drafts with deletions and marginal notes. These can be read as genuine field diaries, written in real time in the weeks following the events. Based on the information gathered in the field by the officials, the three main authorities in the region – the governors of Catanzaro and Cosenza and the vicar general Pignatelli – sent weekly reports to the Neapolitan court, following a relatively uniform structure (number of earthquakes, casualties, health conditions). This internal correspondence within the Kingdom is complemented by the letters exchanged between the Marquis of Sambuca and the Spanish court, which are preserved in the Archivo General de Simancas (Secretaría de Estado collection) and in the State Archives of Naples. These letters, dispatched at regular intervals between February 1783 and January 1784, were intended to present the Spanish crown with an official image of gradual normalisation. This objective is further complemented by the correspondence with the Kingdom's agent in Genoa, Stefano Rati, which was published in the contemporary press almost as an official bulletin.

An additional corpus of sources is provided by the documentation produced by local ecclesiastics. The *"Note dei parroci"* (literally, "Parish Priests' Notes"), collected by Librenti, records the number of victims and, when compared with Pignatelli's data, have made it possible to assess the human losses. Further insights into medium-term demographic dynamics are provided by pastoral visits and reports of the Calabrian dioceses, preserved in the Vatican Apostolic Archives, in Rome.

Within the same archive, particular importance is attached to the document *"Indice generale de' paesi occidentali ed orientali della Calabria Ulteriore del loro stato de' viventi prima del terremoto del 5 febbraio 1783 degli estinti causati dalle rovine colla distinzione del sesso de' monaci e delle monache"*, which was dispatched by the Vicar General for Calabria, Prince Francesco Pignatelli, to the Prime Minister, Marquis of Sambuca, on 28 June 1783. This source documents in detail the degrees of damage (specified as *"distrutto"* – destroyed, *"inabitabile"* – uninhabitable, *"parte distrutto e il resto inabitabile"* – partly destroyed and the remainder uninhabitable, *"poche case lesionate"* – a few cracked houses, etc.) and the number of fatalities for 354 localities, constituting a post-sequence count of considerable completeness and value.

Alongside civil and ecclesiastical administrative documentation, a wide range of contemporary printed material has also been analysed. The earthquake of 1783 prompted a remarkably extensive editorial response, encompassing printed reports, scientific memoirs, chronicles, moral and political pamphlets, and travel accounts. Table 5 list the main ones, sorted by year of production.

Publication date	**Sources**
1783	Vivenzio G., Augusti M., Galimi P., Hamilton W., Gusta F., Gallo A., Torcia M., De Leone A., Campagna G., La Pira G. M., Lamanna G., Minasi G., De Colaci O., Onorati N., Roscitano P., Lallement, Masci A.
1784	Sarconi M., Gallo A., Zupo N., Corrao A., Grimaldi F.A., Pensante Perolitano
1785	De Dolomieu D., Lallement, Minasi G., Mitrowsky J., Serrao E., De Saint-Non J.C.R.
1786	Caristina D., Hamilton W.
1787	Faccioli A.
1788	Vivenzio G., Pignatari D.,
1793	Ippolito F., Hamilton W.
1832	Botta V.C.
1848	Perrey A.

1863	Grimaldi A.
1895	De Lorenzo A., Faggiotto A
1966	Placanica A.
1976	Liberti R., Pugliesi F.
1982	Placanica A.
1985	Despuig A.

Table 5. *Main documentary sources consulted in this study, ordered by date of publication.*

When considered as a whole, these texts constitute a corpus of uneven informational value, yet of great historical and literary interest, offering a valuable perspective on how the disaster was perceived within contemporary society. However, due to the heterogeneity of the texts, caution should be exercised when utilising them for macroseismic purposes.

Among the most important synthetic works produced by official bodies, two texts in particular stand out. The first of these is the "*Istoria de' fenomeni del tremoto avvenuto nelle Calabrie e nel Valdemone*", published by Michele Sarconi in 1784 with the collaboration of Pacifico, Fasano, Minasi, and Father Eliseo della Concezione. This work is the result of the scientific expedition that was initiated on 5 April 1783 under the auspices of the Royal Academy of Sciences and Letters of Naples. It represents the first organised scientific investigation by the State into the effects of an earthquake. The second is the *"Istoria de' Tremuoti avvenuti nella Provincia della Calabria ulteriore, e nella Città di Messina nell'anno 1783 e di quanto nella Calabria fu fatto per lo suo risorgimento fino al 1787 preceduta da una Teoria, ed Istoria Generale de' Tremuoti, 2 voll.",* written by Giovanni Vivenzio in 1788. This work combines a theoretical section with a detailed description of the events, is accompanied by a geographical map, and also incorporates the "*Giornale tremuotico"* by Pignatari; an earlier version of this work had already been composed in 1783 (Fig. 13).

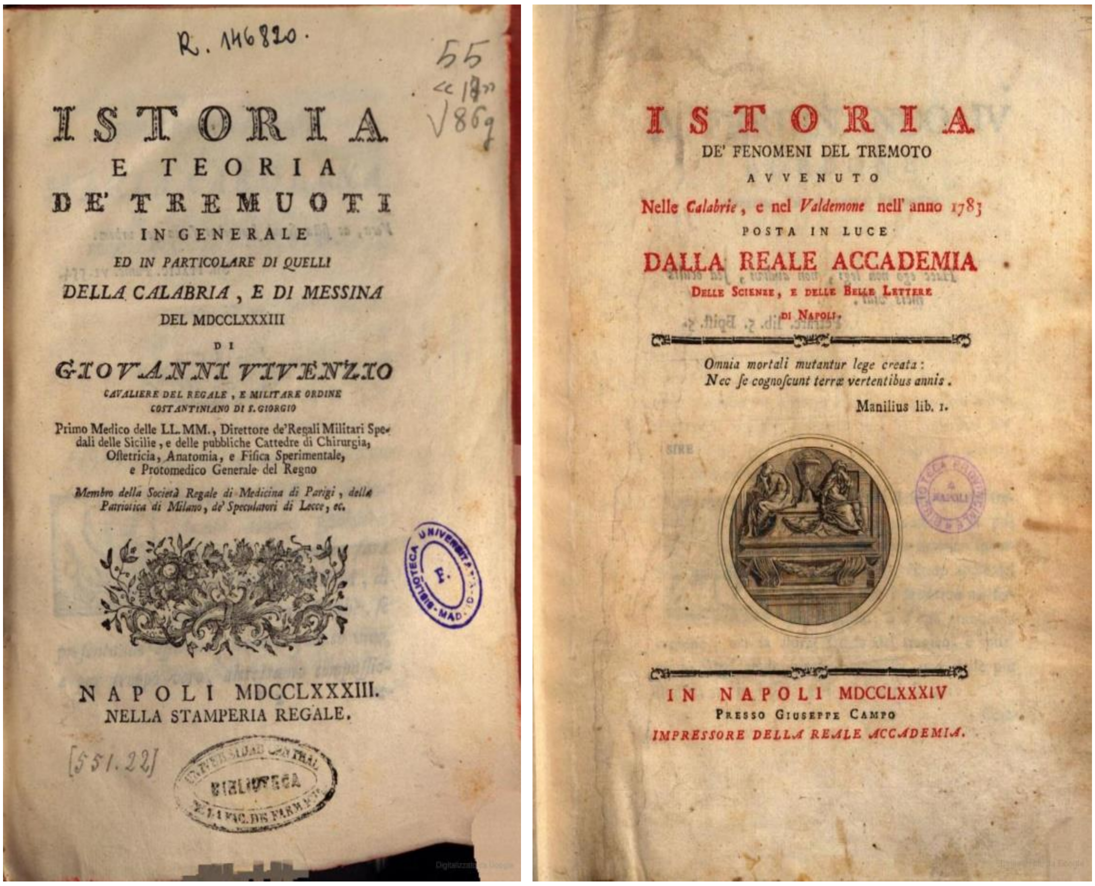

ISTORIA
E TEORIA
DE' TREMUOTI
IN GENERALE
ED IN PARTICOLARE DI QUELLI
DELLA CALABRIA, E DI MESSINA
DEL MDCCLXXXIII
DI
GIOVANNI VIVENZIO
CAVALIERE DEL REGALE, E MILITARE ORDINE
COSTANTINIANO DI S. GIORGIO
Primo Medico delle LL.MM., Direttore de' Regali Militari Spedali delle Sicilie, e delle pubbliche Cattedre di Chirurgia, Ostetricia, Anatomia, e Fisica Sperimentale, e Protomedico Generale del Regno
Membro della Società Regale di Medicina di Parigi, della Patriotica di Milano, de' Speculatori di Lecce, ec.
NAPOLI MDCCLXXXIII.
NELLA STAMPERIA REGALE.

ISTORIA
DE' FENOMENI DEL TREMOTO
AVVENUTO
Nelle Calabrie, e nel Valdemone nell' anno 1783
POSTA IN LUCE
DALLA REALE ACCADEMIA
DELLE SCIENZE, E DELLE BELLE LETTERE
DI NAPOLI.
Omnia mortali mutantur lege creata:
Nec se cognoscunt terrae vertentibus annis.
Manilius lib. 1.
IN NAPOLI MDCCLXXXIV
PRESSO GIUSEPPE CAMPO
IMPRESSORE DELLA REALE ACCADEMIA.

Figure 13: *Front page of the historical-scientific accounts by Vivenzio [1783] – on the left – and by Sarconi [1784] – on the right.*

The study has also taken into account the numerous accounts conveyed by contemporary periodical press. Periodicals from central and northern Italy, including the "Gazzetta Universale" (which carried 67 issues of earthquake-related news between March 1783 and 1786, 38 of which were published in 1783), "Notizie del Mondo" (46 issues), "[Gazzetta di]Bologna" (30 issues), "Avvisi di Genova" (25 issues), "Notizie Diverse" (24 issues), the "Diario Estero" of Rome (19 issues), as well as the "Gazzetta di Mantova" and "Il Messaggiere" of Modena, frequently published reports from the affected areas, often preceding the major official accounts.

In particular, issue no. 16 of the *Gazzetta Universale* of Tuesday, 25 February 1783, in the Naples section dated 17 February, reports the first information concerning the seismic sequence so far identified during the present study, including the description of the earthquake of 5 February and a list of 28 affected localities (Fig. 14).

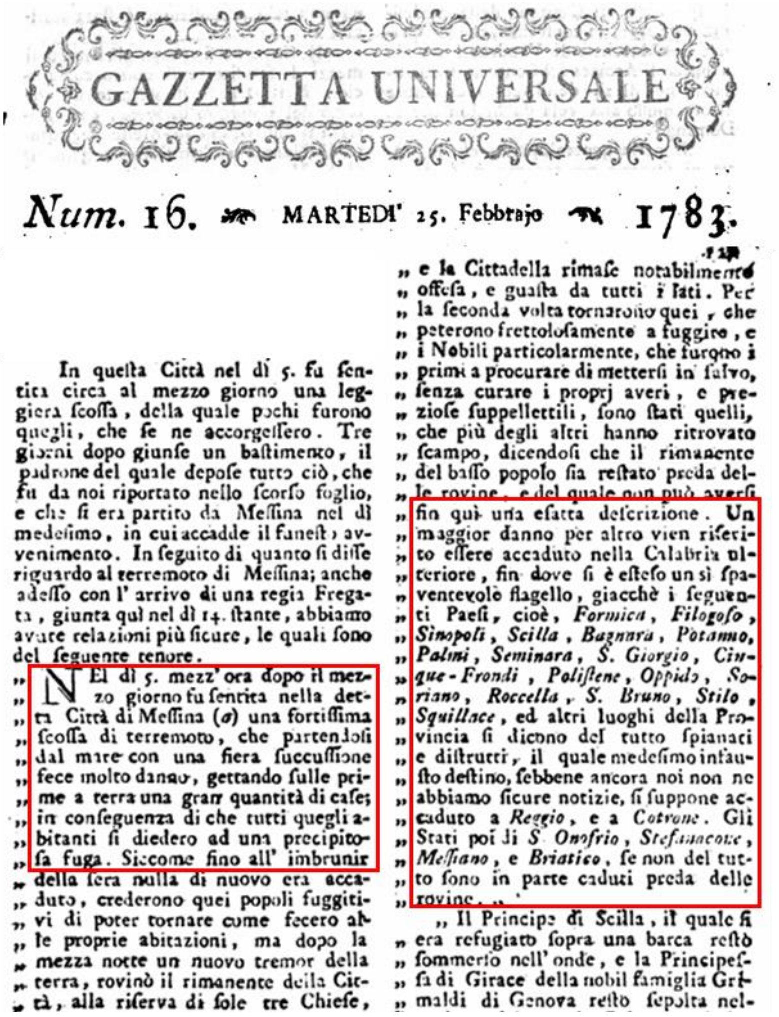

GAZZETTA UNIVERSALE

Num. 16. MARTEDI' 25. Febbrajo 1783.

In questa Città nel dì 5. fu sentita circa al mezzo giorno una leggiera scossa, della quale pochi furono quegli, che se ne accorgessero. Tre giorni dopo giunse un bastimento, il padrone del quale depose tutto ciò, che fu da noi riportato nello scorso foglio, e che si era partito da Messina nel dì medesimo, in cui accadde il funesto avvenimento. In seguito di quanto si disse riguardo al terremoto di Messina; anche adesso con l' arrivo di una regia Fregata, giunta quì nel dì 14. stante, abbiamo avute relazioni più sicure, le quali sono del seguente tenore.

„ NEl dì 5. mezz' ora dopo il mezzo giorno fu sentita nella detta Città di Messina (*a*) una fortissima scossa di terremoto, che partendosi dal mare con una fiera succussione fece molto danno, gettando sulle prime a terra una gran quantità di case; in conseguenza di che tutti quegli abitanti si diedero ad una precipitosa fuga. Siccome fino all' imbrunir della sera nulla di nuovo era accaduto, crederono quei popoli fuggitivi di poter tornare come fecero alle proprie abitazioni, ma dopo la mezza notte un nuovo tremor della terra, rovinò il rimanente della Città, alla riserva di sole tre Chiese,

„ e la Cittadella rimase notabilmente offesa, e guasta da tutti i lati. Per la seconda volta tornarono quei, che poterono frettolosamente a fuggire, e i Nobili particolarmente, che furono i primi a procurare di mettersi in salvo, senza curare i proprj averi, e preziose suppellettili, sono stati quelli, che più degli altri hanno ritrovato scampo, dicendosi che il rimanente del basso popolo sia restato preda delle rovine, e del quale non può aversi fin quì una esatta descrizione. Un maggior danno per altro vien riferito essere accaduto nella Calabria ulteriore, fin dove si è esteso un sì spaventevole flagello, giacchè i seguenti Paesi, cioè, *Formica*, *Filogoso*, *Sinopoli*, *Scilla*, *Bagnara*, *Potamo*, *Palmi*, *Seminara*, *S. Giorgio*, *Cinque-Frondi*, *Polistene*, *Oppido*, *Soriano*, *Roccella*, *S. Bruno*, *Stilo*, *Squillace*, ed altri luoghi della Provincia si dicono del tutto spianati e distrutti, il quale medesimo infausto destino, sebbene ancora noi non ne abbiamo sicure notizie, si suppone accaduto a *Reggio*, e a *Cotrone*. Gli Stati poi di *S. Onofrio*, *Stefanacone*, *Messiano*, e *Briatico*, se non del tutto sono in parte caduti preda delle rovine. „

„ Il Principe di Scilla, il quale si era refugiato sopra una barca restò sommerso nell' onde, e la Principessa di Girace della nobil famiglia Grimaldi di Genova restò sepolta nel-

Figure 14: *Extract from the Gazzetta Universale, no. 16, 25 February 1783, describing the effects of the 5 February 1783 earthquake (left: "On the 5th day, half an hour after midday, a very strong earthquake was felt in the said city of Messina, which, coming from the sea with violent shaking, caused great damage, immediately throwing down a great number of houses; as a consequence, all the inhabitants took to a hasty flight"; right: "Even greater damage, however, is reported to have occurred in Calabria Ulteriore, as far as such a dreadful calamity extended, since the following towns, namely Formica, Filogaso, Sinopoli, Scilla, Bagnara, Potamo, Palmi, Seminara, S. Giorgio, Cinquefrondi, Polistena, Oppido, Soriano, Roccella, S. Bruno, Stilo, Squillace, and other places in the province, are said to have been completely, or almost completely, destroyed. The same unfortunate fate, although no certain reports have yet reached us, is supposed to have befallen Reggio and Crotone. The States of Sant'Onofrio, Stefanaconi, Messiano, and Briatico, if not entirely destroyed, have in part fallen prey to the ruins").*

Despite being filtered through the rhetoric of the press, these sources provide an almost real-time chronicle of how the sequence unfolded and how the progression of damage was perceived.

The 1783 corpus is also exceptionally rich in iconographic sources. Sarconi's work was complemented by an atlas comprising 68 copper-engraved plates, some of which were watercolour-painted by Pietro Fabris. The plates were prepared by the architects Pompeo

Schiantarelli, Ignazio Stile, and Bernardino Rulli, and document a range of phenomena including damage to buildings, landscape transformations, landslides, landslide-dammed lakes, surface faulting, and changes in the coastline [Sarconi, 1784]. The plates also circulated separately from the Istoria as an independent collection, representing the first systematic visual documentation of the effects of an earthquake produced in Italy.

Three examples of these representations, all of which were drawn by Pompeo Schiantarelli, are shown in Figure 15 and depict (a) Francica — the church of Sant'Angelo, which had almost completely collapsed, with only a few walls and a window still standing ; (b) Terranova Sappo Minulio — a ruin that had been completely overturned by the force of the earthquake; and (c) Monteleone di Calabria (present-day Vibo Valentia) — a deep chasm that had opened in the ground near the town, and in the background, a north-west view of the settlement that had been damaged by the earthquake.

Figure 15. *Iconographic representations of the 1783 Calabrian earthquakes from Sarconi [1784]: (a) Francica (tav. X); (b) Terranova Sappo Minulio (tav. XXXIV); (c) Monteleone di Calabria (present-day Vibo Valentia) (tav. V). Drawings by Pompeo Schiantarelli.*

This iconographic material is accessible through CFTIvisual [Bianchi et al., 2022], the INGV atlas of visual sources.

Furthermore, the *Carta corografica della Calabria Ulteriore* (Fig. 16), as depicted by Padre Eliseo della Concezione, holds particular relevance to this study.

Figure 16. *Carta corografica della Calabria Ulteriore by Padre Eliseo della Concezione [1784].*

The map was produced with the aid of an equatorial instrument of his own invention. It documents the territorial transformations caused by the seismic sequence and corrects errors found in pre-existing cartography. The classification of effects severity of each locality is determined by the number of asterisks assigned: with one asterisk indicating partial damage, two asterisks indicating partial destruction and rendering of the settlement uninhabitable, and three asterisks indicating complete destruction. The map represents one of the first instances of a seismic map being produced in Italy.

Numerous works have documented the seismic sequence also in the 19th century. Of particular importance are the works of Mercalli [1897, 1910] and Baratta [1895, 1901, 1905], who dedicated specific studies to Calabrian seismicity and contributed to consolidating, within the seismological field, the image of the 1783 earthquakes as a reference event for the entire region. Among more recent studies, the historical writings of Cortese [1921, 1965] and Pagano[1892], along with the particularly significant contributions of Placanica [1970, 1982, 1988], author of fundamental works on the response of the southern cultural environment to the disaster and on the administration of the Cassa Sacra, deserve particular mention. This research tradition also encompasses the studies by Principe [1985] and by Pugliesi [1976], who examined various aspects of the establishment of new settlements following the earthquake. More recently, the study by Cecere [2017] offers a historical-social perspective complementary to contemporary administrative and scientific sources. Finally, the *"Dizionario geografico-ragionato del Regno di Napoli"*, first published in 1797 by Lorenzo Giustiniani, was also utilised for the identification and location of the localities of interest.

5.2 Macroseismic Data Collection

Following the collection, chronological ordering and critical analysis of the sources, the work proceeded with the identification of all localities affected by the 1783 seismic sequence. Each locality has been georeferenced, and for each one, a summary sheet has been compiled (Fig.17).

Locality	Municipality	Province	Latitude	Longitude	Other toponyms
Gerocarne	Gerocarne	VV	38.587	16.219	Jerocarne, Perocarne

Sources and excerpts
Vivenzio G., [1783]. Istoria e teoria de' tremuoti in generale ed in particolare di quelli della Calabria, e di Messina del MDCCLXXXIII. *[...]Stato di ARENA. Arena, ed i Villaggi Dasà, Aquaro, Potame, Migliana, Bracciara, Limpidi, Pronia, Semiatone, e Jerocarne. Questo Stato, che giace presso Aspromonte, nelle orribili scosse de' cinque, e sette Febbrajo fu danneggiato negli edificj in guisa, che non ne rimase quasi alcuno in piedi [...]*
Gallo A., [1783]. Articolo di lettera del signor D.Andrea Gallo al P. Lettore Augusti in cui si notano per i suoi giorni le scosse sentite in Messina sino ai 5 d'aprile 1783, giorno della data della medesima lettera, in M.Augusti, "Dei terremoti di Messina e di Calabria dell'anno 1783. Memorie e riflessioni", pp.49-50. *[...] Relazione del danno cagionato dal Terremoto della Calabria Ulteriore nei giorni 5, e 7 Febbrajo 1783.[...] Arena, Dasà, Gerucarne, Ciano, Senciatone, Acquaro, Limbidi, Potami, Brastelara, Migliano, Pronia Anime 1369, 1292, 919,100,314,2081,504,264,230,180. Morti 300. Danni Tutti Distrutti[...]*
Sarconi M., [1784]. Istoria de' fenomeni del tremoto avvenuto nelle Calabrie, e nel Valdemone nell'anno 1783 posta in luce dalla Reale Accademia delle Scienze, e delle Belle Lettere di Napoli. *[...]Gli edificj del resto di questo distretto furono ridotti in un confuso rovinio; ma non vi furono fenomeni singolari. I massimi furono quelli , che già altrove notammo allor che parlammo di Jerocarne i mediocri furono quelli , che osservammo in Arena e i minimi furono quelli , che avvertimmo in Dasa , e in Aquaro . Nel resto de' villaggi , cioè Brazzaria, Ciano, Limpide, Meliano, Potamia, Pronia , e Signatone , non vi era fenomeno di conseguenza , in fuori del disastro avvenuto ne' rozzi abituri[...]*
Grimaldi F.A., [1784]. Descrizione de' tremuoti nelle Calabrie nel 1783. *[...]I danni, che cagionò la scossa della mattina dei cinque di Febraìo nella Calabria Meridionale, furono i seguenti. Paesi intieramente distrutti. [...]Stato di Arena, che comprende i seguenti paesi Arena, Basà, Acquaro, Ciano, Porame, Migliano, Bracciara, Limpadi, Oronía, Semiatenì, Perocarne. Paesi' de' mezzani tempi, quando la Provinci*
Faccioli A., [1787]. Delle memorie fisico-tragiche sulla storia del terremoto e suoi fenomeni, accaduti nella provincia di Calabria Ulteriore nell'anno 1783. *[...]Dispianato, e distrutto Gerocarne Picciola casa in pié riserba appena, Potea la gente sua altrove andarne Illesa senz'aver eccidio, e pena! Nò, che per ogni dove umana carne Mirasi al suol d'ogni sua strada piena, Quà le otto donne, e quattro putti estinti, La uomini dieci, alle rovine avvinti. [...]*
Vivenzio G. [1788]. Istoria de' Tremuoti avvenuti nella Provincia della Calabria ulteriore, e nella Città di Messina nell'anno 1783 e di quanto nella Calabria fu fatto per lo suo risorgimento fino al 1787 preceduta da una Teoria, ed Istoria Generale de' Tremuoti, 2 voll. *[...]Gerocarne distrutto. Numero delle anime prima dei de' Tremuoti 803. Morti per le rovine 22[...]*

Figure 17. *Example of locality summary sheet with excerpts from consulted texts.*

This comprises excerpts from all sources providing information relating to that specific locality. The sheet report provides a comprehensive overview of the effects on the built environment, the natural environment, and the population, as documented by contemporary sources. This approach enables the reconstruction of the overall picture of damage and, in some cases, its temporal evolution throughout the entire sequence. This methodological approach enabled the construction of the macroseismic dataset for the 1783 sequence.

Particular attention, for the purposes of this work, was paid to identifying, for each source, information relating to where, when and how strong each seismic event was perceived and what effects it produced on the built environment. An example of this approach is shown in Figure 18.

From the work of Vivenzio [1788], for the localities of Cosoleto and Marcellinara, it is possible to clearly extract the date of the earthquake and the effects it produced on the built environment.

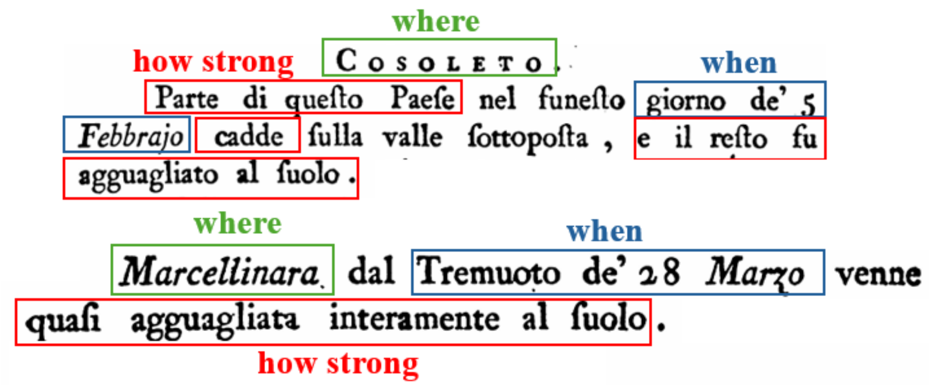

Figure 18. *Extracts from Vivenzio [1788] describing the damage to Cosoleto after the 5 February earthquake (on the top: "Part of this settlement, on the fateful day of 5 February, collapsed into the valley below, and the remainder was levelled to the ground") and to Marcellinara after the 28 March earthquake (on the bottom: "Marcellinara was almost entirely levelled to the ground by the earthquake of 28 March").*

For Cosoleto, for example, the following is reported: *"Parte di questo paese nel funesto giorno de' 5 Febbrajo cadde sulla valle sottoposta, e il resto fu agguagliato al suolo",* a description that undoubtedly allows the damage to be associated with the 5 February earthquake. Similarly, for Marcellinara, the account *"Marcellinara dal Tremuoto de' 28 Marzo venne quasi agguagliata interamente al suolo"* clearly attributes the near-total destruction of the locality to the 28 March earthquake.

One of the most complex aspects of the review involved the chronological ordering of information extracted from the sources, with the aim of reconstructing as accurately as possible the sequence of earthquakes and the evolution of their effects in the localities concerned. Despite the considerable richness of the documentary corpus relating to the 1783 Calabrian sequence, many accounts describe scenarios referring to the combined effects of different earthquakes, without a clear distinction of the contribution of individual events.

A notable example in this regard is provided by the case of the State of Laureana di Borrello, for which the following is reported: *"Or per le scosse de' memorabili Tremuoti furono distrutti gli edifici di questo Stato, restando in piedi soltanto poche fabbriche rovinose, di cui non può farsi alcuno uso"* [Vivenzio, 1788] (Fig. 19). In this type of description, the damage is attributed to the sequence as a whole rather than to a single earthquake; consequently, it must be compared with further information drawn from other sources in order to determine whether at least part of the effects described can be chronologically distinguished.

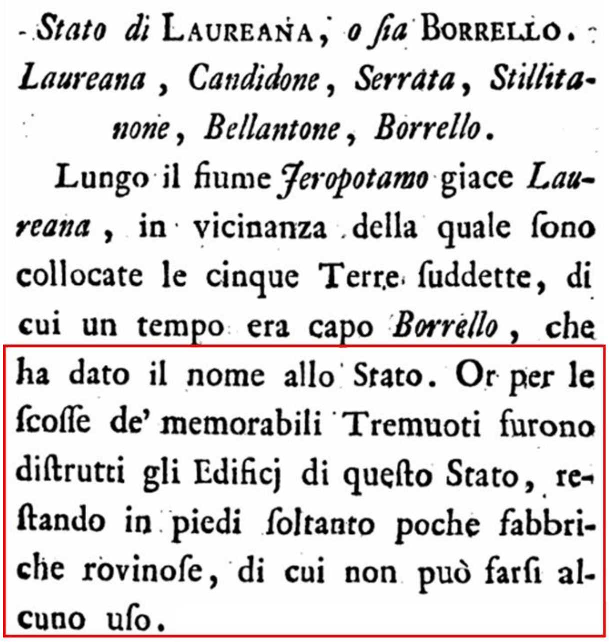

Stato di LAUREANA, o ſia BORRELLO.
Laureana, Candidone, Serrata, Stillitanone, Bellantone, Borrello.
Lungo il fiume Jeropotamo giace Laureana, in vicinanza della quale ſono collocate le cinque Terre ſuddette, di cui un tempo era capo Borrello, che ha dato il nome allo Stato. Or per le ſcoſſe de' memorabili Tremuoti furono diſtrutti gli Edificj di queſto Stato, reſtando in piedi ſoltanto poche fabbriche rovinoſe, di cui non può farſi alcuno uſo.

Figure 19. *Excerpt from Vivenzio [1788] describing the damage in the State of Laureana ("Due to the shocks of the memorable Earthquakes, the buildings of this State were destroyed, leaving standing only a few ruinous masonry buildings, of which no use can be made").*

However, it should be noted that not all cumulative descriptions are equally indeterminate. In some cases, although they refer to the effects produced by multiple events, the sources preserve a temporal scan that makes it possible to recognise a progression of damage. This observation is exemplified in the case of Reggio (RC), as Sarconi [1784] documents: *"Il tremoto del dì cinque ne cominciò il guasto fatale: continuollo quello del dì sette di Febbrajo: quello poi del dì 28 di Marzo vi appose l'ultima mano"*(Fig. 20).

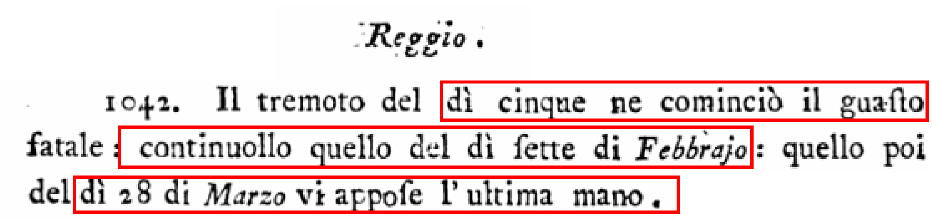

Reggio.
1042. Il tremoto del dì cinque ne cominciò il guaſto fatale: continuollo quello del dì ſette di Febbrajo: quello poi del dì 28 di Marzo vi appoſe l'ultima mano.

Figure 20. *Extract from Sarconi [1784] describing the damage in Reggio ("The earthquake of the fifth began its fatal ruin: that of the seventh of February continued it: then that of 28 March put the final hand to it").*

In order to discriminate, as far as possible, between effects attributable to individual events and cumulative descriptions of the entire sequence, the chronological reconstruction was based on the integration of information from multiple sources relating to the same locality, giving priority to those that were written chronologically closer to the events. When both cumulative descriptions and accounts attributing damage to a single earthquake were available for a given locality, the latter were prioritised. This comparative approach enabled the determination, on a case-by-case basis, of whether a given description referred to a single seismic event or to the cumulative effects of multiple events.

The distinction between the February shocks and those of March was, in general, more readily discernible. Sources dated before March, particularly of a journalistic type, such as the *Gazzetta Universale*, can in fact be attributed with sufficient confidence exclusively to the February events.

Distinguishing between the February earthquakes proved more complex, as many sources describe the effects of the closely spaced shocks in cumulative terms, as in the case of Sinopoli (Fig. 21).

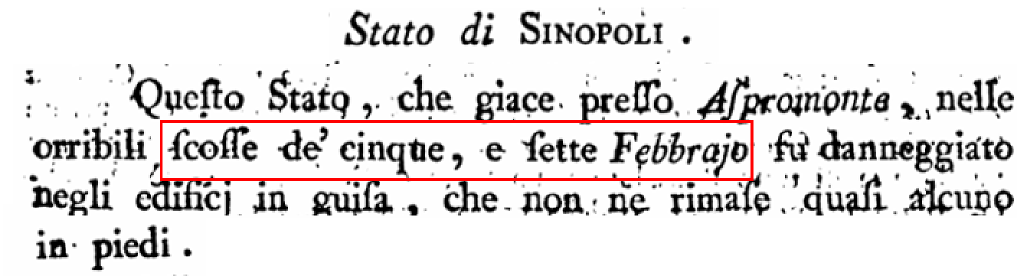
Stato di SINOPOLI.

Queſto Stato, che giace preſſo *Aſpromonte*, nelle orribili ſcoſſe de' cinque, e ſette *Febbrajo* fu danneggiato negli edificj in guiſa, che non ne rimaſe quaſi alcuno in piedi.

Figure 21. *Extract from Vivenzio [1788] describing the damage in Sinopoli ("This State, which lies near Aspromonte, in the terrible shocks of 5 and 7 February, was damaged in its buildings in such a manner that almost none remained standing").*

Vivenzio [1788] reports that *"Questo Stato, che giace presso Aspromonte, nelle orribili scosse de' cinque, e sette Febbrajo fu danneggiato negli edifici in guisa, che non ne rimase quasi alcuni in piedi.",* thus describing the damage to the locality as the result of the combined effects of the shocks of 5 and 7 February.

In such a case, where temporal indicators within the sources were not sufficiently clear, the information was considered cumulative rather than attributed to a particular event (see paragraph 5.3.2).

5.3 Intensity Assessment

The collected accounts have improved our understanding of the sequence of 1783 earthquakes, allowing detailed documentation of the observed effects in each affected locality. This information is then used to assign macroseismic intensity values.

Macroseismic intensity classifies the ground shaking at a locality during an earthquake, based on the effects observed on people, buildings and the natural environment [Musson e Cecić, 2012]. In contrast to instrumental metrics, such as magnitude, which quantifies the energy released at the source of the earthquake, intensity focuses on the consequences of the seismic event at a specific locality. For this reason, macroseismic intensity is a fundamental tool in seismology, as it enables the reconstruction and comparison of the impact of earthquakes across different regions and historical periods, including events that occurred before the advent of instrumental recordings.

The concept of intensity emerged in the mid-19th century and is intrinsically linked to Mercalli [1902]: the evolution of this concept has been addressed among others by Tertulliani [2019].

In practical terms, intensity is expressed as an integer and does not constitute a physical parameter in the strict sense; rather, it is a classification of diagnostic features characteristic of the effects of ground motion, organised in proportion to their severity. An intensity value relating to a specific earthquake and a specific locality, identified by geographical coordinates, constitutes a macroseismic data point (MDP).

Macroseismic intensity has been employed in various fields of seismology. For instance, it has been used for predictive purposes in hazard studies [D'Amico and Albarello, 2008; Gomez-Capera et al., 2010], for loss estimates inferred from expected intensity values [Musson et al., 2010] and for testing probabilistic hazard assessments [Albarello and D'Amico, 2008; Beauval et al., 2020; D'Amico et al., 2024].

However, the most common use of macroseismic data is for assessing the parameters (i.e. macroseismic epicentre and magnitude) of earthquakes that occurred in the pre-instrumental era, whose effects can only be inferred from the analysis of their descriptions in historical documents.

This is the case of the 1783 Calabrian seismic sequence, the subject of this work, for which macroseismic intensity is the only available instrument for the quantitative reconstruction of the effects on the localities.

5.3.1 Macroseismic scales

The ideal intensity scale is required to fulfil three fundamental functions: firstly, to measure the intensity of different earthquakes at the same locality; secondly, to measure the intensity of the same earthquake at different localities; and thirdly, to chart the variation in intensity across the entire macroseismic area. The assignment of a degree is achieved through a comprehensive comparison of the available observations with the diagnostic features that characterise each degree on the adopted scale. From this standpoint, buildings can be regarded as effective

seismic sensors. The degree of damage they incur, in relation to their construction characteristics, provides a reliable indicator of the intensity of the shaking.
Although numerous macroseismic scales have been proposed over the years, the most widely used internationally are the Mercalli-Cancani-Sieberg (MCS) scale [Sieberg, 1930], the Modified Mercalli Intensity (MMI) [Wood and Neumann, 1931], the Medvedev–Sponheuer–Karnik (MSK) scale [Medvedev et al., 1965] and the European Macroseismic Scale (EMS-98) [Grünthal, 1998]. The MMI is predominantly utilised in North America and shares the twelve-degree structure with the MCS. The MSK, which was utilised in Europe from the 1960s until the 1990s, constituted a substantial advancement by introducing, for the first time, a formalisation of building types through three classes of vulnerability and five levels of damage. It is also pertinent to mention the Environmental Seismic Intensity Scale (ESI 2007) [Guerrieri and Vittori, 2007], which differs from traditional scales as it is based exclusively on effects induced on the physical environment, such as surface faulting, liquefaction, landslides and hydrological changes. In recent years, efforts have also been directed towards the development of an International Macroseismic Scale (IMS), aimed at harmonising existing macroseismic practices and providing a more globally applicable framework for intensity assessment [Wald et al., 2024].
In this study, macroseismic intensity is assessed using the MCS and EMS-98 scales.
The Mercalli–Cancani–Sieberg (MCS) scale was introduced in 1930 as the outcome of Sieberg's synthesis of his own 1912 scale with the earlier formulations proposed by Mercalli and Cancani. The scale is divided into twelve degrees of increasing intensity, ranging from I (imperceptible, detectable only by instruments) to XII (highly catastrophic, with complete disruption of the landscape). The scale is organised into three functional bands: degree I describes events recorded exclusively by instruments; degrees II–V describe transient effects on people and household objects; and degrees VI–XII describe permanent effects on buildings and the natural environment, ranging from slight damage (VI) to total collapse of the building stock (XI–XII). In the process of assigning intensities, the effects on buildings – particularly on ordinary dwellings, which represent the most prevalent structures – assume a pivotal role. Conversely, environmental effects (including landslides, ground ruptures, surface faulting, liquefaction, and alterations in surface and groundwater) are typically poorly indicative for three primary reasons: they are profoundly influenced by local factors; they tend to manifest significantly only in earthquakes of relatively substantial magnitude; and they less frequently impact inhabited centres, which are the locations where intensity is typically assessed.

Conversely, such effects can assist in approximating the magnitude of an earthquake occurring within a sparsely populated epicentral region. The MCS scale remains the reference scale of Italian historical seismology, is adopted in the main national macroseismic catalogues, and is currently used by the National Civil Protection Department for rapid damage surveys in the Molin [2008] version. The scale's widespread use in historical seismology is facilitated by the fact that the diagnostic descriptors of its degrees correspond closely to the building stock and material culture of past centuries.

Based on the MSK scale, and in response to the needs of a seismological community increasingly attentive to the diversity of the modern building stock, the European Seismological Commission launched in 1990 a comprehensive revision process that led, in 1998, to the approval of the European Macroseismic Scale EMS-98 [Grünthal, 1998]. The main motivations for this revision were to include building typologies designed according to seismic-resistant criteria, to improve the description of intensity degrees, to provide a tool that could be applied jointly by seismologists and civil engineers, and to ensure full compatibility with the study of historical earthquakes. EMS-98 classifies buildings into six vulnerability classes (A–F, from most to least vulnerable) and uses five damage grades (D1–D5), together with qualitative criteria for estimating the distribution of damage. Today it is used worldwide for both historical and recent earthquakes [among others: Tertulliani et al., 2018; Buforn & Udías, 2022; Triantafyllou et al., 2022], and its guidelines have been translated into numerous languages; in Italy, the first systematic applications date back to the 2009 L'Aquila earthquake [Tertulliani et al., 2011].

In this study, both the MCS and EMS-98 scales are utilised in parallel, a practice that has become common in recent years for all studies reviewing the Italian seismic catalogue [e.g., Tertulliani et al., 2025; Galadini and Tertulliani, 2025; Antonucci et al., 2026].

The MCS was developed during a period when the building stock was predominantly homogeneous, characterised by masonry structures with broadly comparable seismic resistance. This implied an implicit treatment of buildings as sensors, calibrated in a similar manner. The gradual typological and structural diversification of the Italian building stock has rendered this assumption obsolete [Dolce, 2019]: in the presence of an increasing proportion of less vulnerable structures, MCS-based estimates tend to be systematically lower than those obtained with EMS-98, with discrepancies that may exceed one full intensity degree in areas where buildings fall into vulnerability class C or higher (generally reinforced concrete buildings).

However, for the 1783 Calabrian sequence, this limitation is overcome, as the 18th-century building stock consists almost entirely of masonry constructions, often built with earthen materials and lacking any seismic design criteria (Fig. 22). According to the EMS-98, these can be assimilated to vulnerability classes A and, to a lesser extent, B.

Figure 22. *Earthen construction typologies representative of the 18th-century building stock.*

In this context, the two scales tend to yield convergent estimates. The motivation behind their joint utilisation is attributable to the complementarity of their respective strengths. The MCS ensures continuity with the Italian seismological tradition and with existing historical earthquakes catalogues, thereby enabling direct comparison of the new results with previous evaluations for the 1783 sequence. Conversely, the EMS-98 provides a more modern and internationally shared methodological framework. As demonstrated by Del Mese et al. [2023], it has proven to be fully suitable for the study of historical earthquakes and for the analysis of highly vulnerable building stocks.

The assignment of macroseismic intensity from historical sources necessarily requires the translation of qualitative information into data suitable for defining a coherent macroseismic scenario. The descriptions of effects available are quite diversified, depending on the type and style of the documents and on their purpose, whether bureaucratic-administrative texts or journalistic and popular accounts.

A significant part of the documentation concerning the 1783 sequence offers comprehensive and systematic reports, providing detailed descriptions of building damage, the state of localities, and the repercussions for the inhabitants. These characteristics enable a relatively direct comparison with the diagnostics of macroseismic scales. However, a non-negligible number of sources describes the state of a locality using only a single adjective (for example, "*inabitabile*" – uninhabitable, or "*distrutto*" – destroyed) or short phrases (such as "*parte distrutto*" – partly destroyed, or "*parte inabitabile*" – partly uninhabitable).

In cases where the information relating to a given locality is reduced to a single term or concise formula, an attempt was made to identify a correspondence with the diagnostics of the macroseismic scale, following an approach that had been tested in previous studies [i.e. Monachesi et al., 2016].

In order to ensure consistency between the historical terminology and the scale descriptors, a "lexical scale" was developed, in which each level delineates a range of possible intensities. Given the inevitable uncertainty inherent in this type of information, the resulting intensity ranges partially overlap. In accordance with the classification delineated in Table 6, and considering any additional elements (e.g. the number of casualties) where applicable, an intensity value was subsequently assigned to each locality.

Lexical expressions	Intensity Range
intieramente spianati; ne fu compiuta la devastazione; tutte le fabbriche furono rovesciate; adeguato al suolo entirely levelled; its devastation was completed; all the buildings were overturned; levelled to the ground	I ≥10
quasi tutto/ in gran parte/ buona parte, distrutto; sommamente malmenata; distrutto nella maggior parte, il resto inabitabile almost entirely / for the most part / largely destroyed; most severely damaged; destroyed for the most part, the remainder uninhabitable	I 9, 9-10
parte distrutto, parte inabitabile; in parte spiantati, ed in parte sconquassati da non potersi abitare; parte distrutta, parte lesionata; in parte caddero, ed in parte furono fracassate; in porzione sommamente lesi, e in altra porzione distrutti partly destroyed, partly uninhabitable; partly levelled, and partly shattered so as to be uninhabitable; partly destroyed, partly cracked; partly collapsed, and partly were smashed; partly severely cracked, and partly destroyed	I 8-9
non poco malmenata; poche case rovinate, le altre lesionate; inabitabile; molto lesionato considerably damaged; a few ruined houses, the others cracked; uninhabitable; severely cracked	I 8, 7-8
lesionati; percossi cracked; battered	I 7, 6-7
furono inquietati; nulla si presentò agli effetti del tremoto; vi scuotono tuttocché più debolmente were disturbed; no earthquake effects were observed; shaken, though more weakly	I ≤ 6-7

Table 6. *Correspondence between lexical expressions, their translations and the intensity ranges in the present work.*

In some cases, the sources do not provide all the elements necessary to reconstruct the macroseismic scenario. Consequently, the information is insufficient and generalised to the extent that it is not possible to assign a number. Therefore, an indication that encompasses the associated uncertainties was adopted. In light of the aforementioned considerations, the following were occasionally adopted, in accordance with the DBMI15 guidelines [Locati et al., 2022]: NC (Not Classified), SF (Slightly Felt), F (Felt), SD (Slight Damage), and D (Damage). Finally, for a limited number of localities, the available information allows the estimation of the intensity of effects but not their association with a specific earthquake of the sequence. In these cases, an intensity value was assigned without attribution to a specific event.

5.3.2 Cumulative Intensity Issue

One particularly relevant aspect in the analysis of seismic sequences, especially historical ones, concerns the concept of cumulative intensity. When several strong earthquakes occur in rapid succession within a limited geographical area, the effects observed in the affected territory can hardly be attributed to a single event, but rather reflect the progressive and accumulated damage produced by the entire sequence of events. In such cases, the intensity value assigned to a locality necessarily comprises multiple contributions, and is therefore referred to as cumulative intensity [Rossi et al., 2019; Graziani et al., 2022].

From a structural point of view, this phenomenon is related to the progressive degradation of building resistance: theorically, a construction already damaged by a first event is more vulnerable to subsequent shocks and will experience a higher damage level than it would have suffered in an undamaged state [Penna et al., 2014; Grimaz and Malisan, 2017]. As a consequence, the cumulative intensity observed at the end of the sequence tends to systematically overestimate the intensity that could be associated with each individual event if considered in isolation, with likely consequences for the source parameters derived from macroseismic data [Albini and Pantosti, 2004; Stucchi and Rovida, 2008; Graziani et al., 2019]. This distortion becomes more pronounced as the number of strong events increases, as they occur closer in time, and as the building stock affected is more homogeneous and more vulnerable. Macroseismic scales do not provide specific methodological guidelines to separate the damage contributions from successive earthquakes within a sequence, since it is not possible to reliably estimate changes in building vulnerability or the progression of damage during individual events [Graziani et al., 2019; Rossi et al., 2019; Tertulliani et al., 2018]. Consequently, the intensity assigned by an observer who arrived at the site after several earthquakes is necessarily based on cumulative effects. This implies that the intensity in a locality already affected by damage cannot decrease over the course of the sequence, except in cases where a subsequent event is only felt by the population without producing further damage to the building stock.

In the case of recent sequences, timely detailed field surveys may make it possible to identify localities affected by cumulative effects. A prominent recent example is the 2016–2017 Central Italy sequence: in the areas struck by the 24 August, 26 October, and 30 October 2016 earthquakes, the progressive damage to the building stock made it impossible, for many localities, to distinguish the contribution of each event to the final pattern of destruction [Rossi et al., 2019] (Fig. 23).

Figure 23. *Example of the effects of damage progression in a class B building in Castelsantangelo sul Nera: left) August 24; center) October 26; right) October 30 [from Rossi et al., 2019].*

With this in mind it is obvious that, in historical sequences, the possibility of tracking the evolution of damage over time is strongly limited by the availability of sources that describe in detail the chronology of individual events.

With regard to the 1783 seismic sequence, many sources describe the state of the affected area almost exclusively at the end of the sequence, making it difficult to disaggregate the effects of individual earthquakes (see section 5.2). As a result, the intensity assigned to localities affected by multiple events inevitably reflects a cumulated effect. The uncritical use of such values in standard parametrisation methods – which are designed for single events – may therefore introduce systematic bias in the estimates of epicentral location and macroseismic magnitude.

From a macroseismic perspective, it is not possible to establish a simple, general rule for assessing the extent to which the seismic response of a building is influenced by pre-existing damage. However, it is reasonable to assume that once a structure has suffered moderate to severe structural damage, starting from at least damage grade 3 of the EMS-98 scale [Grünthal, 1998], its vulnerability increases significantly. Under these conditions, the building may perform very poorly, such that a relatively weak aftershock can produce a disproportionate amount of damage compared with the energy released [Grünthal, 1998].

In this study, intensity 7 EMS-98 was chosen as the threshold above which the spreading of structural damage is expected to affect a substantial portion of the building stock, resulting in a permanent weakening of structures. At the lower intensity level (6 EMS-98), damage grade 3 is not expected for any vulnerability class, whereas at the higher level (8 EMS-98), all

vulnerability classes – with the exception of those including earthquake-resistant constructions – are subject to structural damage. The adoption of this threshold is also consistent with the historical context considered, since the building stock affected by the 1783 sequence pre-dates any seismic code.
For the MCS scale, an equivalent threshold criterion was adopted by taking degree 7 as reference, which corresponds to moderate damage in numerous well-built structures. From this standpoint, if in a given locality the threshold of 7 EMS-98 (or 7 MCS) was exceeded at an early stage of the sequence, it is plausible that the damage produced by a subsequent event is conditioned by a cumulative effect.

5.4 Earthquake Parameterisation

The parameterisation of an earthquake in the macroseismic field involves the translation of the spatial distribution of seismic effects, as documented by MDPs, into physical and geometric parameters of the seismic source. The parameters include epicentral location, estimation of equivalent magnitude, as well as the dimensions and orientation of the fault. The aim is to derive a quantitative seismological framework, starting from qualitative data (macroseismic intensity). This is a pivotal step, especially in the study of historical earthquakes.
The macroseismic parameterisation is of particular importance when analysing seismotectonic characteristics in regions such as Italy, where the abundance of historical earthquake records extends the observational time window well beyond the instrumental period, which covers only the last few decades. Although empirically determined and sometimes associated with a different physical meaning – particularly with regard to event location – source parameters obtained from macroseismic data are generally recognised as valid substitutes for instrumental ones when the latter are unavailable. The similarity between macroseismic and instrumental source parameters for Italian earthquakes has been extensively documented in the literature [i.e., Cecic et al., 1996; Gasperini et al., 2010; Bakun et al., 2011; Gómez Capera et al., 2015; Vannucci et al., 2019].
Over the years, several algorithmic strategies have been proposed to estimate macroseismic parameters. For instance, the methods by Bakun and Wentworth [1997], MEEP [Musson and Jiménez, 2008], Sirovich and Pettenati [2004], Provost and Scotti [2020], and Sbarra et al. [2019, 2023].
Despite the validity of these methods, the BOXER algorithm [Gasperini et al., 1999; 2010] was selected for the purposes of this thesis because it is the methodological standard of reference

within the Italian seismological community and is adopted for the parametrisation of earthquakes in the CPTI15 [Rovida et al., 2022].

The development of this model is based on the assumption of a direct physical connection between the geometry of the seismogenic source at depth (exemplified by a rectangular box) and the macroseismic field observed at the surface.

The BOXER code enables the epicentral coordinates, equivalent magnitude, and a simplified geometric representation of the source in the form of a "box" from the spatial distribution of the MDPs.

Within the BOXER code, two main computational procedures are implemented, reflecting different theoretical and operational choices about the relationship between the intensity field and the seismic source. The first one, designated Method 0, is based on the barycentre of the area of maximum macroseismic effects. The second approach is implemented in six variants (Methods 1–6) and is based on the intensity attenuation relationship calibrated for the Italian territory as proposed by Pasolini et al. [2008].

In this study, Method 0 was used to maintain consistency with the CPTI15, while Method 1 was employed as a complementary approach to explore potentially more adequate alternative solutions for seismic sequence, as suggested by Vannucci [2025].

In the Method 0, BOXER selects the MDPs with maximum observed intensity $I_{\max}$ and computes their barycenter using a 25% trimmed average of their coordinates (the average of all values included in the interval between the first and third interquartiles of the coordinates of all selected localities). In this way, the influence of outliers, georeferencing errors, or isolated localities is reduced, yielding robust epicentral estimates even in the presence of sub-optimal intensity fields, provided that the epicentral area is reasonably well documented.

If the number of MDPs with $I_{\max}$ is less than 3, the dataset is progressively extended to include data from the lower intensity classes up to $I_{\max} - 1$. For uncertain intensities classes (i.e. 7-8 MCS), the value of the lower intensity class (e.g. 7 MCS) is assigned.

The macroseismic magnitude is computed by combining the epicentral intensity and the isoseismal areas, following the scheme proposed by Galanopoulos (1961) and implemented by Sibol et al. (1987). In particular, the epicentral intensity I_0 is assumed to be equal to $I_{\max}$ if the data with $I_{\max}$ values are more than three and to $I_{\max} - 1$ if less than three values.

The areas of circular isoseismals are computed considering the average distance between the estimated macroseismic epicentre and each locality within an intensity class as their radius.

Macroseismic magnitude (M) is computed as the weighted average of the values independently obtained from each intensity class through the equation:

$$M_I = a + bI_0^2 + c\log_2 A_I$$

where M is the magnitude associated with intensity level I, I_0 is the epicentral intensity calculated for the earthquake and *a*, *b* and *c* are the empirical coefficients estimated through the regression step for each isoseismal intensity.

Instead, Method 1 is based on the intensity attenuation relationship derived by Pasolini et al. [2008] for the Italian territory:

$$I_i = I_E - aD_i^h - b\ln(D_i) - \ln(h)$$

where I_i is the intensity at the i-th site, I_E is the expected intensity at the macroseismic epicentre, *a* and *b* are empirical attenuation coefficients, *h* is the hypocentral depth, and D_i is equal to $\sqrt{(R_i^2 + h^2)}$ is the hypocentral distance of the i-th site.

For Method 1, the localisation problem is formulated in terms of searching for the parameters latE, lonE, h, I_E , a, b that minimise the sum of squared residuals between observed and predicted intensities. The problem is addressed with a probabilistic approach through Maximum Likelihood Estimation (MLE), using the algorithm implemented in the Fortran subroutine BCONF/BCONFD [IMSL, 1991].

In Method 1, the parameters h, I_E, *b* and *a* are constrained to external estimates as in Pasolini et al. [2008], and the algorithm estimates only the epicentral coordinates latE and lonE.

The equivalent magnitude is calculated following the approach of Bakun and Wentworth [1997], through a relationship that allows estimating a magnitude M_j for each MDP in the dataset, obtained from the combination of the attenuation relationship of Pasolini et al.[2008] and the empirical relationship between epicentral intensity and moment magnitude of Fuller [1987].

In both methods adopted, the fault source dimensions are estimated using the log-linear empirical relationships of Wells and Coppersmith [1994], which allow the calculation of subsurface fault rupture length (RLD) and down-dip rupture width (RW) from the moment magnitude:

$$\log_{10}\text{RLD} = 0.59(\pm0.02)M - 2.44(\pm0.11)$$

$$\log_{10}\text{RW} = 0.32(\pm0.02)M - 1.01(\pm0.10)$$

where the coefficients used are those derived by Wells and Coppersmith [1994] as an average of all possible faulting styles, as adopted by Gasperini et al., [1999].

For the estimation of fault orientation (strike), it is assumed that the strike direction is approximated by the azimuths of MDPs with probability increasing with their epicentral distance. The strike direction is thus estimated by performing a weighted axial mean of the azimuths of those sites with intensity above a certain threshold I_{min}. The weights are defined as the ratio between the site's epicentral distance and the epicentral distance predicted by an empirical cubic attenuation relationship [Berardi et al., 1993]. The threshold I_{min} is determined so that the selected sites have a mean epicentral distance as close as possible to the fault length RLD. It is worth noting that while the mathematical procedure is identical for both methods, the azimuths are computed relative to their respective epicenters (the barycenter for Method 0 and the MLE epicenter for Method 1). Empirically, the orientations calculated starting from the Method 0 epicenter yield significantly more reliable results compared to instrumental fault strikes.

In BOXER the source is graphically represented as a rectangle (box) centred on the macroseismic epicentre, with the major dimension equal to RLD parallel to the orientation direction, and the minor dimension corresponding to the surface projection of RW for a fault with a dip angle of 45°. If it is not possible to calculate the fault orientation, a circle centred on the epicentre with a diameter equal to RLD is drawn instead.

In addition to the solutions obtained with the BOXER methods, the CIS (Cumulative Intensity Subtraction) procedure, introduced by Graziani et al. [2022], was also applied. This approach has already been tested on the major seismic sequence of 1703 in central Italy, and requires the exclusion of those localities likely to have been affected by cumulative damage effects from the parameterisation.

6. Results

The study carried out in this thesis enabled the reconstruction of the intensity fields of the five main earthquakes of the 1783 Calabrian seismic sequence according to the EMS-98 and MCS scales, through a critical re-examination of the chronology of the events and of the progression of the effects observed in the different localities.

The documentary research identified a total of 562 localities affected by the seismic sequence as a whole (Appendix A) and significantly increased the number of macroseismic observations available for the five main earthquakes compared with those reported in CFTI4Med [Guidoboni et al., 2007], the current reference for the CPTI15 catalogue (Table 7). Following the chronological reordering of the events, it was not possible to confidently associate the effects with the main earthquakes of the sequence for eight localities (Appendix B, Table 6).

Earthquakes	MDPs [CFTI4med]	MDPs [This study]
5 February 1783	356	438
6 February 1783	8	67
7 February 1783	191	327
1 March 1783	18	22
28 March 1783	323	339
Uncertain date	-	8

Table 7. *Summary of the data of the five main events of the 1783 sequence obtained in this work compared with those reported in CFTI4Med [Guidoboni et al., 2007].*

Of the identified localities, 13 represent (Appendix B; Table 7) new observations of damage or shaking at sites not included in the current macroseismic database [Guidoboni et al., 2007].

One of the most methodologically challenging aspects of the revision concerned the attribution of damage to individual earthquakes. In most cases, historical sources describe overall damage scenarios that are likely to reflect the combined effects of successive events rather than the effects produced by a single earthquake. Consequently, assigning each locality to one of the five main earthquakes was a crucial step for the subsequent intensity assessment.

For the 5 February earthquake, a direct correlation between the seismic event and the observed effects could be established. The evaluation of the subsequent events, however, proved more complex, as it required cumulative damage to be taken into account. In localities already affected by a previous earthquake, the effects of later events are rarely distinguishable from the pre-existing damage pattern; the most reliable approach is therefore to consider the overall worsening of damage.

For this reason, in the present study the intensities assigned to the earthquakes following that of 5 February were evaluated in light of the cumulative effects produced by the sequence up to that point. As a consequence of this approach, intensity cannot decrease during the sequence in localities that had already sustained damage, except in cases where a subsequent event was only felt and did not produce any additional effects on the building stock.

A significant example of the approach adopted is provided by the case of Laureana di Borrello (RC). In the reference study, Guidoboni et al. [2007] assign to this locality an intensity of 9–10 MCS for the earthquake of 5 February and 8–9 MCS for that of 7 February, without taking into account the shock of 6 February. However, an intensity of 9–10 MCS implies a near-total destruction of the building stock, making any subsequent worsening of damage difficult to assess. This attribution appears inconsistent with the historical evidence.

In particular, the Gazzetta Universale of 11 March 1783 reports that Laureana was *"nella notte de' 7. [fu] diroccata in buona parte, e nel venerdì rovinata quasi tutta con morte di molti" ("in the night of the 7th [it was] largely ruined, and on Friday almost completely destroyed with the death of many")*, thus distinguishing two successive stages in the worsening of damage, referable respectively to the night between 6 and 7 February and to the day of 7 February. Sarconi [1784] also explicitly links Laureana to destructive effects already produced by the earthquake of 5 February, noting that "*in questo aggregato di valli, di stagni, e di picciole colline nel dì 5 di Febbrajo si produsse sotto l'impeto del tremoto un generale rivolgimento" ("in this cluster of valleys, ponds, and small hills, a general upheaval occurred under the impact of the earthquake on the 5 of February")*. In turn, De Dolomieu [1785], referring to the event of 7 February, states that it *"terminò di rovesciare Laureana, Galatro, Arena e altri paesi convicini" ("finished destroying Laureana, Galatro, Arena, and other neighbouring villages")*, clearly indicating that the damage observed on 7 February represented the completion of a destructive process already initiated by the preceding events. Finally, Vivenzio [1788] describes Laureana as *"parte distrutto e parte inabitabile"("partly destroyed and partly uninhabitable")*, thus conveying an overall picture consistent with the cumulative outcome of the sequence.

In light of these testimonies, it therefore appears more consistent to interpret the damage at Laureana di Borrello as the result of a destructive progression developed over the course of several closely spaced events. For this reason, in the present study Laureana di Borrello was assigned an intensity of 8-9 EMS-98 (8-9 MCS) for 5 February, 8-9 EMS-98 (8-9 MCS) for 6

February, and 9 EMS-98 (9 MCS) for 7 February, with the latter two intensities to be regarded as cumulative.

This approach was consistently applied to all affected localities, with the aim of providing intensity assessments that reflect the progressive and cumulative nature of the effects documented in the historical sources.

Furthermore, in particular cases, such as evidence referring to single buildings, very small localities, or contexts documented in an extremely generic manner, it was preferred not to force the assignment of a conventional intensity degree, but instead to use a descriptive code, in accordance with the DBMI15 [Locati et al., 2022]. In some cases, very small localities located close to larger centres were merged with the latter when the available information did not allow a sufficiently robust independent assessment. In other cases, where the descriptions were too ambiguous or did not allow a reliable relationship between event and effects to be established, the code NC (Not Classifiable) was assigned.

The results of the five earthquakes are described in detail below.

5.1 The 5 February 1783 Earthquake

The earthquake of 5 February 1783 is the best documented event of the entire Calabrian seismic sequence, as nearly all available historical sources refer to it. The critical review of these sources enabled the definition of a dataset of 438 macroseismic observations (Appendix B; Table 1). The resulting intensity distribution is shown in Figure 24 for both EMS-98 and MCS scales.

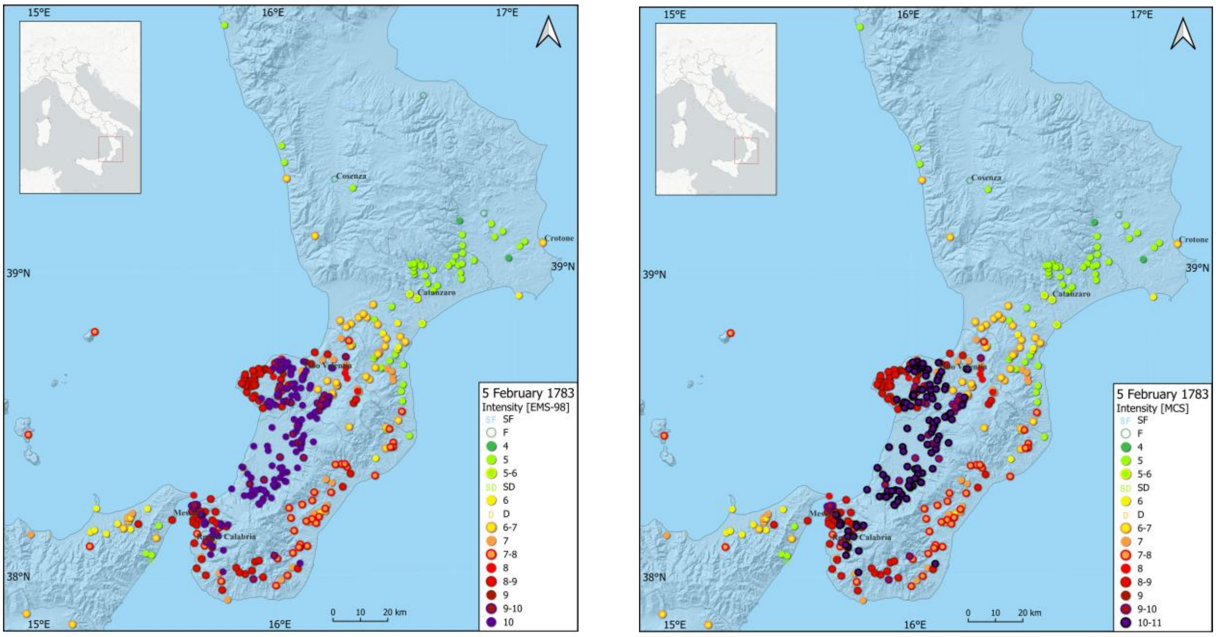

Figure 24. *Macroseismic intensity distributions for 5 February 1783 earthquake in the EMS-98 scales (on the left) and in the MCS (on the right).*

In comparison with the 356 observations reported in Guidoboni et al. [2007], the dataset reconstructed in this study includes 82 additional localities. This expansion was made possible by the critical review of the sources, particularly the accounts by Grimaldi [1784], Sarconi [1784] and Vivenzio [1788], from which damage information attributable to the 5 February earthquake was recovered for these sites. In many cases, however, this information is reported together with that relating to the 7 February event.

Among the newly identified localities, several are located in the provinces of Vibo Valentia and Reggio Calabria and are assigned macroseismic intensities higher than 6 EMS-98 (6 MCS), thereby improving the characterization of effects in the epicentral area. The remaining sites, characterised by lower intensities, are concentrated mainly in the provinces of Catanzaro and Crotone and allow a more detailed reconstruction of the earthquake effects in the far field.

Overall, the maximum intensity reached is 10 EMS-98 (10-11 MCS), assigned to 114 localities. This cluster is distributed mainly in the western sector of the Aspromonte and in the Mesima Valley, near Vibo Valentia, with a further concentration of high-intensity sites in the Reggio Calabria area and along the Strait of Messina. A belt of intensities ranging between 7-8 to 9 EMS-98 (7-8 to 9 MCS), associated with 150 localities, also extends along the Ionian side, in the Mesima Valley, and near the Strait of Messina. Lower values, up to 6-7 EMS-98 (6-7 MCS) are instead recorded in the Catanzaro area, in the sector between Crotone and Catanzaro, and along the north-eastern margin of Sicily, involving 138 localities.

The macroseismic epicentre and magnitude were estimated on the basis of this new dataset using BOXER code, with both the EMS-98 and MCS intensity dataset, and applying calculation methods 0 (Bx0) and 1 (Bx1). The results are shown in Figure 25 and Table 8.

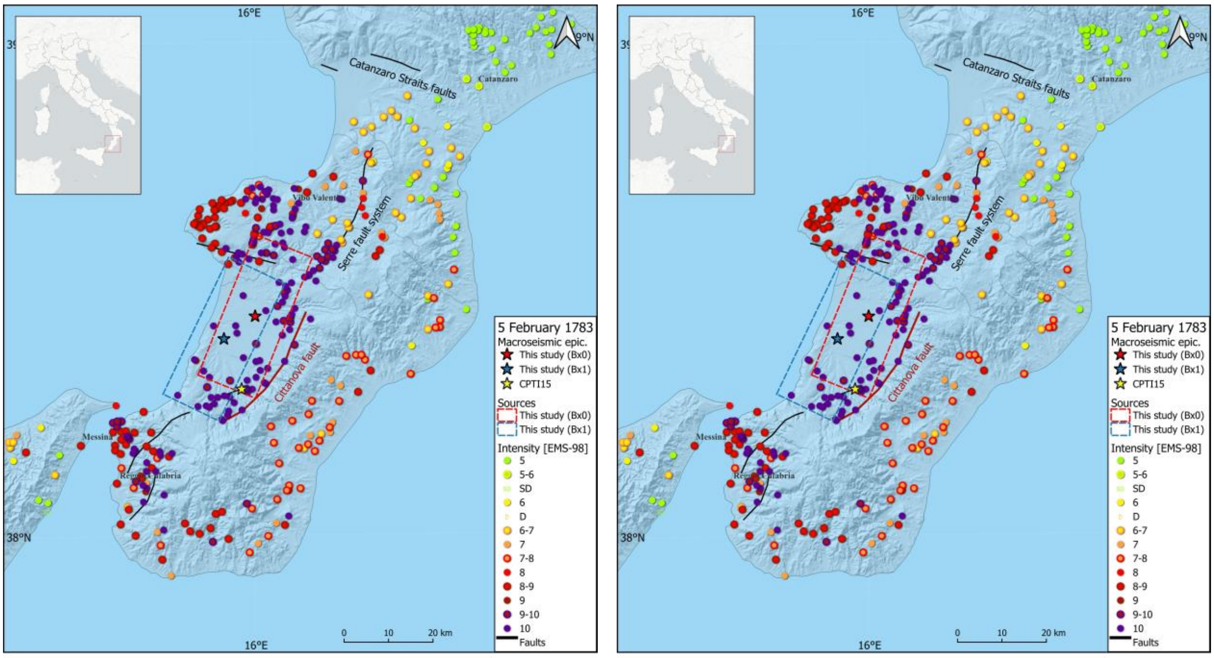

***Figure 25**. Macroseismic intensity distributions for 5 February 1783 earthquake in the EMS-98 scales (on the left) and in the MCS (on the right), with the macroseismic epicentres estimated in this study and the corresponding seismogenic boxes. The red and blue stars indicate the epicentres estimated in this study using Bx0 and Bx1, respectively, whereas the yellow star indicates the epicentre reported in CPTI15.*

Ref.	Lat	Lon	M_w	I_o	I_{max}
This study (Bx0) [EMS-98]	38.4446	16.0068	6.73±0.03	10	10
This study (Bx0) [MCS]	38.4446	16.0068	6.9±0.03	10-11	10-11
This study (Bx1) [EMS-98]	38.3993	15.9258	6.74±0.03	10	10
This study (Bx1) [MCS]	38.3951	15.9324	6.9±0.03	10	10
CPTI15	38.297	15.970	7.10 ± 0.10	11	11

***Table 8.** Macroseismic parameters estimated with the data in the EMS-98 and MCS scale with different method for the earthquake of 5 February1783.*

Both calculation methods indicate a northward shift of the epicentre relative to the coordinates reported in the catalogue CPTI15. Method 0, which determines the barycentre using only the highest-intensity observations, yields coincident epicentral locations for the two macroseismic scales, with a displacement of about 17 km towards N-NE with respect to CPTI15. In contrast, method 1, which incorporates lower intensities through an iterative optimization procedure based on attenuation laws, locates the epicentre approximately 12 km to the N-NW of the CPTI15 location. The two solutions differ by about 8.5 km, with the estimate Bx1 located SW of the Bx0. This discrepancy reflects the different approaches, as Bx1 accounts for the full macroseismic field and the reduced attenuation observed towards the Strait of Messina. Despite these differences, both methods relocate the epicentre further north than CPTI15.

In contrast, magnitude estimates are only marginally affected by the calculation method. For a given macroseismic scale, the values obtained with Bx0 and Bx1 are in close agreement: using the EMS-98 scale, the difference amounts to only 0.01, with values of 6.73 and 6.74, respectively, whereas with the MCS scale both methods yield a magnitude of 6.9. This indicates that the macroseismic scale, rather than the calculation method, exerts the primary control on magnitude estimates.

Overall, all analyses performed in this study point to a downscaling of the 5 February earthquake parameters relative to those reported in the CPTI15. The catalogue assigns a magnitude of 7.10 and locates the epicentre in the southern Gioia Tauro Plain. The present revision instead yields magnitudes between and 6.73 and 6.90. This revision reflects the critical reassessment of the sources and the reassignment of the highest intensities. The northward relocation of the epicentre also contrasts with the more southerly barycentre proposed in the CPTI15, while the BOXER-derived solutions place it closer to the centre of the overall damage distribution.

The source dimensions, derived from seismogenic boxes whose length and width are computed using empirical scaling relationships implemented in the code (see chapter 5.4), show an orientation consistent with the major axis of the macroseismic field, suggesting a predominantly longitudinal rupture development.

Two main models have been proposed for the source of the 5 February 1783 mainshock. The first associates the event with the Cittanova Fault, an extensional structure dipping towards NW, supported by both historical accounts of coseismic surface faulting [De Dolomieu, 1784], paleoseismological evidence of Holocene activity [Galli and Bosi, 2002] and distribution of coseismic hydrological anomalies [Cucci, 2022]. The second model instead links the event to the Gioia Tauro Fault, interpreted as a low-angle blind structure dipping towards the southeast [Valensise and D'Addezio, 1994], based on geochemical data [Pizzino et al., 2004] and geomorphological evidence related to drainage evolution [Tiberti et al., 2017].

The analytically derived source dimensions obtained in this study support the first model. As shown in Figure 25, the seismogenic boxes derived from both datasets, irrespective of the method used, are elongated parallel to the Cittanova Fault. Moreover, the highest macroseismic intensities fall within the hanging wall of the fault, indicating that this structure likely played a primary role in the 5 February 1783 earthquake. Finally, the estimated source dimensions are consistent with the length of the Cittanova fault system reported in the literature.

5.2 The 6 February 1783 Earthquake

The 6 February 1783 earthquake, the second event in the sequence, is recorded in the CFTI4Med catalogue with a magnitude of 6.3 and a maximum intensity of 8–9 MCS, whereas it is not parametrised in CPTI15, most likely owing to the limited reliability of the available intensity data.

In the present study, a total of 67 macroseismic observations were collected, a number significantly higher than that reported in the current reference study [Guidoboni et al., 2007], which considers only 10 (Appendix B; Table 2). The spatial distribution of macroseismic observations for this earthquake, according to both the EMS-98 and MCS scales, is shown in Figure 26.

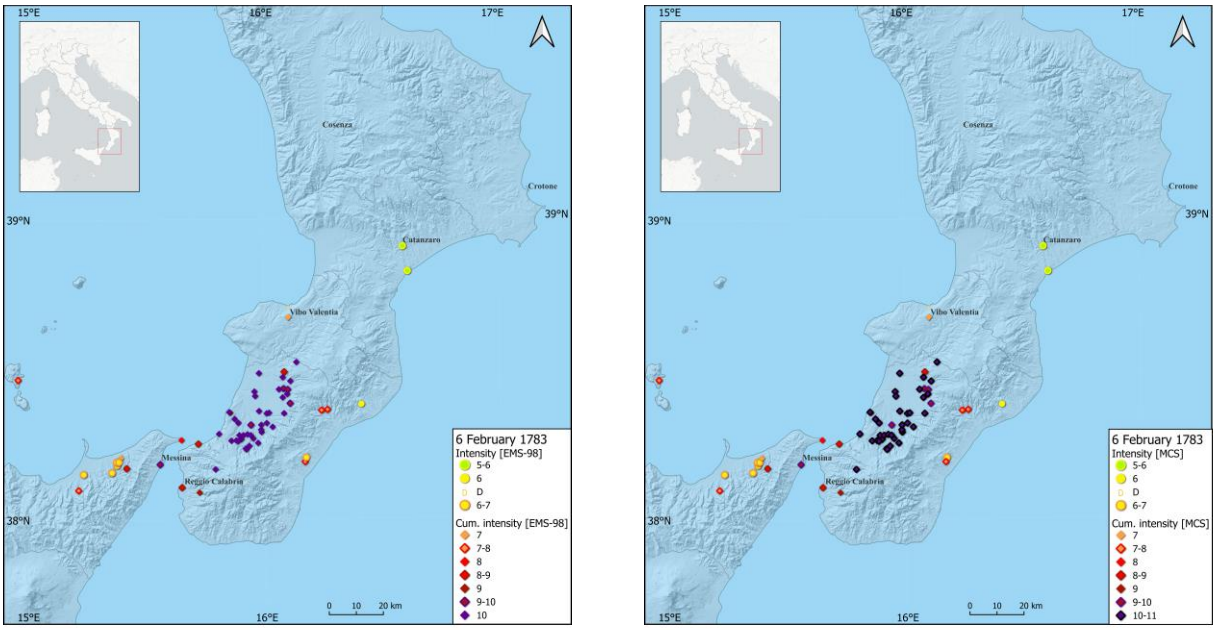

Figure 26. *Macroseismic intensity distributions for 6 February 1783 earthquake in the EMS-98 scales (on the left) and in the MCS (on the right).*

The critical analysis of the sources and their chronological reordering revealed that the available information is insufficient to delineate a clear and consistent picture of the effects of this event. In most accounts, reference is made almost exclusively to the earthquakes of 5 and 7 February, whereas the 6 February event is mentioned only in a limited number of testimonies and, in any case, in association with the 5 February shock. These include, among others, the works by De Leone [1783], Torcia [1783], Hamilton [1783], Mercalli [1897], which provide explicit information on the 6 February event.

Localities for which non-cumulative effects can be attributed to this event are only eleven (represented by circles in Fig. 26), all characterized by intensities lower than 6-7 EMS-98 (6-7 MCS) and in any case also associated with the 5 February earthquake. In the remaining 56 localities (shown as diamonds in Fig. 26), the descriptions report aggravations that do not substantially modify the pre-existing damage scenario and therefore do not lead to an increase in the assigned intensity.

The maximum intensity reached is 10 EMS-98 (10 MCS) and was assigned to 37 localities; in all these cases the values are cumulative, as these settlements had already been heavily damaged by the 5 February earthquake

Overall, the available information, which is fragmentary and incomplete, does not allow a well-defined macroseismic pattern to be outlined for the 6 February 1783 earthquake. The collected data only make it possible to identify a strong aftershock, but with lower energy than the 5 and 7 February shocks, capable of causing slight aggravation of damage in some already affected localities in the province of Reggio Calabria and a perceptible shaking in north-eastern Sicily.

In light of these considerations, the 6 February earthquake was not subjected to an autonomous macroseismic parametrization in the present study. The available intensity dataset was in fact considered insufficient for a robust and independent determination of the epicentral parameters.

5.3 The 7 February 1783 Earthquake

As for the previous events, this study significantly increases the number of macroseismic observations also for the 7 February 1783 earthquake, bringing the total to 327 MDPs, that is, 136 more than in the reference study [Guidoboni et al., 2007] adopted by the CPTI15. This new dataset extends the intensity range both in the far field and in the epicentral area (Appendix B; Table 3).

The distribution of intensities for this earthquake, according to the EMS-98 and MCS scales, is shown in Figure 27.

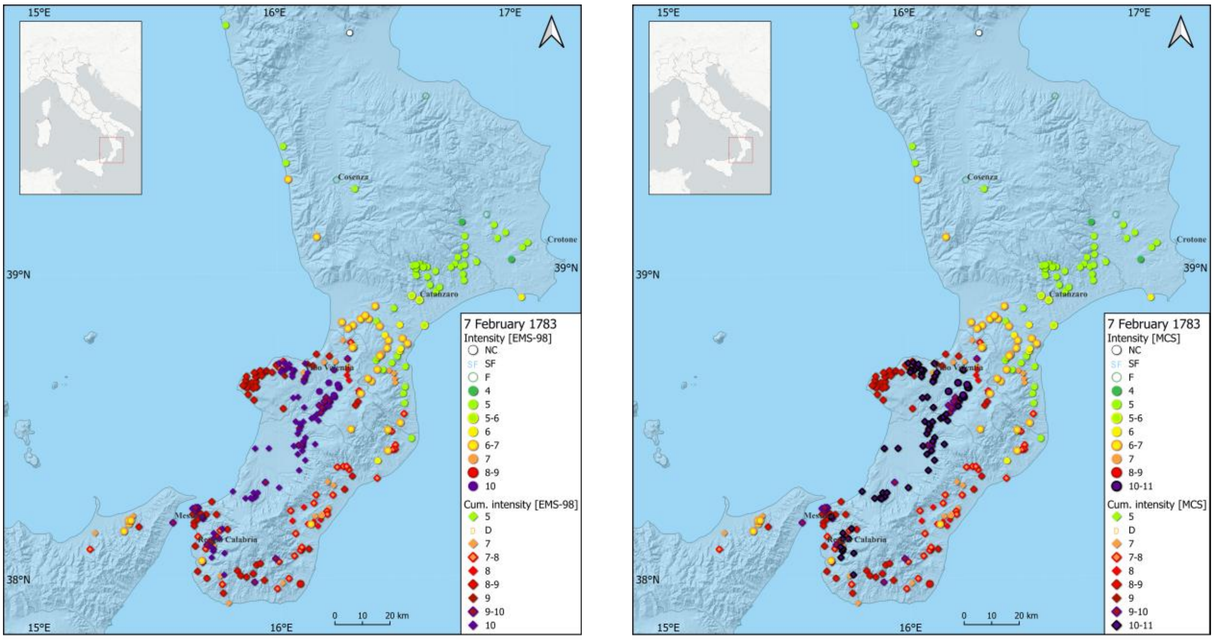

Figure 27. *Macroseismic intensity distributions for 7 February 1783 earthquake in the EMS-98 scales (on the left) and in the MCS (on the right).*

The maximum assigned intensity is 10 EMS-98 (10-11 MCS) and has been attributed to 72 localities, most of which are located in the area already heavily damaged by the 5 February earthquake (see diamonds in Fig. 27).

However, for seven of these localities, all situated in the province of Vibo Valentia (Pizzoni, San Basilio, Santa Barbara, Sant'Angelo, Sorianello, Soriano Calabro and Vazzano), it was possible to distinguish specifically the effects of the 7 February earthquake thanks to the descriptions found in the historical sources.

In particular, Sarconi [1784] notes that the houses of Soriano *"furono rispettate in quel giorno stesso, in cui la massima parte della Calabria Ultra fu nel dì 5 di Febbrajo desolata"("were spared on that very same day, when most of Calabria Ultra was devastated on 5 February"),* and then specifies that *"nel dì 7 di Febbrajo, alle ore 22, Soriano e Sorianello passarono in un punto solo dall'esistenza alla più miserabile, e indistinta annichilazione"("on 7 February, at the 22nd hour, Soriano and Sorianello passed in a single moment from existence to the most miserable and indistinct annihilation").* Consistently, Vivenzio [1788] reports that *"l'orribile scuotimento de' 7 ebbe la sua principal fede in questa contrada"("the horrible shaking of the 7 had its main seat in this district")*, explicitly referring to the State of Soriano (which includes Soriano and the hamlets of Sorianello, Pizzoni, San Basilio, Vazzano, Santa Barbara and Sant'Angelo). Such descriptions clearly indicate that, in these localities, the 5 February shock did not cause damage comparable to that produced by the 7 February earthquake, and therefore allow the effects described in the sources to be attributed non-cumulatively to the latter. Further macroseismic observations attributable to this event amount to 102, all characterised by intensities lower than 7 EMS-98 (7 MCS) and located mainly in the Catanzaro area and surrounding sectors, where they document the shaking produced by the 7 February earthquake in the north-eastern far field.

The overall picture emerging from this analysis shows that the macroseismic field of the 7 February earthquake is strongly affected by the cumulative damage produced by the previous shocks. To address this issue and define the macroseismic parameters, calculations with the BOXER code were carried out using both the standard approach and the CIS approach [Graziani et al., 2022]: the former applies the classical Bx0 and Bx1 methods to the entire dataset, while the latter discards localities strongly damaged by the early earthquakes from the intensity distributions used to compute the macroseismic source parameters. Simulations were performed in parallel using both the EMS-98 and the MCS scales.

The results (Figure 28 and Table 9) show how the macroseismic parameters of the 7 February 1783 earthquake change with the processing method adopted.

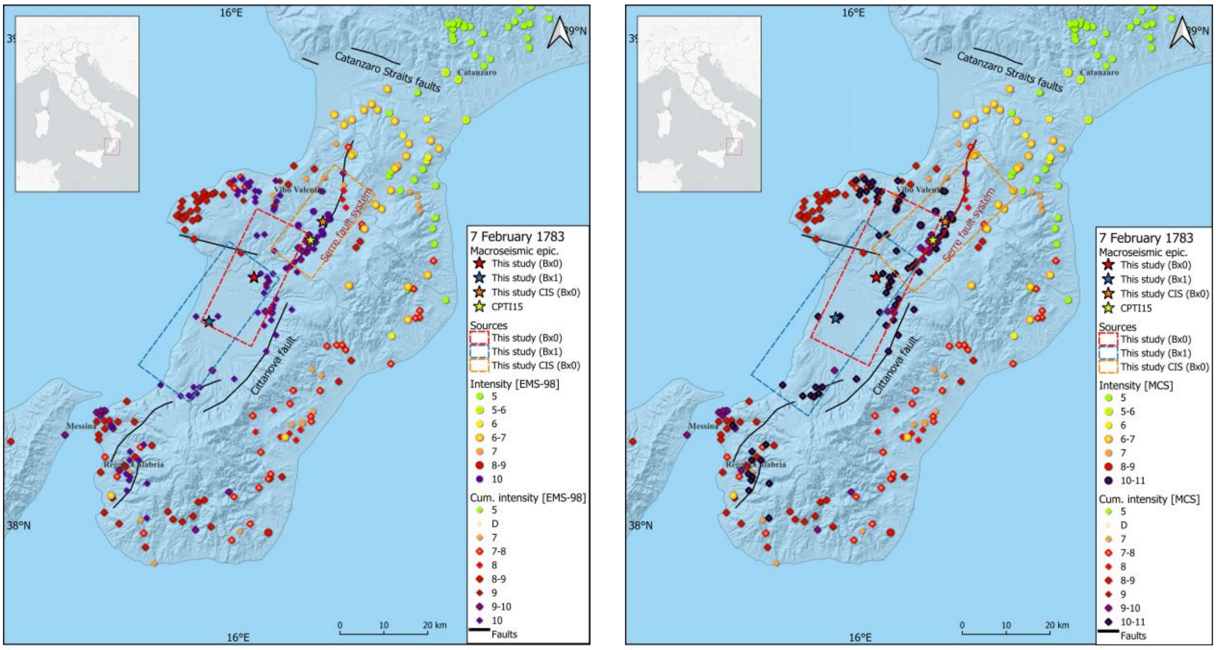

Figure 28. *Macroseismic intensity distributions for 7 February 1783 earthquake in the EMS-98 scales (on the left) and in the MCS (on the right), together with the macroseismic epicentres estimated in this study. The red, blue, and orange stars indicate the epicentres estimated in this study using Bx0, Bx1, and CIS Bx0, respectively, whereas the yellow star indicates the epicentre reported in CPTI15.*

Ref	Lat	Lon	M_w	I_o	I_{max}
This study (Bx0) [EMS-98]	38.5048	16.052	6.61±0.08	10	10
This study (Bx0) [MCS]	38.5048	16.052	6.81±0.08	10-11	10-11
This study (Bx1) [EMS-98]	38.4148	15.9331	6.75±0.04	10	10
This study (Bx1) [MCS]	38.422	15.9461	6.91±0.04	10	10-11
This study (CIS_Bx0) [EMS-98]	38.6174	16.2338	6.48±0.16	10	10
This study (CIS_Bx0) [MCS]	38.6174	16.2338	6.7±0.16	10-11	10-11
CPTI15	38.580	16.201	6.74 ± 0.10	10-11	10-11

Table 9. *Macroseismic parameters estimated with the data in the EMS-98 and MCS scale with different method for the earthquake of 7 February1783.*

With regard to epicentral location, the Bx0 solutions for both the EMS-98 and MCS scales converge on the same coordinates, whereas the Bx1 solutions yield very closely spaced epicentres, placing the event in both cases within the south-western sector already heavily affected by the 5 February shock. In contrast, the CIS approach provides the same epicentral solution for the two scales, relocating the epicentre to the north-east, at a distance of about 12 km from the Bx0 solution and about 24 km from the Bx1 solution.

From an energetic point of view, the magnitude estimates span a relatively wide range depending on the adopted method. The Bx0 method yield higher magnitude values than the CIS solutions, both for EMS-98 and MCS, while the Bx1 method tend to fall at intermediate values. The CIS method, by isolating the effects that can be attributed exclusively to the 7 February shock, provides the lowest magnitude estimates in both scales, highlighting the non-negligible contribution of cumulative sequence intensities to the overestimation of the energetic parameters.

Overall, these results show how strongly the cumulative intensity value affects the computation of macroseismic parameters: approaches that do not explicitly discriminate the effects of the different shocks tend to yield epicentres located within the areas that experienced the highest intensity levels during the sequence and systematically higher magnitudes, whereas the CIS elaboration shows that a rigorous selection of the effects attributable to the 7 February event alone leads to a relocation of the epicentre and to a systematic reduction of the magnitude estimates.

Finally, all analytically reconstructed sources (Bx0, Bx1 and CIS) are oriented approximately NE–SW; in this framework, the CIS source differs not so much in its geometric trend as in its position and in its closer overlap with the Serre Fault. This result fits into the seismotectonic

debate concerning the 7 February event, which reflects the same interpretative dichotomy discussed for the 5 February earthquake. On the basis of geomorphological and paleoseismological evidence, a first group of authors [Tortorici et al., 1995; Jacques et al., 2001; Galli et al., 2007; Monaco & Tortorici, 2007] attributes the event to the activation of the southern segment of the Serre Fault, an extensional structure dipping westward. In sharp contrast, a second line of research proposes the Upper Mesima Basin as the responsible source, interpreted as a blind east-dipping fault in possible tectonic and kinematic continuity with the deeper Gioia Tauro fault system [DISS Working Group, 2025]. Nevertheless, the available geological evidence is limited and the interpretation remains uncertain.
The geographical projection of the seismogenic box calculated by means of the CIS method provides an additional spatial constraint for discussing this seismotectonic controversy. Overall, the distribution of damage and the analytical azimuth derived from it yield solutions that appear more consistent with the seismotectonic model attributing the 7 February 1783 earthquake to the southern segment of the Serre Fault, which thus emerges as the source most compatible with the currently available data.

5.4 The 1 March 1783 Earthquake

The fourth event in the sequence is listed in CFTI4Med with a magnitude of 5.9 and a maximum intensity of 8–10 MCS, whereas CPTI15 does not provide macroseismic parameters.
The resulting macroseismic pattern is essentially analogous to that already described for the 6 February event. The overall dataset includes 22 macroseismic observations, 13 of which are classified as cumulative intensities, since the available sources do not allow the specific effects of this earthquake to be distinguished in a consistent way from those produced by the preceding events, nor to delineate its impact on the affected area independently (Appendix B; Table 4). Compared with CFTI, which lists 18 MDPs for this event, a slight increase in the number of observations is observed; however, this increase is modest and does not substantially modify the overall interpretative picture.
The spatial distribution of the EMS-98 and MCS intensities assigned to this shock is shown in Figure 29.

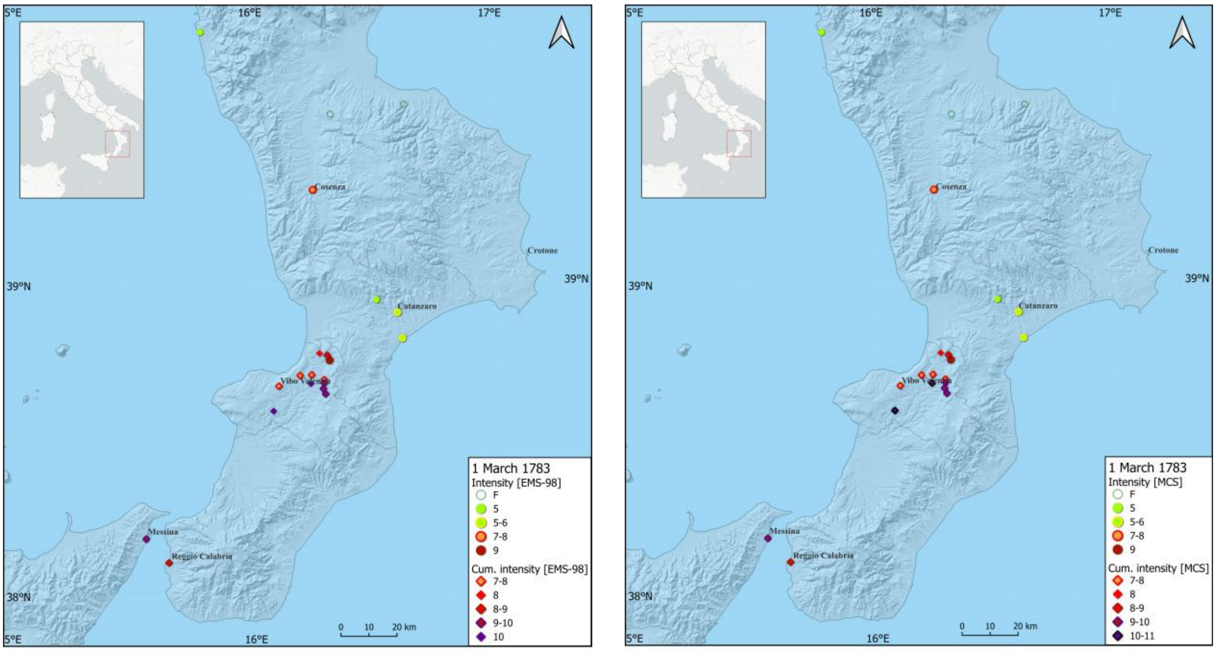

Figure 29. *Macroseismic intensity distributions for 1 March 1783 earthquake in the EMS-98 scales (on the left) and in the MCS (on the right).*

The maximum intensity reached is 10 EMS-98 (10-11 MCS), attributed to the localities of Panaia (VV) and Mileto (VV), both of which had already been significantly affected by the previous earthquakes in the sequence. The only localities for which it has been possible to identify a non-cumulative intensity are Poliolo (VV) and Trecroci (VV) (referred to in the sources also as Polia Antica), for which an intensity of 9 EMS-98 (9 MCS) has been assigned; this therefore represents the highest value that can be discriminated with a reasonable degree of reliability for this event.

Only a few accounts refer explicitly to the 1 March earthquake. Masci [1783], Vivenzio [1788], and later Baratta [1901], document the effects of this event with specific reference to the localities of Monteleone, Poliolo and Castelmonardo.

For example, Vivenzio [1788] reports that "*Il Tremuoto avvenuto alle ore otto, e mezza Italiane nella mattina del primo di Marzo del 1783 cagionò sommo danno in Polia con distruggere gran parte delle abitazioni"("the earthquake that occurred at half past eight, Italian time, on the morning of 1 March 1783 caused immense damage in Polia by destroying a large part of the houses").*

This very limited documentary basis, confined to a small set of settlements, is not sufficient to support a methodologically robust macroseismic parametrisation of the event, which is therefore considered here only within the broader framework of the 1783 sequence.

5.4 The 28 March 1783 Earthquake

The last earthquake of the sequence occurred on 28 March 1783. The macroseismic observations collected in this study for this event amount to 339, compared with the 323 reported in CFTI4Med; this increase is numerically limited with respect to what is observed for the preceding earthquakes (Appendix B; Table 5).

As already noted for the 7 February event, in this case as well the macroseismic field is strongly influenced by the combined effects produced by the previous events: the total cumulative intensity associated with this earthquake is 134. The distribution of intensities according to the EMS-98 and MCS scales is shown in Figure 30.

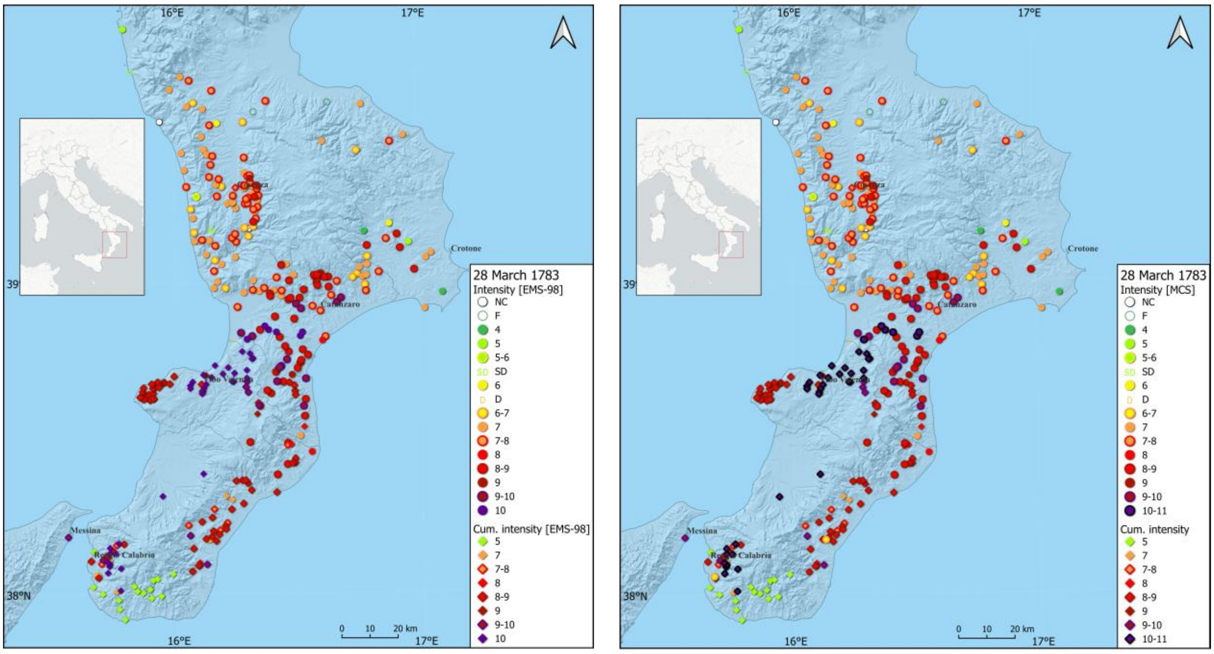

Figure 30. *Macroseismic intensity distributions for 28 March 1783 earthquake in the EMS-98 scales (on the left) and in the MCS (on the right).*

The maximum intensity reached is 10 EMS-98 (10–11 MCS) and has been assigned to 39 localities. Among these, only for six sites – Jacurso, Maida, Borgia, Cortale and San Floro, in the province of Catanzaro, and Montesoro, in the province of Vibo Valentia – was it possible to attribute the damage specifically to the 28 March earthquake, unaffected or only marginally affected (I < 7) by the previous shocks. As evidence of this, Vivenzio [1788] notes for the State of Maida that *"per cagione de' tremuoti accaduti nel mese di febbrajo, e soprattutto per quello de' 28 marzo furono rovesciati quasi tutti gli edifici di questo Stato"("due to the earthquakes that occurred in the month of February, and especially the one on 28 March, almost all the* *buildings of this State were destroyed")*, while Sarconi [1784], for the locality of Borgia, reports that *"fra i diversi paesi rovinati col tremoto de' 28 di marzo, fu interamente rovesciata la terra di Borgia"("among the various towns ruined by the earthquake of 28 March, the town of Borgia was completely destroyed").*

For the remaining localities with an intensity of 10 EMS-98 (10-11 MCS), the values instead reflect a combination of the effects of the 28 March earthquake and of the previous events, which the available sources do not allow to separate reliably.

Overall, compared with the events that preceded this earthquake, the highest intensities show a shift towards the north-east, concentrating mainly between the Isthmus of Catanzaro and the northern Tyrrhenian margin, where intensities of degree 8–9 EMS-98 (8-9 MCS) prevail.

In addition to the accounts by Vivenzio[1788] and Sarconi [1784], the *"Gazzetta Universale"* of 15 April 1783, provides further evidence for attributing the observed effects to this specific event. It documents new information about severe damage and reports that many towns in the surroundings of Cosenza were heavily affected.

The estimation of the macroseismic parameters of the 28 March earthquake follows the same criteria adopted for the 7 February event; the results are shown in Figure 31 and Table 10.

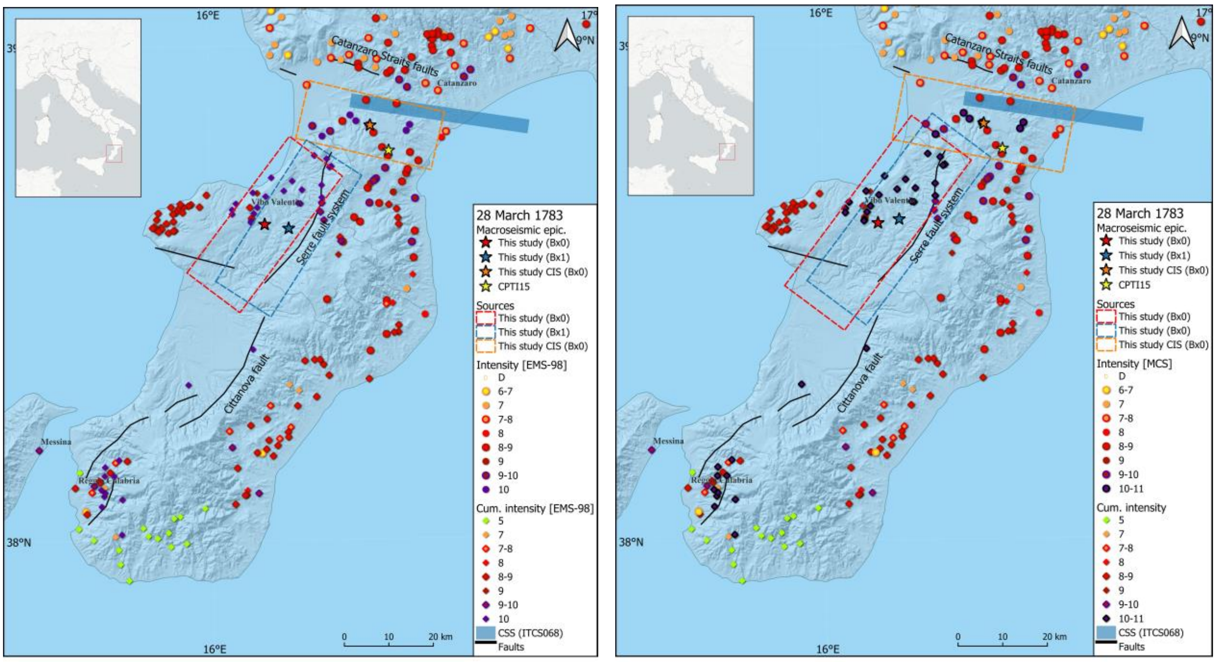

Figure 31. Macroseismic intensity distributions for 28 March 1783 earthquake in the EMS-98 scales (on the left) and in the MCS (on the right), together with the macroseismic epicentres estimated in this study. The red, blue, and orange stars indicate the epicentres estimated in this study using Bx0, Bx1, and CIS Bx0, respectively, whereas the yellow star indicates the epicentre reported in CPTI15.

Ref	Lat	Lon	M_w	I_o	I_{max}
This study (Bx0) [EMS-98]	38.6385	16.141	6.82± 0.03	10	10
This study (Bx0) [MCS]	38.6173	16.1247	6.98± 0.03	10-11	10-11
This study (Bx1) [EMS-98]	38.6346	16.2054	6.81± 0.03	10	10
This study (Bx1) [MCS]	38.6405	16.1934	6.97± 0.03	10-11	10-11
This study (CIS_Bx0) [EMS-98]	38.8365	16.4168	6.67± 0.04	10	10
This study (CIS_Bx0) [MCS]	38.8365	16.4168	6.83± 0.04	10-11	10-11
CPTI15	38.785	16.464	7.03 ± 0.10	11	11

Table 10. *Macroseismic parameters estimated with the data in the EMS-98 and MCS scale with different method for the earthquake of 28 March 1783.*

The standard Bx0 and Bx1 solutions, for both the EMS-98 and MCS scales, yield very closely spaced epicentres and place the event in the south-western sector, clearly overlapping the areas already affected by the previous earthquakes. In contrast, the CIS processing relocates the macroseismic epicentre approximately 10 km to the north-east: the distances from the Bx0/Bx1 solutions obtained in this study range between about 29 and 35 km, while the offset from the epicentre adopted in the CPTI15 catalogue is about 7 km. Overall, these differences indicate that the CIS, after removal of cumulative effects, shifts the spatial barycentre of the macroseismic field significantly with respect to the standard solutions.
As regards the macroseismic magnitude, the use of the full dataset in the standard elaborations leads to a systematic overestimation of the magnitudes. The Bx0 and Bx1 solutions provide moment magnitudes of 6.98 on the MCS scale and 6.82 on the EMS-98 scale, whereas the CIS processing yields lower estimates, with magnitudes of 6.83 on the MCS scale and 6.67 on the EMS-98 scale. The comparison between these values shows that including the cumulative damage from the previous earthquakes results in systematically higher energy estimates, while the CIS approach highlights a significantly lower energy level.
Finally, the analytically reconstructed seismogenic sources for this event display markedly different geometries. The boxes calculated on the full dataset are elongated in a NW–SE direction and are located to the south-west of the Isthmus of Catanzaro, largely overlapping the areas struck by the previous earthquakes. By contrast, the source derived exclusively from non-cumulative data is shifted north-eastwards and is oriented approximately E–W beneath the Catanzaro basin, revealing a position and trend of the seismogenic structure that differ significantly from the other solutions.
For the 28 March earthquake, unlike the preceding events, no unequivocal evidence of coeval surface faulting has been identified, although its origin has been generically placed within the

transtensional and normal fault systems of the Lamezia area [Moretti, 2000; Pirrotta et al., 2021]. The DISS Working Group [2025] further proposes that the composite Caraffa–Squillace Gulf source (shown in blue in Fig. 31) includes the fault segment responsible for the 28 March 1783 earthquake; in this context, the box obtained with the CIS method is consistent with this structure.

7. Discussion and Conclusions

The principal objective of this study was to analyse the seismic sequence that occurred in Calabria between February and March 1783 from a historical seismology perspective, with the innovative purpose of reconstructing its evolution and of improving its knowledge. The complex and systematic process of documentary revision, based on the analysis of archival sources, contemporary periodicals, chronicles and iconographic material, enabled information that had not previously been considered to be integrated, thereby expanding and redefining the macroseismic database of the sequence. The investigation of historical sources was the most substantial and demanding phase of the work, given the extraordinary volume of available documents.

From a methodological point of view, the research was structured around the collection and cataloguing (by typology and year of production) of all the recovered material, followed by its subsequent analysis. This approach enabled the identification of all the affected localities. Subsequently, for each locality, the relevant information and descriptions of the damage extrapolated from the various sources were collected (see Appendix C).

Once identified, the historical localities were georeferenced. This operation was sometimes challenging due to toponymic variations, administrative mergers, and the abandonment or relocation of numerous settlements following the earthquakes. The information collected for each locality was then compiled into a summary sheet, to enable systematic comparison of the different damage descriptions. This step was essential for converting qualitative data into quantitative data and for assigning a macroseismic intensity. This evaluation was based on the specific descriptions collected in the sheets, which were, however, constantly interpreted and assessed within the framework outlined by the historical sources.

The entire reconstruction process involved overcoming various interpretative difficulties. Sometimes, practical difficulties arose simply from reading historical documents. At other times, it was necessary to identify and correct 'false attributions', i.e. reports of damage assigned to the wrong localities and later propagated uncritically in subsequent sources. Another issue was cumulative descriptions: often, documents described the total destruction of an entire 'state' (an administrative unit comprising several inhabited centres), applying the same level of damage to the entire jurisdiction. However, cross-referencing allowed these effects to be differentiated. In many cases, individual localities presented damage scenarios that were very different from each other and often less severe than that described for the entire 'state'. In order to assign the correct intensity, it was therefore necessary to disaggregate this summary

information and evaluate the actual impact on each individual locality. Throughout this evaluation process, greater relevance was given to contemporary sources in order to assess the reliability of the texts and resolve contradictions.
This critical reassessment of the available evidence led to a substantial redefinition of the macroseismic dataset, reflected in the increased number of macroseismic data points (MDPs) for most of the main events (see Table 7). Notably, the MDPs increased for both the 5 and 6 February events. A similar trend was observed for the 7 February event and the 28 March shock. By contrast, the increase was more limited for the 1 March earthquake.
As a result of this study, the entire seismic sequence is now documented by 1193 macroseismic observations, distributed across about 562 localities. Intensities were estimated using both the MCS scale, in order to ensure continuity with the Italian seismological tradition and with the existing catalogues of historical earthquakes, and the EMS-9, to align with the modern, international methodological framework.
At the same time, the methodological approach adopted revealed the factors of uncertainty that characterise complex phenomena, such as historical seismic sequences. Unlike isolated events, the detailed analysis highlighted the critical nature of macroseismic intensity assessment within seismic sequences. However, this process still presents open methodological problems, such as the absence of suitable indicators in macroseismic scales and practice for evaluating the cumulative impact of multiple earthquakes and the challenge of clearly identifying the cause-and-effect relationships between individual earthquakes and their consequences on the built environment. Therefore, when studying seismic sequences such as that of 1783, attempts to isolate the effects produced by each main event must be integrated with reconstructions capable of providing an overall picture of the seismic sequence [Rossi et al., 2019; Graziani et al., 2017; Azzaro et al., 2019].
In this study, emphasis was placed on these issues, from the interpretation of the information to mapping and subsequent parameterisation. This was done to clearly highlight the critical nature of the topics addressed. The uncertainty arising from these issues is at risk of being underestimated when the data are synthesised into catalogue records.
In the case of the 1783 Calabrian sequence, the assessment of cumulative damage constitutes a methodological innovation: this factor had not previously been considered in relation to this sequence and only recently to some other seismic sequence [Graziani et al., 2017; Azzaro et al., 2019; Graziani et al., 2022]. In this context, the cumulative intensity field, i.e., the maximum values for each locality, representative of the cumulative effect of all the earthquakes in the

sequence, is the most realistic representation. It is not susceptible to interpretative errors when the chronology of the earthquakes is reconstructed, and it shows the overall severity reached at the end of the sequence.

This type of representation, recently adopted in field studies during the 2016–2017 seismic sequence [Rossi et al., 2019] and for the historical 1703 seismic sequence[Tertulliani et al., 2022; Graziani et al., 2022] both in central Italy, although it does not provide elements for seismotectonic interpretations of individual sources, is nevertheless important in view of the fact that macroseismic intensities form the basis of local seismic histories and seismic hazard studies.

The 1783 sequence was characterised by three strong and two other significant earthquakes, which occurred over a short period of time and were documented to different extents. The estimated macroseismic parameters vary depending on the processing method and the selected dataset.

The 5 February earthquake, whose maximum intensities fall within the Gioia Tauro Plain, is well constrained by the intensity data and, following the revision, is enriched by information relating both to the epicentral area and to the far field. The new parametric estimates indicate a relocation of the macroseismic epicentre northwards with respect to the CPTI15 catalogue, together with a reduced magnitude estimate. The geometry of the estimated source shows an orientation consistent with the Cittanova Fault, with the highest intensities concentrated in the hanging wall of the extensional structure. This evidence provides elements in support of the interpretative model linked to that fault [Jacques et al., 2001; Galli and Bosi, 2002; Cucci 2022].

A different scenario emerges for the earthquake that struck the coastal area south of Palmi on 6 February. The accuracy of this event is greatly affected by the presence of cumulative damage, which directly impacts the estimation of macroseismic intensity. Even when the few pieces of information free from cumulative effects are isolated, the available data are insufficient to guarantee reliable parameterisation. Nevertheless, the 6 February earthquake may plausibly represent a relatively strong aftershock of the 5 February event and is therefore probably generated by the same seismogenic structure.

As regards the 7 February earthquake, the dataset is enriched by information that is largely referable to a cumulative damage scenario. The failure to consider this factor in previous studies has a direct effect on the estimated macroseismic parameters. The application of different methodological approaches produces divergent results: analysis carried out on the entire dataset localises the epicentre to the south, whereas the selection of non-cumulative data alone leads to an epicentral localisation towards the northeast, with a lower magnitude estimate. This divergence in the estimated parameters highlights the influence of dataset selection on the reconstruction process. In this context, the source geometry derived from the non-cumulative data shows an orientation consistent with the Serre Fault, providing indications in support of this seismogenetic interpretation [Galli and Bosi, 2002; Galli et al., 2007].

The 1 March earthquake, by contrast, is characterised by a significant margin of uncertainty due to its poor documentation and frequent disregard by contemporary sources. Analysis of these sources revealed only a small number of intensity data points, which were largely cumulative. This leaves the interpretation of this event uncertain.

Finally, the 28 March earthquake, which propagated as far as the Catanzaro basin, presents a macroseismic framework strongly conditioned by the cumulative damage scenario. The marked discrepancy between the estimated parameters shows how deeply the reconstruction is affected by the adopted methodology: processing the entire dataset localises the epicentre southwest of the Isthmus of Catanzaro, defining a NW-SE oriented source. By contrast, the approach based exclusively on non-cumulative data locates the epicentre towards the northeast, beneath the Catanzaro basin, with an E-W geometry. This configuration converges with the trend of the strike-slip structure known as the Caraffa-Squillace Gulf.

The analyses carried out show that cumulative damage has a significant effect on the estimation of macroseismic parameters. Comparing different methodologies revealed significant differences in epicentral location, magnitude estimates and source geometry. Specifically, the comparison between Method 0, used in CPTI15, and Method 1 of the Boxer code shows substantial overlap in the results. Although Method 1 is considered a more robust approach for analysing seismic sequences in the literature, no significant discrepancies between the two methods emerge in the case of the 1783 seismic sequence. However, this methodological convergence does not mitigate the limitations posed by cumulative effects, which remain a conditioning factor in the parametrisation of events within a seismic sequence.

The CIS approach, which excludes localities likely affected by prior damage from the parametrisation, allows isolation of macroseismic observations specific to each event. Applying this procedure to the 7 February and 28 March earthquakes resulted in substantial variations in both epicentral location and magnitude estimates compared to standard processing of the full dataset. In particular, for the 28 March event, the procedure defined a seismogenic source geometry with an E–W orientation, consistent with the local seismotectonic framework, diverging significantly from standard processing, which locates the epicentre in areas already struck by preceding events. These discrepancies confirm the necessity of a rigorous selection of intensity data to minimise the bias introduced by cumulative damage and to improve the reliability of seismogenic source characterisation in seismic sequences.

In conclusion, this study aimed to highlight the challenges of historical seismology and macroseismic source interpretation, particularly in seismic sequences, where the final data parametrised in the catalogues are affected by significant uncertainty. Therefore, the use of these data, particularly for seismotectonic characterisation and seismological parameterisation, requires caution and critical evaluation.

References

Albarello, D., & D'Amico, V. (2008). Testing probabilistic seismic hazard estimates by comparison with observations: an example in Italy. Geophys. J. Int., 175, 1088–1094.

Albini, P., & Pantosti, D. (2004). The 20 and 27 April 1894 (Locris, central Greece) earthquake sources through coeval records on macroseismic effects. Bull. Seismol. Soc. Am., 94(4), 1305-1326. https://doi.org/10.1785/012003174

Amato, A., Alessandrini, B., Cimini, G. B., Frepoli, A., & Selvaggi, G. (1993). Active and remnant subducted slabs beneath Italy: evidence from seismic tomography and seismicity. Ann. Geofis., 36, 201-214.

Amodio Morelli, L., Bonardi, G., Colonna, V., Dietrich, D., Giunta, G., Ippolito, F., Liguori, V., Lorenzoni, S., Paglionico, A., Perrone, V., Piccarreta, G., Russo, M., Scandone, P., Zanettin Lorenzoni, E., & Zuppetta, A. (1976). L'arco Calabro-Peloritano nell'orogene appenninico Maghrebide. Mem. Soc. Geol. It., 17, 1-60.

Andrenacci, C., Bello, S., Barbano, M. S., de Nardis, R., Pirrotta, C., Pietrolungo, F., & Lavecchia, G. (2023). Reappraisal and Analysis of Macroseismic Data for Seismotectonic Purposes: The Strong Earthquakes of Southern Calabria, Italy. Geosciences, 13(7), 212. https://doi.org/10.3390/geosciences13070212

Antonucci, A., Castellano, C., Cucci, L., & Tertulliani, A. (2026). A thorough review of the 5 May 1990 Potenza (Southern Italy) earthquake: constraints from macroseismology and insights from hydrology. NHESS. https://doi.org/10.5194/nhess-26-1105-2026

Augusti, M.: Dei terremoti di Messina e di Calabria dell'anno 1783, memorie e riflessioni, Bologna, 1783.

Azzaro, R., Barbano, M. S., Tertulliani, A., & Pirrotta, C. (2019). A reappraisal of the 1968 Valle del Belìce seismic sequence (Western Sicily): a case study of intensity assessment with cumulated damage effects. Annals of Geophysics. https://doi.org/10.4401/ag-8308

Azzaro, R., Barbano, M. S., Tertulliani, A., & Pirrotta, C. (2020). A Reappraisal of the 1968 Valle Del Belice Seismic Sequence (Western Sicily): A case study of Intensity Assessment with Cumulated Damage Effects. Annals of Geophysics, 63(1), SE105. https://doi.org/10.4401/ag-8308

Bakun, W. H., & Wentworth, C. M. (1997). Estimating earthquake location and magnitude from seismic intensity data. Bull. Seismol. Soc. Am., 87(6), 1502–1521.

Bakun, W. H., Gomez-Capera, A. A., & Stucchi, M. (2011). Epistemic uncertainty in the location and magnitude of earthquakes in Italy from macroseismic data. Bull. Seismol. Soc. Am., 101(6), 2712–2725. https://doi.org/10.1785/0120110118

Baranello, S., Camassi, R., & Castelli, V. (2025). Materiali per un catalogo dei terremoti italiani. Terremoti del Trevigiano e Bellunese tra '700 e '900. Quaderni di Geofisica, 197, 1-150. https://doi.org/10.13127/qdg/19

Baratta, M. (1895). Notizie sui terremoti osservati in Italia durante l'anno 1895, compilate da M. Baratta, 1895. Appendice al Bollettino della Società Sismologica Italiana.

Baratta, M. (1897). Materiali per un catalogo dei fenomeni sismici avvenuti in Italia (1800-1872). Memorie della Società Geografica Italiana, 7, 81-164. Roma.

Baratta, M. (1899). Saggio dei materiali per una storia dei fenomeni sismici avvenuti in Italia raccolti dal Prof. Michele Stefano De Rossi. Bollettino della Società Geologica Italiana, 18, 432-460.

Baratta, M. (1901). I terremoti d'Italia; saggio di storia geografia e bibliografia sismica italiana. Torino, p. 950.

Beauval, C., Bard, P. Y., & Danciu, L. (2020). The influence of source- and ground-motion model choices on probabilistic seismic hazard levels at 6 sites in France. Bull. Earthquake Eng., 18, 4551–4580.

Berardi, R., Petrungara, C., Zonetti, C., Magri, L., & Mucciarelli, M. (1993). Mappe di sismicita per l'area italiana. ISMES. Bergamo, Italy.

Bianchi, M. G., Tarabusi, G., Ciuccarelli, C., Maresci, M., Baranello, S., Taccone, R. C., & Ferrari, G. (2022). CFTIvisual, Atlante delle fonti visive dei terremoti italiani. Istituto Nazionale di Geofisica e Vulcanologia (INGV). https://doi.org/10.13127/cfti/visual

Bordoni, P., & Valensise, G. (1998). Deformation of the 125 ka marine terrace in Italy: tectonic implications. In I. S. Stewart & C. Vita-Finzi (Eds.), Coastal tectonics. Geological Society, London, Special Publications, 146, 71–110.

Boschi, E., Guidoboni, E., Ferrari, G., Valensise, G., & Gasperini, P. (Eds.) (1997). Catalogo dei forti terremoti in Italia dal 461 a.C. al 1990, vol. 2. ING-SGA, Bologna, 644 pp.

Buforn, E., & Udías, A. (2022). The 1620 and 1644 earthquakes in alcoy and the Eastern region of Spain. Seismol. Res. Lett., 93, 2335–2346. https://doi.org/10.1785/0220220053

Camassi, R., & Stucchi, M. (Eds.) (1997). NT4.1: un catalogo parametrico di terremoti di area italiana al di sopra della soglia di danno (versione 4.1.1). Milano, 93 pp.

Camassi, R., Castelli, V., Molin, D., Bernardini, F., Caracciolo, C. H., Ercolani, E., & Postpischl, L. (2011). Materiali per un catalogo dei terremoti italiani: eventi sconosciuti, rivalutati o riscoperti. Quaderni di Geofisica, 96, INGV, Roma, 51 + 391 pp.

Camassi, R., Castelli, V., Serpelloni, E., & Pondrelli, S. (2023). Reappraising the 25 February 1695 Asolano Earthquake. Seismological Research Letters. https://doi.org/10.1785/0220230238

Carrozzo, M. T., Cosentino, M., Ferlito, A., Giorgetti, F., Patanè, G., & Riuscetti, M. (1975). Earthquakes Catalogue of Calabria and Sicily (1783-1973). Quaderni de "La Ricerca Scientifica", 93, CNR, Roma, 194 pp

Cecere, D. (2017). Scritture del disastro e istanze di riforma nel Regno di Napoli (1783). Alle origini delle politiche. Studi Storici, 58(1), 187-214.

Cecic, I., Musson, R. M. W., & Stucchi, M. (1996). Do Seismologists Agree Upon Epicentre Determination from Macroseismic Data? A Survey of ESC Working Group 'Macroseismology'. Ann. Geophys., 39(5). https://doi.org/10.4401/ag-4031

Chiarabba, C., De Gori, P., & Speranza, F. (2008). The southern Tyrrhenian subduction zone: Deep geometry, magmatism and Plio-Pleistocene evolution. Earth Planet. Sci. Lett., 268, 408–423. https://doi.org/10.1016/j.epsl.2008.01.036

Cinti, F. R., Cucci, L., Pantosti, D., D'Addezio, G., & Meghraoui, M. (1997). A major seismogenic fault in a "silent area": the Castrovillari Fault (southern Apennines, Italy). Geophys. J. Int., 130, 595–605.

Cortese, N. (1965). Il Mezzogiorno ed il Risorgimento Italiano.

Cortese, N. (n.d.). La Calabria Ulteriore alla fine del secolo XVIII. Rivista di Cultura Calabrese, a.1, fascc.3-4.

Cosentino, M., Imposa, S., Lombardo, G., & Patané, G. (1982). Progetto Finalizzato Geodinamica, CNR. Personal communication.

Cotecchia, V., Melidoro, G., & Travaglino, G. (1969). I movimenti franosi e gli sconvolgimenti della rete idrografica prodotti in Calabria dal terremoto del 1783. Geol. Appl. Idrogeol., 4, 1–24.

CPTI Working Group (2004). Catalogo Parametrico dei Terremoti Italiani, versione 2004 (CPTI04). Istituto Nazionale di Geofisica e Vulcanologia (INGV), Bologna. https://doi.org/10.6092/INGV.IT-CPTI04

Cucci, L. (2004). Raised marine terraces in the northern Calabrian Arc (southern Italy): a ~600 000 yr-long geological record of regional tectonic deformation. Ann. Geophys., 47, 1391–1406.

Cucci, L. (2022). NW-dipping versus SE dipping causative faults of the 1783 M7.1 Southern Calabria (Italy) earthquake: The contribution from the analysis of the coseismic hydrological changes. Front. Earth Sci., 10:987731. https://doi.org/10.3389/feart.2022.987731

Cucci, L., & Cinti, F. R. (1998). Regional uplift and local tectonic deformation recorded by the Quaternary marine terraces on the Ionian coast of northern Calabria (southern Italy). Tectonophysics, 292, 67–83.

Cucci, L., & Tertulliani, A. (2010). The Capo Vaticano (Calabria) coastal terraces and the 1905 M7 earthquake: the geomorphological signature of regional uplift and coseismic slip in southern Italy. Terra Nova, 22, 378–389.

D'Agostino, N., and Selvaggi, G. (2004). Crustal motion along the Eurasia-Nubia plate boundary in the Calabrian Arc and Sicily and active extension in the Messina Straits from GPS measurements. J. Geophys. Res. Solid Earth 109 (B11), B11402. doi:10.1029/2004JB002998

D'Agostino, N., D'Anastasio, E., Gervasi, A., Guerra, I., Nedimović, M. R., Seeber, L., & Steckler, M. (2011). Forearc extension and slow rollback of the Calabrian Arc from GPS measurements. Geophys. Res. Lett., 38, L17304. https://doi.org/10.1029/2011GL048270

D'Amico, V., & Albarello, D. (2008). SASHA: A computer program to assess seismic hazard from intensity data. Seismol. Res. Lett., 79, 663-671. https://doi.org/10.1785/gssrl.79.5.663

D'Amico, V., Visini, F., Rovida, A., Marzocchi, W., & Meletti, C. (2024). Scoring and ranking probabilistic seismic hazard models: an application based on macroseismic intensity data. Nat. Hazards Earth Syst. Sci., 24, 1401–1413.

De Dolomieu, D. (1785). Memoria sopra i tremuoti della Calabria dell'anno 1783.

De Leone, A.: Giornale e notizie de' tremuoti accaduti l'anno 1783 nella provincia di Catanzaro, Napoli, 1783.

De Lorenzo, A.: Memorie da servire alla storia sacra e civile di Reggio e delle Calabrie, Cronache e Documenti inediti o rari, vol. I, Reggio Calabria, 1877.

De Lorenzo, A.: Un secondo manipolo di monografie e memorie reggine e calabresi, Siena, 1895

De Stefano, D. (1987). I Terremoti in Calabria e nel Messinese. Ed. Sci. Ital., Naples, Italy.

Del Mese, S., Graziani, L., Meroni, F., et al. (2023). Considerations on using MCS and EMS-98 macroseismic scales for the intensity assessment of contemporary Italian earthquakes. Bull. Earthquake Eng., 21, 4167–4189. https://doi.org/10.1007/s10518-023-01703-0

Dellong, D., Klingelhoefer, F., Dannowski, A., Kopp, H., Murphy, S., Graindorge, D., et al. (2020). Geometry of the deep Calabrian subduction (central Mediterranean Sea) from wide-angle seismic data and 3-D gravity modeling. Geochem. Geophy. Geosy. 21, 3. doi:10.1029/2019GC008586

Devoti, R., Riguzzi, F., Cuffaro, M., and Doglioni, C. (2008). New GPS constraints on the kinematics of the Apennines subduction. Earth Planet Sci. Lett. 273, 163–174. doi:10.1016/j.epsl.2008.06.031

DISS Working Group (2025). Database of Individual Seismogenic Sources (DISS), Version 3.3.1: A compilation of potential sources for earthquakes larger than M 5.5 in Italy and surrounding areas. Istituto Nazionale di Geofisica e Vulcanologia (INGV). https://doi.org/10.13127/diss3.3.1

Doglioni, C. (1991). A proposal for the kinematic modelling of W-dipping subductions: Possible application to the Tyrrhenian-Apennines system. Terra Nova, 3, 423–434.

Dolce, M. (2019). Prefazione all'edizione italiana della Scala Macrosismica Europea 1998. In: Tertulliani, A., Azzaro, R., Buffarini, G. (Eds.), Scala Macrosismica Europea 1998 - EMS-98, Centre Européen de Géodynamique et de Séismologie. Luxembourg, p. 99.

Dolomieu, D. (1784). Memoria Sopra i Tremuoti della Calabria nell'Anno 1783. G. P. Merande, Naples, Italy.

Dumas, B., & Raffy, J. (2004). Late Pleistocene tectonic activity deduced from uplifted marine terraces in Calabria, facing the Strait of Messina. Quat. Nova, 8, 79–100

Eliseo della Concezione, (1784). Carta corografica della Calabria Ulteriore, allegata a "Istoria de' fenomeni del tremuoto avvenuto nelle Calabrie e nel Valdemone nell'anno 1783".

ENEL (1985). Studi e indagini per l'accertamento della idoneità tecnica delle aree suscettibili di insediamento di impianti nucleari per le Regioni Piemonte, Lombardia e Puglia: indagini di sismica storica. Rapporti tecnici predisposti da ISMES-SGA, Roma.

Faccenna, C., Davy, P., Brun, J.-P., Funiciello, R., Giardini, D., Mattei, M., et al. (1996). The dynamics of back-arc extension: an experimental approach to the opening of the Tyrrhenian Sea. Geophys. J. Int. 126, 781–795. doi:10.1111/j. 1365-246x.1996.tb04702.x

Finetti, I., & Morelli, C. (1973). Geophysical exploration of the Mediterranean Sea. Boll. Geofis. Teor. Appl., 15, 263–344

Fuller, W. A. (1987). Measurement Error Models. Wiley. New York, p. 440.

Galadini, F., & Tertulliani, A. (2025). Il terremoto di Rosciolo dei Marsi del 24 febbraio 1904 (Abruzzo, Italia centrale): revisione dei dati e nuove acquisizioni storiche. Quaderni di Geofisica, 196. https://doi.org/10.13127/qdg/196

Galanopoulos, A. G. (1961). On magnitude determination by using macroseismic data. Ann. Geophys., 14(3), 225–253.

Galli, P. A. C., & Peronace, E. (2015). Lowslip rates and multimillennial return times for Mw 7 earthquake faults in southern Calabria (Italy). Geophys. Res. Lett., 42, 5258–5265. https://doi.org/10.1002/2015GL064062

Galli, P., & Bosi, V. (2002). Paleoseismology along the Cittanova fault: Implications for seismotectonics and earthquake recurrence in Calabria (southern Italy). J. Geophys. Res., 107(B3). https://doi.org/10.1029/2001JB000234

Galli, P., & Bosi, V. (2003). Catastrophic 1638 earthquakes in Calabria (southern Italy): New insights from paleoseismological investigation. J. Geophys. Res., 108(B1). https://doi.org/10.1029/2001JB001713

Galli, P., & Scionti, V. (2006). Two unknown M >6 historical earthquakes revealed by palaeoseismological and archival researches in eastern Calabria (southern Italy): Seismotectonic implications. Terra Nova, 18, 44–49. https://doi.org/10.1111/j.1365-3121.2005.00658.x

Galli, P., Galadini, F., & Pantosti, D. (2008). Twenty years of paleoseismology in Italy. Earth Sci. Rev., 88, 89–117. https://doi.org/10.1016/j.earscirev.2008.01.001

Galli, P., Muto, F., & Peronace, E. (2025). Palaeoseismic evidence of a mainshock in the Lamezia Terme area during the March 1638 seismic sequence (MW ~7, Calabria, southern Italy). Bull. Geophysics Oceanography, XX, in press. doi: 10.4430/bgo00500

Galli, P., Scionti, V., & Spina, V. (2007). New paleoseismic data from the Lakes and Serre faults (Calabria, southern Italy). Seismotectonic implication. Boll. Soc. Geol. Ital., 126, 347–364.

Galli, P., Spina, V., Ilardo, I., & Naso, G. (2010). Evidence of active tectonics in southern Italy: the Rossano Fault (Calabria). *Recent progress on earthquake geology*, 49-78.

Gallo, A.: Lettera istorico-fisica de' terremoti accaduti in Messina nel mese di febbraio di quest'anno 1783, Messina, 8 marzo 1783, Bologna, 1784.

Gasperini, P., Bernardini, F., Valensise, G., & Boschi, E. (1999). Defining seismogenic sources from historical earthquake felt reports. Bull. Seismol. Soc. Am., 89, 94-110. https://doi.org/10.1785/BSSA0890010094

Gasperini, P., Vannucci, G., Tripone, D., & Boschi, E. (2010). The Location and Sizing of Historical Earthquakes Using the Attenuation of Macroseismic Intensity with Distance. Bull. Seismol. Soc. Am., 100, 2035-2066. https://doi.org/10.1785/0120090330

Gazzetta Universale, 1783.02.25, n.16.

Ghisetti, F. (1981). Evoluzione neotettonica dei principali sistemi di faglie della Calabria centrale. Boll. Soc. Geol. It., 99, 387–430.

Ghisetti, F., & Vezzani, L. (1982). Different styles of deformation in the Calabrian Arc (southern Italy): Implication for a seismotectonic zoning. Tectonophysics, 25, 149–165.

Gomez-Capera, A. A., D'Amico, V., Meletti, C., Rovida, A., & Albarello, D. (2010). Seismic hazard in terms of macroseismic data intensity in Italy: a critical analysis from the comparison of different computational procedures. Bull. Seismol. Soc. Am., 100(4), 1614–1631.

Gomez-Capera, A. A., Rovida, A., Gasperini, P., Stucchi, M., & Viganò, D. (2015). The determination of earthquake location and magnitude from macroseismic data in Europe. Bull. Earthq. Eng., 13, 1249–1280.

Graziani, L., Del Mese, S., Tertulliani, A., Arcoraci, L., Maramai, A., & Rossi, A. (2019). Macroseismic assessment (EMS-98) of damage progression during the 2016-17 seismic sequence in central Italy. Bull. Earthq. Eng., 17, 5535–5558. https://doi.org/10.1007/s10518-019-00645-w

Graziani, L., Maramai, A., & Tinti, S. (2006). A revision of the 1783–1784 Calabrian (southern Italy) tsunamis. Nat. Hazards Earth Syst. Sci., 6, 1053–1060. https://doi.org/10.5194/nhess-6-1053-2006

Graziani, L., Rovida, A., & Tertulliani, A. (2022). The Influence of Cumulative Intensity on Macroseismic Source Parameters: The Case of 2016–2017 and 1703 Seismic

Sequences (Central Italy). Seismol. Res. Lett., 94, 759–774. https://doi.org/10.1785/0220220038

Graziani, L., Tertulliani, A., Maramai, A., Rossi, A., & Arcoraci, L. (2017). The 7 and 11 May, 1984 earthquakes in Abruzzo-Latium (Central Italy): reappraisal of the existing macroseismic datasets according to the EMS98. J. Seismol., 21, 1219-1227. https://doi.org/10.1007/s10950-017-9663-3

Grimaldi, F. A. (1784). Descrizione de' tremuoti nelle Calabrie nel 1783.

Grimaz, S., & Malisan, P. (2017). How could cumulative damage affect the macroseismic assessment? Bull. Earthq. Eng., 15, 2465–2481. https://doi.org/10.1007/s10518-016-0016-3

Grünthal, G. (Ed.) (1998). European Macroseismic Scale 1998 (EMS-98). European Seismological Commission, subcommission on Engineering Seismology, Working Group Macroseismic Scales. Conseil de l'Europe, Cahiers du Centre Européen de Géodynamique et de Séismologie 15. Luxembourg.

Guerrieri, L., & Vittori, E. (Eds.) (2007). Intensity Scale ESI 2007. Memorie Descrittive della Carta Geologica d'Italia, Vol. 74. Roma: Servizio Geologico d'Italia – Dipartimento Difesa del Suolo, APAT.

Guidoboni, E., & Ebel, J. E. (2009). Earthquakes and Tsunamis in the Past. A Guide to Techniques in Historical Seismology. Cambridge University Press, Cambridge.

Guidoboni, E., Ferrari, G., Mariotti, D., Comastri, A., Tarabusi, G., & Valensise, G. (2007). CFTI4Med, Catalogue of Strong Earthquakes in Italy (461 B.C.-1997) and Mediterranean Area (760 B.C.-1500). INGV-SGA. https://storing.ingv.it/cfti/cfti4/

Guidoboni, E., Ferrari, G., Mariotti, D., Comastri, A., Tarabusi, G., Sgattoni, G., & Valensise, G. (2018). CFTI5Med, Catalogo dei Forti Terremoti in Italia (461 a.C.-1997) e nell'area Mediterranea (760 a.C.-1500). Istituto Nazionale di Geofisica e Vulcanologia (INGV). https://doi.org/10.6092/ingv.it-cfti5

Hamilton, W. (1783). Relazione dell'ultimo terremoto delle Calabrie e della Sicilia, tradotta dall'inglese da Gasparo Sella.

Hollenstein, C., Kahle, H. G., Geiger, A., Jenny, S., Goes, S., and Giardini, D. (2003). New GPS constraints on the Africa-Eurasia plate boundary zone in southern Italy. Geophys. Res. Lett. 30 (18), 1935. doi:10.1029/2003gl017554.

IMSL (1991). International Mathematic Statistic Library IMSL 1991 MATHLibrary User's Manual Version 2.0. Visual Numerics Inc. Huston, Texas, p. 1313

Infelise, M. (2002). Prima dei giornali: alle origini della pubblica informazione, secoli 16 e 17. Roma-Bari, Laterza.

ISIDe Working Group (2007). Italian Seismological Instrumental and Parametric Database (ISIDe). Istituto Nazionale di Geofisica e Vulcanologia (INGV). https://doi.org/10.13127/ISIDE

Jacques, E., Monaco, C., Tapponnier, P., Tortorici, T., & Winter, T. (2001). Faulting and earthquake triggering during the 1783 Calabria seismic sequence. Geophys. J. Int., 147, 499–516.

Locati, M., Camassi, R., Rovida, A., Ercolani, E., Bernardini, F., Castelli, V., Caracciolo, C. H., Tertulliani, A., Rossi, A., Azzaro, R., D'Amico, S., & Antonucci, A. (2022). Database Macrosismico Italiano (DBMI15), versione 4.0. Istituto Nazionale di Geofisica e Vulcanologia (INGV). https://doi.org/10.13127/DBMI/DBMI15.4

Malinverno, A., and Ryan, W. B. F. (1986). Extension in the Tyrrhenian Sea and shortening in the Apennines as result of arc migration driven by sinking of the lithosphere. Tectonics 5 (2), 227–245. doi:10.1029/TC005i002p00227.

Medvedev, S. V., Sponheuer, W., & Karnik, V. (1965). Seismic intensity scale version MSK 1964. Academy of Sciences of the USSR, Soviet Geophysical Committee, Moscow.

Mercalli, G. (1897). I terremoti della Calabria meridionale e del messinese. In Memorie della Società Italiana delle Scienze [detta dei XL], s.III, tomo 11, 117-266.

Mercalli, G. (1902). Sulle modificazioni proposte alla scala sismica De Rossi-Forel. Boll. Soc. Sism. It., vol. VIII, Roma.

Mercalli, G. (1910). I danni prodotti dai terremoti nella Basilicata e nelle Calabrie. In Relazione della Sotto Giunta Parlamentare d'Inchiesta sulle condizioni dei contadini nelle provincie meridionali e nella Sicilia, vol.5, tomo 3 (Basilicata e Calabria).

Michetti, A. M., Ferreli, L., Serva, L., & Vittori, E. (1997). Geological evidence for strong historical earthquakes in an 'aseismic' region: the Pollino case. J. Geodyn., 24, 67–86.

Minasi, G. (1785). Continuazione ed appendice sopra i tremuoti descritti nella relazione colla data di Scilla del 30 settembre 1783, con altro che accadde in progresso.

Minelli, L., & Faccenna, C. (2010). Evolution of the Calabrian accretionary wedge (central Mediterranean). Tectonics, 29, TC4004. https://doi.org/10.1029/2009TC002562

Minelli, L., Vecchio, A., Speranza, F., Nicolosi, I., D'Ajello Caracciolo, F., Chiappini, S., Carluccio, R., & Chiappini, M. (2016). Aeromagnetic investigation of southern Calabria and the Messina Straits (Italy): Tracking seismogenic sources of 1783 and

1908 earthquakes. J. Geophys. Res. Solid Earth, 121, 1297–1315. https://doi.org/10.1002/2015JB012305

Molin, D., Bernardini, F., Camassi, R., Caracciolo, C. H., Castelli, V., Ercolani, E., & Postpischl, L. (2008). Materiali per un catalogo dei terremoti italiani: revisione della sismicità minore del territorio nazionale. Quaderni di Geofisica, Vol. 57, 78 (+1444 pp. su CD-Rom).

Monachesi, G., Castelli, V., & Camassi, R. (2016). Aggiornamento delle conoscenze sul terremoto del 28 luglio 1799 nel sub-Appennino maceratese. Quaderni di Geofisica, 138, 212 pp. https://doi.org/10.13127/qdg/138

Monaco, C., & Tortorici, L. (2000). Active faulting in the Calabrian arc and eastern Sicily. J. Geodynamics, 29, 407–424.

Moretti, A., & Guerra, I. (1997). Tettonica dal Messiniano ad oggi in Calabria: implicazioni sulla geodinamica del sistema Tirreno-Arco Calabro. Boll. Soc. Geol. Ital., 116, 125–142.

Musson, R. M. W., & Jiménez, M. J. (2008). Macroseismic estimation of earthquake parameters. NERIES Project Report, Module NA4, Deliverable D3, 31 pp. https://nora.nerc.ac.uk/id/eprint/533370/

Musson, R. M. W., Grünthal, G., & Stucchi, M. (2010). The comparison of macroseismic intensity scales. J. Seismol., 14. https://doi.org/10.1007/s10950-009-9172-0

Musson, R. M., & Cecić, I. (2012). Intensity and Intensity Scales. In: Bormann, P. (Ed.), New Manual of Seismological Observatory Practice 2 (NMSOP-2), Potsdam: Deutsches GeoForschungsZentrum GFZ, 1-41. https://doi.org/10.2312/GFZ.NMSOP-2_ch12

Neri, G., Marotta, A. M., Orecchio, B., Presti, D., Totaro, C., Barzaghi, R., et al. (2012). How lithospheric subduction changes along the Calabrian Arc in southern Italy: geophysical evidences. Int. J. Earth Sci. 101, 1949–1969. doi:10.1007/s00531-012-0762-7.

Neri, G., Orecchio, B., Totaro, C., Falcone, G., and Presti, D. (2009). Subduction beneath southern Italy close the ending: results from seismic tomography. Seismol. Res. Lett. 80 (1), 63–70. doi:10.1785/gssrl.80.1.63.

Nijholt, N., Govers, R., and Wortel, R. (2018). On the forces that drive and resist deformation of the south-central Mediterranean: a mechanical model study. Geophys. J. Int. 214 (2), 876–894. doi:10.1093/gji/ggy144.

Pagano, F. M. (1892). Studi sulla Calabria, 2 voll.

Pasolini, C., Albarello, D., Gasperini, P., D’Amico, V., & Lolli, B. (2008). The attenuation of seismic intensity in Italy, part II: modeling and validation. Bull. Seismol. Soc. Am., 98, 692–708.

Patacca, E., R. Sartori, and P. Scandone (1990), Tyrrhenian basin and Apenninic arcs: Kinematic relations since late tortonian times, Mem.Geol. Soc. Ital., 45, 425–451.

Penna, A., Morandi, P., Rota, M., Manzini, C. F., da Porto, F., & Magenes, G. (2014). Performance of masonry buildings during the Emilia 2012 earthquake. Bull. Earthq. Eng., 12, 2255–2273.

Perrey, A. (1848). Memoire sur les tremblements de terre de la peninsule Italique. Mem. Cour. et Mem. Sav. Ètran., Acad. R. des Sciences, Lettres et Beaux-Arts de Belgique, 145 pp. Bruxelles.

Peterschmitt, E. (1956). Quelques donnees nouvelles sur les seismes profonds de la Mer Tyrrhenienne. Ann. Geofis., 9, 305–334.

Piromallo, C., & Morelli, A. (2003). P wave tomography of the mantle under the Alpine–Mediterranean area. J. Geophys. Res., 108, 2156–2202. https://doi.org/10.1029/2002JB001929

Pirrotta, C., Barberi, G., Barreca, G., Brighenti, F., Carnemolla, F., De Guidi, G., Monaco, C., Pepe, F., & Scarfì, L. (2021). Recent Activity and Kinematics of the Bounding Faults of the Catanzaro Trough (Central Calabria, Italy): New Morphotectonic, Geodetic and Seismological Data. Geosciences, 11, 405. https://doi.org/10.3390/geosciences11100405

Pizzino, L., Burrato, P., Quattrocchi, F., et al. (2004). Geochemical signatures of large active faults: The example of the 5 February 1783, Calabrian earthquake (southern Italy). Journal of Seismology, 8, 363–380. https://doi.org/10.1023/B:JOSE.0000038455.56343.e7

Placanica, A. (1970). Cassa Sacra e beni della chiesa nella Calabria del Settecento.

Placanica, A. (1982). L’Iliade funesta. Storia del terremoto calabro-messinese del 1783. Corrispondenza e relazioni della Corte, del Governo e degli Ambasciatori.

Placanica, A. (1988). La catastrofe sismica calabro-peloritana del 1783. La resistibile ascesa degli elettricisti. In Il Meridione e le scienze (secoli XVI-XIX), Atti del Convegno, Palermo 14-16 maggio 1985, a cura di P. Nastasi, pp. 525-539.

Postpischl, D. (1985). Catalogo dei terremoti italiani dall'anno 1000 al 1980. Quaderni della Ricerca Scientifica, 114, 2B, Bologna, 239 pp.

Principe, I. (1985). 1783. Il progetto della forma, la ricostruzione della Calabria negli Archivi di Cassa Sacra a Catanzaro e Napoli.

Provost, L., & Scotti, O. (2020). QUake-MD: Open-source code to quantify uncertainties in magnitude–depth estimates of earthquakes from macroseismic intensities. Seismological Research Letters, 91(5), 2520-2530. https://doi.org/10.1785/0220200064.

Pugliesi, F. (1976). Ricerche sulla storia di Bocchigliero, aggiornate da B. Pugliesi.

Ricchetti, E., & Ricchetti, G. (1991). Aspetti della morfogenesi pleistocenico-olocenica su versante tirrenico della Calabria. Mem. Soc. Geol. It., XLVII, 655–663.

Rovida, A., Camassi, R., Gasperini, P., & Stucchi, M. (Eds.) (2011). CPTI11, the 2011 version of the Parametric Catalogue of Italian Earthquakes. Istituto Nazionale di Geofisica e Vulcanologia (INGV), Milano, Bologna. https://doi.org/10.6092/INGV.IT-CPTI11

Rovida, A., Locati, M., Antonucci, A., & Camassi, R. (Eds.) (2017). Archivio Storico Macrosismico Italiano (ASMI). Istituto Nazionale di Geofisica e Vulcanologia (INGV). https://doi.org/10.13127/asmi

Rovida, A., Locati, M., Camassi, R., Lolli, B., Gasperini, P., & Antonucci, A. (2022). Italian Parametric Earthquake Catalogue (CPTI15), version 4.0. Istituto Nazionale di Geofisica e Vulcanologia (INGV). https://doi.org/10.13127/cpti/cpti15.4

Sarconi, M. (1784). Istoria de' fenomeni del tremoto avvenuto nelle Calabrie, e nel Valdemone nell'anno 1783 posta in luce dalla Reale Accademia delle Scienze, e delle Belle Lettere di Napoli.

Sbarra, P., Burrato, P., De Rubeis, V., Tosi, P., Valensise, G., Vallone, R., & Vannoli, P. (2023). Inferring the depth and magnitude of pre-instrumental earthquakes from intensity attenuation curves. Natural Hazards and Earth System Sciences, 23(3), 1007–1028. https://doi.org/10.5194/nhess-23-1007-2023

Sbarra, P., Burrato, P., Tosi, P., De Rubeis, V., Valensise, G., & Vannoli, P. (2019). Inferring the depth of pre-instrumental earthquakes from macroseismic intensity attenuation curves. Scientific Reports, 9(1), 15611.

Scionti, V., Galli, P., & Chiodo, G. (2006). The Calabrian seismicity during the Viceroyalty of Naples: sources silence or silent sources? The case of the strong 1744 earthquake. Boll. Geof. Teor. Appl., 47, 53–72.

Sibol, M. S., Bollinger, G. A., & Birch, J. B. (1987). Estimation of magnitudes in central and eastern North America using intensity and felt area. Bull. Seismol. Soc. Am., 77(5), 1635–1654.

Sieberg, A. (1930). Geologie der Erdbeben. Handbuch der Geophysik, Gebrüder Bornträger, Berlin, vol. 2, pt 4, 550-555.

Stucchi, M. (1993). Historical seismology and seismic hazard. Annals of Geophysics, 36(1). https://doi.org/10.4401/ag-4314

Stucchi, M., & Rovida, A. (2008). Investigating historical earthquake sequences. MERCEA'08 Seismic Engineering International Conference, Messina e Reggio Calabria, 8–11 luglio 2008.

Stucchi, M., Albini, P., Mirto, C., & Rebez, A. (2004). Assessing the completeness of Italian historical earthquake data. Annals of Geophysics, 47, 28. https://doi.org/10.4401/ag-3330

Stucchi, M., Meletti, C., Montaldo, V., Crowley, H., Calvi, G. M., & Boschi, E. (2011). Seismic hazard assessment (2003-2009) for the Italian building code. Bull. Seismol. Soc. Am., 101, 1885-1911.

Tertulliani, A. (2019). Storia delle scale macrosismiche. Duecento anni di osservazione degli effetti del terremoto. Quaderni Di Geofisica, 150. https://doi.org/10.13127/qdg/150

Tertulliani, A., Antonucci, A., Bernardini, F., Castelli, V., Ercolani, E., Graziani, L., Maramai, A., Orlando, M., Rossi, A., & Tuvè, T. (2025). A comprehensive integrated macroseismic dataset from multiple earthquake studies. Earth Syst. Sci. Data, 17, 4063–4077. https://doi.org/10.5194/essd-17-4063-2025

Tertulliani, A., Arcoraci, L., Berardi, M., et al. (2011). An application of EMS98 in a medium-sized city: the case of L'Aquila (Central Italy) after the April 6, 2009 Mw 6.3 earthquake. Bull. Earthq. Eng., 9, 67–80. https://doi.org/10.1007/s10518-010-9188-4

Tertulliani, A., Cecić, I., Meures, R., Sović, I., Kaiser, D., Grünthal, G., Pazdirkova, J., Sira, C., Guterch, B., Kysel, R., Camelbeeck, T., Lecocq, T., & Szanyi, G. (2018). The 6 May 1976 Friuli earthquake: re-evaluation and unification of transnational macroseismic data. Boll. Geophys. Teor. App., 59, 417–444. https://doi.org/10.4430/bgta0234

Tertulliani, A., Graziani, L., & Locati, M. (2022). Nuovo studio della sequenza sismica del gennaio-febbraio 1703 in Italia centrale. Quaderni di Geofisica, 178, 576. https://doi.org/10.13127/qdg/178

Tiberti, M. M., Vannoli, P., Fracassi, U., Burrato, P., Kastelic, V., & Valensise, G. (2017). Understanding seismogenic processes in the Southern Calabrian Arc: a geodynamic perspective. Italian Journal of Geosciences, 136(3), 365–388. https://doi.org/10.3301/IJG.2016.12.

Torcia, M.: Tremuoto avvenuto nella Calabria e a Messina all 5 febbrajo 1783 descritto da Michele Torcia– Archiviario di S. M. Siciliana e Membro della Accademia Regia, Napoli, 1783.

Tortorici, L., Monaco, C., Tansi, C., & Cocina, O. (1995). Recent and active tectonics in the Calabrian arc (southern Italy). Tectonophysics, 243, 37–55.

Triantafyllou, I., Koukouvelas, I., Papadopoulos, G. A., & Lekkas, E. (2022). A reappraisal of the destructive earthquake (Mw5.9) of 15 July 1909 in Western Greece. Geosciences, 12, 374. https://doi.org/10.3390/geosciences12100374

Tripodi, V., Gervasi, A., La Rocca, M., et al. (2022). Seismotectonics of Southern Calabria Terrane (South Italy). Journal of Mountain Science, 19(11). https://doi.org/10.1007/s11629-022-7354-1

Valensise, G., & D'Addezio, G. (1994). Il contributo della geologia di superficie all'identificazione delle strutture sismogenetiche della Piana di Gioia Tauro. Istituto Nazionale di Geofisica, pubbl. 559, 21 pp.

Vannucci, G. (2025). Analysis of the macroseismic cumulative damage in the seismic sequences in Italy. Bull. Earthquake Eng., 23, 759–778. https://doi.org/10.1007/s10518-024-02073-x

Vannucci, G., Gasperini, P., Lolli, B., & Gulia, L. (2019). Fast characterization of sources of recent Italian earthquakes from macroseismic intensities. Tectonophysics, 750, 70–92.

Vivenzio, G. (1783). Istoria e teoria de' tremuoti in generale ed in particolare di quelli della Calabria, e di Messina del MDCCLXXXIII.

Vivenzio, G. (1788). Istoria de' tremuoti avvenuti nella provincia della Calabria ulteriore, e nella città di Messina nell'anno 1783, e di quanto nella Calabria fu fatto per lo suo risorgimento fino al 1787, preceduta da una teoria, ed istoria generale de' tremuoti (2 voll.).

Wald, D. J., Goded, T., Hortacsu, A., & Loos, S. C. (2024). Developing and implementing an International Macroseismic Scale (IMS) for earthquake engineering, earthquake science, and rapid damage assessment. U.S. Geological Survey Open-File Report 2023–1098, 55 p. https://doi.org/10.3133/ofr20231098

Wells, D. L., & Coppersmith, K. J. (1994). New empirical relationships among magnitude, rupture length, rupture width, rupture area, and surface displacement. Bulletin of the Seismological Society of America, 84(4), 974–1002.

Westaway, R. (1993). Quaternary uplift of southern Italy. J. Geophys. Res., 98, 21,741–21,772.

Wood, H. O., & Neumann, F. (1931). Modified Mercalli Intensity scale of 1931. Bull. Seismol. Soc. Am., 21, 277-283

Zatta, A., Zuliani, G., & Pitteri, G. (1782). L'Italia. Venezia, 1782. David Rumsey Historical Map Collection.

Appendix A

The table reports the 562 localities identified in this study as affected by the 1783 seismic sequence, in alphabetical order. For each site, the locality name, municipality, province, coordinates (latitude and longitude), alternative toponyms, and the number of documentary source excerpts related to the locality are provided.

Locality	Municipality	Prov.	Lat.	Long.	Other toponyms	No. excerpts
Accaria	Serrastretta	CZ	38.98	16.365		4
Acciarello	Villa San Giovanni	RC	38.212	15.638	Asciarello	3
Acconia	Curinga	CZ	38.837	16.267	Lacconia, Lauconi	4
Acquaro	Cosoleto	RC	38.268	15.899	Aquano	13
Acquaro	Acquaro	VV	38.555	16.189		6
Africo [vecchio]	Africo	RC	38.065	15.98	Affrico	5
Agnana Calabra	Agnana Calabra	RC	38.302	16.224		6
Agrigento	Agrigento	AG	37.312	13.578	Girgenti	1
Agropoli	Agropoli	SA	40.35	14.99		3
Aiello Calabro	Aiello Calabro	CS	39.117	16.166		3
Alafito	Parghelia	VV	38.672	15.919	Alafiro	4
Albi	Albi	CZ	39.024	16.597		5
Altavilla	Lappano	CS	39.333	16.311	Corno	2
Altilia	Altilia	CS	39.129	16.252	Pietra Irta	3
Altilia	Santa Severina	KR	39.182	16.882		4
Altolia	Messina	ME	38.075	15.446	Artalia	5
Amantea	Amantea	CS	39.132	16.081		4
Amaroni	Amaroni	CZ	38.792	16.447		6
Amato	Amato	CZ	38.942	16.463		8
Amendolea [vecchia]	Condofuri	RC	37.988	15.892		4
Andali	Andali	CZ	39.013	16.77		7
Angoli	Serrastretta	CZ	38.971	16.436		4
Anoia (Inferiore)	Anoia	RC	38.435	16.08	Anoja	9
Anoia Superiore	Anoia	RC	38.432	16.097	Anoja	8

Antonimina	Antonimina	RC	38.272	16.15		5
Apriglianello	Crotone	KR	39.086	17.052	Apriglianella	6
Aprigliano	Aprigliano	CS	39.24	16.342		2
Arasì	Reggio di Calabria	RC	38.139	15.737		5
Ardore	Ardore	RC	38.191	16.168		6
Arena	Arena	VV	38.562	16.209		8
Argusto	Argusto	CZ	38.679	16.437	Argusta	7
Arietta	Petronà	CZ	39.052	16.789	Arieta	6
Armo	Reggio di Calabria	RC	38.07	15.715		6
Arzona	Filandari	VV	38.622	16.046	Larzona	9
Augusta	Augusta	SR	37.231	15.221		3
Badia	Nicotera	VV	38.564	15.956		7
Badolato	Badolato	CZ	38.568	16.524		5
Bagaladi	Bagaladi	RC	38.026	15.821		8
Bagnara Calabra	Bagnara Calabra	RC	38.286	15.805		24
Barbalaconi	Ricadi	VV	38.634	15.873		4
Barcellona Pozzo di Gotto	Barcellona Pozzo di Gotto	ME	38.146	15.215	Barcellonetta	4
Bari	Bari	BA	41.129	16.869		1
Belcastro	Belcastro	CZ	39.017	16.785		6
Bellantone	Laureana di Borrello	RC	38.497	16.091	Bellantoni	5
Belmonte Calabro	Belmonte Calabro	CS	39.16	16.079		4
Belsito	Belsito	CS	39.174	16.287		2
Benestare	Benestare	RC	38.184	16.139		5
Bianco [vecchio]	Bianco	RC	38.095	16.118		5
Bisignano	Bisignano	CS	39.513	16.285		2
Bivona	Vibo Valentia	VV	38.709	16.103	Bujona	2
Bivongi	Bivongi	RC	38.482	16.453		6
Bocchigliero	Bocchigliero	CS	39.418	16.751		2

Bombile	Ardore	RC	38.205	16.173	Bombilii	5
Borgia	Borgia	CZ	38.825	16.51		8
Borgo Partenope	Cosenza	CS	39.27	16.304	Torzano	2
Borrello	Serrata	RC	38.513	16.069	Borello	8
Bova	Bova	RC	37.994	15.932		10
Bovalino Superiore	Bovalino	RC	38.17	16.156	Motta Bovalina	5
Bovetto	Reggio di Calabria	RC	38.06	15.674		6
Bracciara	Dasà	VV	38.565	16.168	Brazzaria	7
Brancaleone Superiore	Brancaleone	RC	37.981	16.081		10
Brattirò	Drapia	VV	38.642	15.887		6
Briatico Vecchio	Briatico	VV	38.707	16.023		14
Brivadi	Ricadi	VV	38.636	15.856		4
Brognaturo	Brognaturo	VV	38.602	16.342		6
Bruzzano Vecchio	Bruzzano Zeffirio	RC	38.021	16.077		5
Calabrò	Mileto	VV	38.613	16.076		9
Calanna	Calanna	RC	38.183	15.724		8
Calimera	San Calogero	VV	38.556	16.018	Catimero	6
Calvaruso	Villafranca Tirrena	ME	38.222	15.453		2
Camini	Camini	RC	38.432	16.483		4
Campo Calabro	Campo Calabro	RC	38.213	15.659		3
Campoli Vipere	Caulonia	RC	38.449	16.393	Campoli	1
Canale	Benestare	RC	38.176	16.128		1
Candidoni	Candidoni	RC	38.505	16.086	Candidone	8
Cannavò	Reggio di Calabria	RC	38.099	15.69		6
Cannitello	Villa San Giovanni	RC	38.234	15.657	Cannetello	4
Canolo	Canolo	RC	38.314	16.2		6
Capistrano	Capistrano	VV	38.692	16.289		5

Caraffa del Bianco	Caraffa del Bianco	RC	38.092	16.087	Carafa	5
Caraffa di Catanzaro	Caraffa di Catanzaro	CZ	38.88	16.486		2
Carciadi	Spilinga	VV	38.628	15.908		4
Cardeto	Cardeto	RC	38.084	15.768		6
Cardinale	Cardinale	CZ	38.642	16.387		8
Careri	Careri	RC	38.177	16.115		4
Caria	Drapia	VV	38.646	15.905		4
Carlopoli	Carlopoli	CZ	39.055	16.456	Carrapoli	5
Carolei	Carolei	CS	39.253	16.218		2
Caroni	Limbadi	VV	38.567	15.96	Carone	4
Caroniti	Joppolo	VV	38.593	15.905	Baroniti	6
Carpanzano	Carpanzano	CS	39.147	16.303	Carpenzano	2
Casalnuovo	Africo	RC	38.055	15.993	Casalnuovo di Affrico	5
Casignana	Casignana	RC	38.101	16.089	Casignano	5
Casole Bruzio	Casali del Manco	CS	39.281	16.331	Casola	2
Cassano allo Ionio	Cassano all'Ionio	CS	39.784	16.318		1
Castagna	Carlopoli	CZ	39.053	16.436		2
Castellace	Oppido Mamertina	RC	38.315	15.94	Castellaci	11
Castelmonardo	Filadelfia	VV	38.77	16.303	Nuova Filadelfia	7
Castiglione Cosentino	Castiglione Cosentino	CS	39.351	16.288		3
Castiglione Marittimo	Falerna	CZ	38.981	16.159		2
Castrolibero	Castrolibero	CS	39.307	16.194	Castelfranco	2
Castroreale	Castroreale	ME	38.099	15.211	Castroregale	5
Catania	Catania	CT	37.502	15.087		4
Catanzaro	Catanzaro	CZ	38.905	16.594		13
Catanzaro Lido	Catanzaro	CZ	38.822	16.613		1
Catona	Reggio di Calabria	RC	38.185	15.643		4

Caulonia	Caulonia	RC	38.381	16.409	Castelvetere	7
Celico	Celico	CS	39.309	16.34		3
Cenadi	Cenadi	CZ	38.719	16.415	Conadi	5
Centrache	Centrache	CZ	38.729	16.43	Contrache	5
Cerasi	Reggio di Calabria	RC	38.159	15.751	Ceraso	6
Cerisano	Cerisano	CS	39.276	16.175	Ceriliano	2
Certosa di Santo Stefano del Bosco	Serra San Bruno	VV	38.564	16.319		7
Cerva	Cerva	CZ	39.022	16.745		6
Cessaniti	Cessaniti	VV	38.663	16.026	Cestaniti	5
Cetraro	Cetraro	CS	39.516	15.941		2
Chiaravalle Centrale	Chiaravalle Centrale	CZ	38.68	16.412		7
Ciano	Gerocarne	VV	38.576	16.213		6
Ciaramiti	Ricadi	VV	38.65	15.862		5
Cicala	Cicala	CZ	39.021	16.486		4
Ciminà	Ciminà	RC	38.245	16.141		5
Cinquefrondi	Cinquefrondi	RC	38.417	16.095	Cinquefronti	18
Cirella	Platì	RC	38.232	16.099		5
Cittanova	Cittanova	RC	38.353	16.081	Casalnuovo,Curtoladi, Curtuladi	18
Coccorino	Joppolo	VV	38.604	15.872	Cuccurino	4
Comerconi	Nicotera	VV	38.583	15.933	Commerconi	5
Comparni	Mileto	VV	38.568	16.056	Compami, Camparni, Caneparni	9
Condofuri	Condofuri	RC	38.005	15.858	Condufori, Codafuri, Condofuro	6
Condojanni	Sant'Ilario dello Ionio	RC	38.208	16.196	Condojanni, Condojanne	4
Condrò	Condrò	ME	38.173	15.328		2
Conflenti (Conflenti Inferiore)	Conflenti	CZ	39.071	16.286		1

Conflenti Superiore	Conflenti	CZ	39.067	16.293		1
Conidoni	Briatico	VV	38.698	16.035	Canidoni	5
Cortale	Cortale	CZ	38.838	16.412		7
Cosenza	Cosenza	CS	39.303	16.252		13
Cosoleto Vecchio	Cosoleto	RC	38.284	15.925	Casoleto,Cosolero, Cusoleto, Cosoleti, Cossoleto	15
Cotronei	Cotronei	KR	39.159	16.778		4
Cristò	Taurianova	RC	38.389	16.008		1
Croce Valanidi	Reggio di Calabria	RC	38.055	15.677	Valanidi, Velamide	6
Cropani	Cropani	CZ	38.967	16.782		4
Crosia	Crosia	CS	39.566	16.773		4
Crotone	Crotone	KR	39.081	17.128	Cotrone	7
Curinga	Curinga	CZ	38.826	16.313	Coringa, Caringa	7
Cuti	Rogliano	CS	39.183	16.32		1
Cutro	Cutro	KR	39.033	16.982		9
Cuturella	Cropani	CZ	38.987	16.778		5
Daffinà	Zambrone	VV	38.68	15.951	Dafinà	4
Daffinà	Dinami	VV	38.559	16.105	Daffinità, Dafina	7
Daffinacello	Zambrone	VV	38.677	15.944	Dafinacello	4
Dasà	Dasà	VV	38.564	16.196	Basà	6
Davoli	Davoli	CZ	38.649	16.485		5
Delianuova	Delianuova	RC	38.236	15.918	Pedavali	11
Diamante	Diamante	CS	39.678	15.82		2
Diminniti	Reggio di Calabria	RC	38.173	15.696	Dimminiti, Diminiti	4
Dinami	Dinami	VV	38.528	16.147	Denami	6
Dipignano	Dipignano	CS	39.237	16.252		2
Donnici Inferiore	Cosenza	CS	39.251	16.29	Donnici Sottani	2
Donnici Superiore	Cosenza	CS	39.252	16.301	Donnici soprani	2

Drapia	Drapia	VV	38.664	15.911		5
Drosi	Rizziconi	RC	38.426	15.956	Drosia	13
Engreste	Reggio di Calabria	RC	38.204	15.674	Engristi, Cencristi	3
Fabrizia	Fabrizia	VV	38.486	16.299		4
Fagnano Castello	Fagnano Castello	CS	39.564	16.054		3
Falconara Albanese	Falconara Albanese	CS	39.275	16.091		1
Falerna	Falerna	CZ	39.002	16.173		2
Favelloni	Cessaniti	VV	38.682	16.028		6
Feroleto Antico	Feroleto Antico	CZ	38.962	16.388	Feroleto Superiore	6
Feroleto della Chiesa	Feroleto della Chiesa	RC	38.465	16.064	Ferolito	6
Ferrito	Villa San Giovanni	RC	38.234	15.66	Ferlito	3
Ferruzzano	Ferruzzano	RC	38.039	16.087	Ferrazzano, Perghizzano	5
Figline Vegliaturo	Figline Vegliaturo	CS	39.225	16.331		2
Filandari	Filandari	VV	38.615	16.031	Fialandare, Fialandari	6
Filogaso	Filogaso	VV	38.681	16.228	Filogoso, Filogasi	11
Fitili	Parghelia	VV	38.675	15.931		4
Fiumara (San Nicola)	Fiumara	RC	38.211	15.693	Fiumara de Mori, Fiumara di muro, Cenide	8
Fiumefreddo Bruzio	Fiumefreddo Bruzio	CS	39.235	16.066		2
Flavetto	Rovito	CS	39.311	16.319		2
Fondaco Vecchio	Curinga	CZ	38.813	16.234		3
Fontanelle	Reggio di Calabria	RC	38.175	15.643		2
Fossato Ionico	Montebello Jonico	RC	38.013	15.766		2

Fossato Serralta	Fossato Serralta	CZ	38.995	16.58		4
Francavilla Angitola	Francavilla Angitola	VV	38.777	16.271		6
Francica	Francica	VV	38.616	16.099		10
Fuscaldo	Fuscaldo	CS	39.415	16.03		2
Gagliano	Catanzaro	CZ	38.92	16.562		5
Gagliato	Gagliato	CZ	38.676	16.462		4
Galatoni	Terranova Sappo Minulio	RC	38.339	16.037		5
Galatro	Galatro	RC	38.46	16.109		9
Gallicianò	Condofuri	RC	38.016	15.886		5
Gallico	Reggio di Calabria	RC	38.168	15.657		4
Gallipoli	Gallipoli	LE	40.055	17.988		4
Garavati	Rombiolo	VV	38.593	16	Caravate	7
Garopoli	San Pietro di Caridà	RC	38.526	16.145		6
Gasperina	Gasperina	CZ	38.739	16.508		3
Gasponi	Drapia	VV	38.661	15.904		4
Gerace	Gerace	RC	38.271	16.22		9
Gerocarne	Gerocarne	VV	38.587	16.219	Jerocarne, Perocarne	6
Giampilieri Superiore	Messina	ME	38.069	15.47		5
Giffone	Giffone	RC	38.438	16.149	Giffoni	6
Gimigliano	Gimigliano	CZ	38.973	16.527	Gimiliano	6
Gioia Tauro	Gioia Tauro	RC	38.426	15.899	Gioja, Giojosa	13
Gioiosa Ionica	Gioiosa Ionica	RC	38.332	16.302	Giojosa, Giujosa	6
Girifalco	Girifalco	CZ	38.822	16.425		14
Gizzeria	Gizzeria	CZ	38.981	16.206	Gizarria	5
Grimaldi	Grimaldi	CS	39.142	16.235		2
Grotteria	Grotteria	RC	38.364	16.265		6
Guardavalle	Guardavalle	CZ	38.505	16.505		5
Iatrinoli	Taurianova	RC	38.353	16.007	Jatrinoli	9

Ievoli	Feroleto Antico	CZ	38.972	16.404	Jevoli	4
Ioggi	Santa Caterina Albanese	CS	39.576	16.08	Joggi	2
Isca sullo Ionio	Isca sullo Ionio	CZ	38.6	16.52	Isca	5
Isola di Capo Rizzuto	Isola di Capo Rizzuto	KR	38.959	17.096		6
Jacurso	Jacurso	CZ	38.846	16.38	Jacursi, Iacurso	2
Jonadi	Ionadi	VV	38.627	16.055	Ionadi	6
Joppolo	Joppolo	VV	38.585	15.896		4
Laganadi	Laganadi	RC	38.173	15.741		5
Laghitello	Lago	CS	39.167	16.153		1
Lago	Lago	CS	39.169	16.147		1
Lamezia Terme (Nicastro)	Lamezia Terme	CZ	38.974	16.318		7
Lampazzone	Ricadi	VV	38.631	15.875	Lampazoni, Lampazodi	4
Lappano	Lappano	CS	39.319	16.312		3
Laureana di Borrello	Laureana di Borrello	RC	38.491	16.083	Lauriana, Laureano	12
Laurignano	Dipignano	CS	39.277	16.241	Lorignano	2
Le Castella	Isola di Capo Rizzuto	KR	38.908	17.022		5
Limbadi	Limbadi	VV	38.555	15.966	Limbade	5
Limpidi	Acquaro	VV	38.541	16.174	Limpide, Limapadi, Limbidi	6
Linguaglossa	Linguaglossa	CT	37.842	15.139	Linguagrossa	2
Lipari	Lipari	ME	38.467	14.955		5
Longobardi	Longobardi	CS	39.206	16.076	Longoburgo	3
Longobardi	Vibo Valentia	VV	38.702	16.122	Longovardo	4
Longobucco	Longobucco	CS	39.449	16.611		3
Lubrichi	Santa Cristina d'Aspromonte	RC	38.27	15.95	Lumbrichi	13
Macchia Albanese	San Demetrio Corone	CS	39.58	16.381		2

Magisano	Magisano	CZ	39.013	16.628	Maggisano, Mugisano	4
Magli	Casali del Manco	CS	39.278	16.312		2
Maida	Maida	CZ	38.858	16.365		12
Maierato	Maierato	VV	38.706	16.191	Majorato	7
Malito	Malito	CS	39.154	16.248		2
Mammola	Mammola	RC	38.362	16.24	Mamola	6
Mandaradoni	Limbadi	VV	38.574	15.965	Mandarano	3
Mandaradoni	Briatico	VV	38.683	15.985	Mondaradoni	5
Mangone	Mangone	CS	39.203	16.334		2
Mantineo	Cessaniti	VV	38.683	16.057	Mandineo	5
Maranise	Fossato Serralta	CZ	39.012	16.577		4
Marano Marchesato	Marano Marchesato	CS	39.313	16.172		3
Marcedusa	Marcedusa	CZ	39.027	16.836		5
Marcellinara	Marcellinara	CZ	38.928	16.494	Marcinara	8
Maropati	Maropati	RC	38.441	16.097		7
Martirano	Martirano	CZ	39.08	16.248	Martorano	3
Martone	Martone	RC	38.354	16.288	Martoni, Mastoni	4
Marzi	Marzi	CS	39.171	16.306		2
Melicuccà	Dinami	VV	38.536	16.158	Melicucca	6
Melicuccà	Melicuccà	RC	38.302	15.881	Melicucca del Priorato	4
Melicucco	Melicucco	RC	38.433	16.06		8
Melito di Porto Salvo	Melito di Porto Salvo	RC	37.92	15.784		5
Mesiano	Filandari	VV	38.624	16.011		10
Mesoraca	Mesoraca	KR	39.077	16.789	Mesuraca, Misuraca	4
Messignadi	Oppido Mamertina	RC	38.297	15.997	Mesignadi, Mesignati	7
Messina	Messina	ME	38.185	15.555		28
Mezzocasale	San Gregorio d'Ippona	VV	38.646	16.106		4

Miglianò	Gerocarne	VV	38.591	16.197	Migliana, Meliano	7
Miglierina	Miglierina	CZ	38.947	16.472	Migliarina, Magliarina	4
Migliuso	Serrastretta	CZ	38.954	16.433		4
Milazzo	Milazzo	ME	38.224	15.24	Melazzo	6
Mileto [vecchio]	Mileto	VV	38.593	16.08		18
Mili San Pietro	Messina	ME	38.126	15.488	Sampiero	2
Mineo	Mineo	CT	37.266	14.691		1
Modica	Modica	RG	36.858	14.761		1
Moladi	Rombiolo	VV	38.59	16.002		8
Molochiello	Molochio	RC	38.31	16.028	Moloquiello	6
Molochio	Molochio	RC	38.308	16.032		9
Monasterace	Monasterace	RC	38.453	16.551	Monastarace, Monesterace	4
Monforte San Giorgio	Monforte San Giorgio	ME	38.155	15.382		6
Monopoli	Monopoli	BA	40.951	17.296		3
Monsoreto	Dinami	VV	38.515	16.164		6
Montalto Uffugo	Montalto Uffugo	CS	39.405	16.158		2
Montauro	Montauro	CZ	38.747	16.512		4
Montebello Ionico	Montebello Jonico	RC	37.982	15.758		5
Montepaone	Montepaone	CZ	38.722	16.497	Montepavone	5
Monterosso Calabro	Monterosso Calabro	VV	38.717	16.289		4
Montesanto	Maierato	VV	38.708	16.238		5
Montesoro	Filadelfia	VV	38.816	16.292		4
Morano Calabro	Morano Calabro	CS	39.844	16.136		1
Mosorrofa	Reggio di Calabria	RC	38.098	15.724	Mosorroma	7
Motta	Zumpano	CS	39.31	16.286	Motta Zumpano	1
Motta Filocastro	Limbadi	VV	38.571	15.975		5
Motta San Giovanni	Motta San Giovanni	RC	38.002	15.694		6

Mottafollone	Mottafollone	CS	39.648	16.064		2
Motticella	Bruzzano Zeffirio	RC	38.025	16.055	Motta bruzzano	4
Musalà	Campo Calabro	RC	38.214	15.671	Musola	3
Mutari	Francica	VV	38.625	16.14		5
Nao	Ionadi	VV	38.628	16.062		7
Napoli	Napoli	NA	40.849	14.25		11
Nasiti	Reggio di Calabria	RC	38.112	15.696		5
Natile Vecchio	Careri	RC	38.188	16.051		4
Nicastrello	Capistrano	VV	38.681	16.289		4
Nicotera	Nicotera	VV	38.551	15.938		8
Noce	Sorbo San Basile	CZ	39.017	16.573		3
Nocera Terinese	Nocera Terinese	CZ	39.036	16.16		2
Olivadi	Olivadi	CZ	38.725	16.424		4
Oppido Mamertina	Oppido Mamertina	RC	38.291	15.985	Opido	20
Orsigliadi	Ricadi	VV	38.629	15.861		4
Orsigliadi	Rombiolo	VV	38.6	16.003		7
Ortì Superiore	Reggio di Calabria	RC	38.15	15.724	Urti	6
Otranto	Otranto	LE	40.144	18.491		3
Palermiti	Palermiti	CZ	38.75	16.454		4
Palermo	Palermo	PA	38.115	13.362		2
Palinudo	Bianchi	CS	39.114	16.422	Paliduro	1
Palinuro	Centola	SA	40.033	15.288		2
Palizzi	Palizzi	RC	37.966	15.986		4
Palmi	Palmi	RC	38.358	15.849		19
Panaia	Filogaso	VV	38.68	16.234	Panaja	7
Panaia	Spilinga	VV	38.623	15.892	Panaya	4
Pannaconi	Cessaniti	VV	38.692	16.041	Pannacone	4
Paola	Paola	CS	39.36	16.041	Paula	3
Papaglionti	Zungri	VV	38.645	16.016	Papaglionte	7

Papanice	Crotone	KR	39.071	17.03		6
Paracorio	Delianuova	RC	38.234	15.92	Palagorio	11
Paradisoni	Briatico	VV	38.701	16.045		4
Paravati	Mileto	VV	38.591	16.06	Paravadi	8
Parghelia	Parghelia	VV	38.681	15.923	Parghili	7
Patti	Patti	ME	38.138	14.966		4
Pavigliana	Reggio di Calabria	RC	38.104	15.714	Pattigliana, Paviglione, Pavigliano	5
Pazzano	Pazzano	RC	38.475	16.452		7
Pedace	Casali del Manco	CS	39.274	16.34	Partocise	3
Pellaro	Reggio di Calabria	RC	38.025	15.656		3
Pentedattilo	Melito di Porto Salvo	RC	37.953	15.762		5
Pentimele	Reggio di Calabria	RC	38.139	15.659		2
Pentone	Pentone	CZ	38.986	16.583	Pentoni	4
Perito	Casali del Manco	CS	39.273	16.33		2
Perlupo	Reggio di Calabria	RC	38.132	15.723		5
Pernocarello	Rombiolo	VV	38.613	16.007		7
Pernocari	Rombiolo	VV	38.61	16.006		7
Petilia Policastro	Petilia Policastro	KR	39.112	16.789		4
Petrizzi	Petrizzi	CZ	38.701	16.474		6
Petronà	Petronà	CZ	39.043	16.758		5
Pezzo Inferiore	Villa San Giovanni	RC	38.231	15.638		3
Piale	Villa San Giovanni	RC	38.224	15.648		3
Piane Crati	Piane Crati	CS	39.233	16.325		2
Pianopoli	Pianopoli	CZ	38.954	16.389	Feroleto Piano, Feroleto Inferiore	5

Pietrafitta	Pietrafitta	CS	39.26	16.34		3
Pietrapennata	Palizzi	RC	37.984	16.008		3
Pimene	Maierato	VV	38.726	16.213	Case Pimé	4
Piscopio	Vibo Valentia	VV	38.661	16.113		6
Pizzinni	Filandari	VV	38.626	16.048		7
Pizzo	Pizzo	VV	38.733	16.159		11
Pizzoni	Pizzoni	VV	38.623	16.252	Pizzone, Pizzola	7
Placanica	Placanica	RC	38.414	16.451		4
Plaesano	Feroleto della Chiesa	RC	38.473	16.077	Plaisani, Plaisiano	6
Platania	Platania	CZ	39.005	16.32		5
Platì	Platì	RC	38.221	16.044	Mottaplati	3
Podargoni	Reggio di Calabria	RC	38.162	15.781	Podargone, Perdagoni	6
Poliolo	Polia	VV	38.753	16.31		5
Polistena	Polistena	RC	38.406	16.076		17
Pongadi	Francica	VV	38.615	16.136		5
Porticato	Villa San Giovanni	RC	38.234	15.649		2
Portigliola	Portigliola	RC	38.228	16.202		4
Porto Salvo	Vibo Valentia	VV	38.706	16.08	P. Salvo	1
Potami	Gerocarne	VV	38.579	16.207		6
Potenzoni	Briatico	VV	38.689	16.003		5
Pozzo di Gotto	Barcellona Pozzo di Gotto	ME	38.152	15.232		3
Preitoni	Nicotera	VV	38.576	15.922		5
Presinaci	Rombiolo	VV	38.607	16.018		7
Pronia	Gerocarne	VV	38.578	16.189		6
Pulsano	Dipignano	CS	39.253	16.238		2
Radicena	Taurianova	RC	38.355	16.017		13
Randazzo	Randazzo	CT	37.877	14.948		3
Reggio di Calabria	Reggio di Calabria	RC	38.108	15.647		21
Rende	Rende	CS	39.331	16.183		2

Riace	Riace	RC	38.418	16.482		4
Ricadi	Ricadi	VV	38.626	15.867		4
Rizziconi	Rizziconi	RC	38.411	15.959	Riziconi	8
Rocca Angitola	Maierato	VV	38.748	16.223	Rocca	1
Roccabernarda	Roccabernarda	KR	39.133	16.868	Rocca Bernalda	6
Roccaforte del Greco	Roccaforte del Greco	RC	38.045	15.9		4
Roccavaldina	Roccavaldina	ME	38.182	15.373	Valdino	3
Roccella Jonica	Roccella Ionica	RC	38.324	16.405		9
Roccelletta	Borgia	CZ	38.81	16.601		2
Roggiano Gravina	Roggiano Gravina	CS	39.615	16.157	Ruggiano	2
Roghudi Vecchio	Roghudi	RC	38.049	15.916		4
Rogliano	Rogliano	CS	39.178	16.323		2
Rombiolo	Rombiolo	VV	38.596	16.005		7
Rometta	Rometta	ME	38.172	15.414	Rametta	5
Rosalì	Reggio di Calabria	RC	38.198	15.68		4
Rosarno	Rosarno	RC	38.487	15.976		15
Rose	Rose	CS	39.399	16.288		2
Rossano	Rossano	CS	39.574	16.635		1
Rota Greca	Rota Greca	CS	39.467	16.113		2
Rovella	Zumpano	CS	39.303	16.288		3
Rovito	Rovito	CS	39.308	16.321		2
Salerno	Salerno	SA	40.68	14.76		1
Salice Calabro	Reggio di Calabria	RC	38.197	15.659		2
Sambatello	Reggio di Calabria	RC	38.178	15.692		6
Sambiase	Lamezia Terme	CZ	38.966	16.282	S. Biagio	4
Samo	Samo	RC	38.073	16.058	Crepacore, Precacori, Precacore	5
San Basilio	Pizzoni	VV	38.623	16.25	S. Basile	6

San Benedetto in Guarano	San Pietro in Guarano	CS	39.339	16.302		2
San Benedetto Ullano	San Benedetto Ullano	CS	39.426	16.123		2
San Calogero	San Calogero	VV	38.573	16.024	S. Caloggero	5
San Cono	Cessaniti	VV	38.683	16.013		4
San Costantino	Briatico	VV	38.705	16.002		4
San Costantino Calabro	San Costantino Calabro	VV	38.631	16.073		4
San Domenico	Reggio di Calabria	RC	38.203	15.676		2
San Fili	San Fili	CS	39.338	16.144		2
San Fili	Melicucco	RC	38.456	16.034		5
San Filippo Superiore	Messina	ME	38.166	15.5		1
San Floro	San Floro	CZ	38.837	16.519		6
San Giorgio	Palmi	RC	38.356	15.853		2
San Giorgio Morgeto	San Giorgio Morgeto	RC	38.386	16.107	Sangiorgis	11
San Giovanni	Albi	CZ	39.018	16.594		4
San Giovanni	Zambrone	VV	38.675	15.973		4
San Giovanni	Mileto	VV	38.584	16.084		7
San Giovanni di Gerace	San Giovanni di Gerace	RC	38.364	16.279		4
San Giovanni di Sambatello	Reggio di Calabria	RC	38.169	15.689		4
San Gregorio d'Ippona	San Gregorio d'Ippona	VV	38.643	16.105	San Gregorio di mezzo, San Gregorio superiore	4
San Leo Vecchio	Briatico	VV	38.711	16.02		5
San Lorenzo	San Lorenzo	RC	38.01	15.834		8
San Luca	San Luca	RC	38.146	16.064		3
San Luca	Montebello Jonico	RC	38.009	15.75		2
San Lucido	San Lucido	CS	39.307	16.049		6

San Mango d'Aquino	San Mango d'Aquino	CZ	39.058	16.191		2
San Marco	Cessaniti	VV	38.675	16.01		4
San Marco Argentano	San Marco Argentano	CS	39.556	16.119		3
San Martino	Spadafora	ME	38.207	15.39		1
San Martino	Taurianova	RC	38.361	15.975		7
San Mauro Marchesato	San Mauro Marchesato	KR	39.103	16.925		6
San Nicola	Ardore	RC	38.202	16.145		5
San Nicola da Crissa	San Nicola da Crissa	VV	38.663	16.285		4
San Nicola de' Legistis	Limbadi	VV	38.561	15.992		5
San Nicolò	Ricadi	VV	38.633	15.851	S. Niccolò	4
San Pier Niceto	San Pier Niceto	ME	38.158	15.352	San Piero di Monforte	2
San Pietro	Magisano	CZ	39.012	16.612		4
San Pietro	San Calogero	VV	38.573	16.037		6
San Pietro a Maida	San Pietro a Maida	CZ	38.846	16.345		4
San Pietro Apostolo	San Pietro Apostolo	CZ	39.003	16.467	San Pietro di Tiriolo	2
San Pietro di Bivona	Vibo Valentia	VV	38.703	16.111		4
San Pietro di Caridà (Caridà)	San Pietro di Caridà	RC	38.523	16.135		8
San Pietro in Amantea	San Pietro in Amantea	CS	39.136	16.112		4
San Pietro in Guarano	San Pietro in Guarano	CS	39.342	16.311	San Pietro del Corno	2
San Procopio	San Procopio	RC	38.281	15.891		10
San Roberto	San Roberto	RC	38.211	15.736	Fossa S. Roberto	4
San Sisto dei Valdesi	San Vincenzo La Costa	CS	39.377	16.15		2
San Sostene	San Sostene	CZ	38.636	16.487	S. Soste	4
San Sosti	San Sosti	CS	39.66	16.028	S. Soste	2

San Vito sullo Ionio	San Vito sullo Ionio	CZ	38.71	16.408		4
Santa Barbara	Pizzoni	VV	38.639	16.209		6
Santa Caterina dello Ionio	Santa Caterina dello Ionio	CZ	38.534	16.521		5
Santa Cristina d'Aspromonte	Santa Cristina d'Aspromonte	RC	38.255	15.97		15
Santa Domenica	Ricadi	VV	38.663	15.866		5
Santa Giorgia	Scido	RC	38.253	15.936		7
Santa Lucia del Mela	Santa Lucia del Mela	ME	38.14	15.281		2
Santa Severina	Santa Severina	KR	39.147	16.913		6
Santa Sofia d'Epiro	Santa Sofia d'Epiro	CS	39.546	16.329		3
Sant'Agata	Reggio di Calabria	RC	38.091	15.721		6
Sant'Agata del Bianco	Sant'Agata del Bianco	RC	38.091	16.083		4
Sant'Agata di Esaro	Sant'Agata di Esaro	CS	39.619	15.983		3
Sant'Alessio in Aspromonte	Sant'Alessio in Aspromonte	RC	38.172	15.758		4
Sant'Andrea Apostolo dello Ionio	Sant'Andrea Apostolo dello Ionio	CZ	38.622	16.528		5
Sant'Angelo	Gerocarne	VV	38.611	16.169		6
Sant'Anna	Seminara	RC	38.322	15.887		6
Sant'Elia	Palmi	RC	38.339	15.846		2
Sant'Eufemia	Lamezia Terme	CZ	38.92	16.254	S. Eufemia del Golfo	5
Sant'Eufemia d'Aspromonte	Sant'Eufemia d'Aspromonte	RC	38.263	15.857	Santa Eufemia di Sinopoli	11
Sant'Ilario dello Ionio	Sant'Ilario dello Ionio	RC	38.218	16.195		4
Sant'Ippolito	Cosenza	CS	39.266	16.295		2
Santo Stefano di Rogliano	Santo Stefano di Rogliano	CS	39.193	16.324		2

Santo Stefano in Aspromonte	Santo Stefano in Aspromonte	RC	38.168	15.789		5
Sant'Onofrio	Sant'Onofrio	VV	38.695	16.144		7
Sartano	Torano Castello	CS	39.51	16.178		2
Satriano	Satriano	CZ	38.667	16.482		5
Savuci	Fossato Serralta	CZ	39.009	16.582	Sauci	4
Savuto	Cleto	CS	39.071	16.164		2
Scala Coeli	Scala Coeli	CS	39.445	16.89		4
Scalea	Scalea	CS	39.814	15.792		1
Scaletta Superiore	Scaletta Zanclea	ME	38.051	15.466		2
Scaliti	Filandari	VV	38.614	16.042	Scalite	7
Scandale	Scandale	KR	39.121	16.96	Gaudioso	6
Schindilifà	Reggio di Calabria	RC	38.164	15.76		5
Sciacca	Sciacca	AG	37.508	13.083		1
Sciconi	Briatico	VV	38.691	16.031		5
Scido	Scido	RC	38.245	15.933		10
Scilla	Scilla	RC	38.253	15.717		15
Scrofario	Terranova Sappo Minulio	RC	38.335	16.018	Scrofonio	6
Sellia	Sellia	CZ	38.981	16.629		5
Seminara	Seminara	RC	38.335	15.872		16
Serra d'Aiello	Serra d'Aiello	CS	39.089	16.129		2
Serra Pedace	Casali del Manco	CS	39.277	16.346		2
Serra San Bruno	Serra San Bruno	VV	38.576	16.33		6
Serrastretta	Serrastretta	CZ	39.013	16.416		4
Serrata	Serrata	RC	38.512	16.101		8
Sersale	Sersale	CZ	39.011	16.728		5
Settingiano	Settingiano	CZ	38.913	16.514		4
Siderno Superiore	Siderno	RC	38.289	16.269		5
Simbario	Simbario	VV	38.611	16.335		6

Simeri	Simeri Crichi	CZ	38.932	16.662	Simmari	4
Simeri Crichi (Crichi)	Simeri Crichi	CZ	38.954	16.639		4
Simiatoni	Acquaro	VV	38.558	16.179	Semiatone, Signatoni, Semiateni	6
Sinopoli (Superiore)	Sinopoli	RC	38.264	15.878		8
Sinopoli Inferiore	Sinopoli	RC	38.261	15.886		10
Sinopoli Vecchio	Sinopoli	RC	38.281	15.908	Sinopoli Greco	14
Siracusa	Siracusa	SR	37.073	15.286		2
Sitizano	Cosoleto	RC	38.281	15.939	Sitizzano, Sitizani	9
Sorbo San Basile	Sorbo San Basile	CZ	39.019	16.569		6
Sorianello	Sorianello	VV	38.592	16.233		5
Soriano Calabro	Soriano Calabro	VV	38.598	16.23		16
Soverato Superiore	Soverato	CZ	38.688	16.53		4
Soveria Simeri	Soveria Simeri	CZ	38.946	16.679		5
Spadola	Spadola	VV	38.603	16.337		7
Spezzano della Sila	Spezzano della Sila	CS	39.299	16.34	Spezzano Grande	2
Spilinga	Spilinga	VV	38.627	15.905		4
Squillace	Squillace	CZ	38.781	16.519		10
Staiti	Staiti	RC	37.999	16.034		4
Stalettì	Stalettì	CZ	38.764	16.54	Stallatti, Stalletti	5
Stefanaconi	Stefanaconi	VV	38.673	16.122	Stefanacone	7
Stelletanone	Laureana di Borrello	RC	38.485	16.084	Stillitanone, Stiritantone, Stillitanoni	7
Stignano	Stignano	RC	38.417	16.471		4
Stilo	Stilo	RC	38.477	16.468		8
Straorino	Reggio di Calabria	RC	38.132	15.747	Stravorino	5

Stromboli (San Vincenzo)	Lipari	ME	38.806	15.235	Strongoli	4
Taverna	Taverna	CZ	39.02	16.582		4
Terranova Sappo Minulio	Terranova Sappo Minulio	RC	38.321	16.007		16
Terrati	Lago	CS	39.134	16.142		2
Terravecchia	Terravecchia	CS	39.465	16.946		3
Terreti	Reggio di Calabria	RC	38.119	15.711		5
Tessano	Dipignano	CS	39.256	16.241		2
Tindari	Patti	ME	38.141	15.045		1
Tiriolo	Tiriolo	CZ	38.947	16.509		7
Torano Castello	Torano Castello	CS	39.504	16.147		3
Torre di Ruggiero	Torre di Ruggiero	CZ	38.651	16.372		4
Torre Faro	Messina	ME	38.266	15.646		6
Trecroci	Polia	VV	38.755	16.315	Polia Antica	7
Trenta	Casali del Manco	CS	39.283	16.321		3
Tresilico	Oppido Mamertina	RC	38.299	15.983	Trisilico, Tricilico	9
Triparni	Vibo Valentia	VV	38.681	16.067		4
Tritanti	Maropati	RC	38.448	16.101	Tiritanti, Siritanti	5
Trizzino	Reggio di Calabria	RC	38.122	15.709		6
Tropea	Tropea	VV	38.675	15.899		11
Vaccarizzo	Montalto Uffugo	CS	39.41	16.135		2
Valdina	Valdina	ME	38.193	15.371		2
Vallefiorita	Vallefiorita	CZ	38.775	16.461	Sant'Elia	6
Vallelonga	Vallelonga	VV	38.646	16.294		5
Varapodio	Varapodio	RC	38.315	15.984	Varapodi	8
Vatoni	Taurianova	RC	38.378	16.014	Vatome	1
Vazzano	Vazzano	VV	38.632	16.247	Vezzano, Vassano	7

Vena di Maida	Maida	CZ	38.888	16.407		4
Vena Media	Vibo Valentia	VV	38.669	16.057	Vena inferiore	4
Vena Superiore	Vibo Valentia	VV	38.66	16.057		4
Venetico	Venetico	ME	38.193	15.381		3
Vibo Valentia	Vibo Valentia	VV	38.673	16.103	Monteleone, Monteleone di Calabria, Vibona Valentia, Montelione	12
Vietri di Potenza	Vietri di Potenza	PZ	40.599	15.509		1
Vietri sul Mare	Vietri sul Mare	SA	40.67	14.729		1
Villa San Giuseppe	Reggio di Calabria	RC	38.187	15.671		3
Vinco	Reggio di Calabria	RC	38.108	15.723		5
Vincolise	Magisano	CZ	39.018	16.612		4
Zaccanopoli	Zaccanopoli	VV	38.664	15.929		4
Zagarise	Zagarise	CZ	38.999	16.663		4
Zambrone	Zambrone	VV	38.699	15.991		5
Zammarò	San Gregorio d'Ippona	VV	38.651	16.107	Tammarò	5
Zangarona	Lamezia Terme	CZ	38.97	16.344	Zingarona, Zangarone	5
Zumpano	Zumpano	CS	39.31	16.291		2
Zungri	Zungri	VV	38.654	15.984		7
Zurgonadio	Oppido Mamertina	RC	38.298	15.979		6

Appendix B

The following tables report the Macroseismic Data Points for the five earthquakes of the 1783 seismic sequence, together with a table containing intensity data of uncertain date. For each locality, intensity values are provided in both the EMS-98 and MCS scales. Cumulative intensities are marked with an asterisk (*). The final table lists additional localities identified.

Table 1. MACROSEISMIC FIELD – 5 February 1783

MDPs 438

Locality	Province	Lat.	Long.	Intensity [EMS-98]	Intensity [MCS]
Panaia	VV	38.68	16.234	10	10-11
Armo	RC	38.07	15.715	10	10-11
Cardeto	RC	38.084	15.768	10	10-11
Filogaso	VV	38.681	16.228	10	10-11
Fossato Ionico	RC	38.013	15.766	10	10-11
Mezzocasale	VV	38.646	16.106	10	10-11
Mosorrofa	RC	38.098	15.724	10	10-11
Ortì Superiore	RC	38.15	15.724	10	10-11
Pavigliana	RC	38.104	15.714	10	10-11
Perlupo	RC	38.132	15.723	10	10-11
Piscopio	VV	38.661	16.113	10	10-11
San Gregorio d'Ippona	VV	38.643	16.105	10	10-11
San Pietro di Bivona	VV	38.703	16.111	10	10-11
Schindilifà	RC	38.164	15.76	10	10-11
Stefanaconi	VV	38.673	16.122	10	10-11
Straorino	RC	38.132	15.747	10	10-11
Triparni	VV	38.681	16.067	10	10-11
Vena Media	VV	38.669	16.057	10	10-11
Vena Superiore	VV	38.66	16.057	10	10-11
Mileto [vecchio]	VV	38.593	16.08	10	10-11
Acquaro	RC	38.268	15.899	10	10-11
Bagnara Calabra	RC	38.286	15.805	10	10-11
Cinquefrondi	RC	38.417	16.095	10	10-11
Cittanova	RC	38.353	16.081	10	10-11
Drosi	RC	38.426	15.956	10	10-11
Galatro	RC	38.46	16.109	10	10-11
Melicucco	RC	38.433	16.06	10	10-11
Plaesano	RC	38.473	16.077	10	10-11
Polistena	RC	38.406	16.076	10	10-11
San Pietro di Caridà (Caridà)	RC	38.523	16.135	10	10-11
San Procopio	RC	38.281	15.891	10	10-11
Sant'Eufemia d'Aspromonte	RC	38.263	15.857	10	10-11
Sinopoli (Superiore)	RC	38.264	15.878	10	10-11

Sinopoli Inferiore	RC	38.261	15.886	10	10-11
Sinopoli Vecchio	RC	38.281	15.908	10	10-11
Arena	VV	38.562	16.209	10	10-11
Bellantone	RC	38.497	16.091	10	10-11
Borrello	RC	38.513	16.069	10	10-11
Briatico Vecchio	VV	38.707	16.023	10	10-11
Candidoni	RC	38.505	16.086	10	10-11
Conidoni	VV	38.698	16.035	10	10-11
Daffinà	VV	38.559	16.105	10	10-11
Dinami	VV	38.528	16.147	10	10-11
Engreste	RC	38.204	15.674	10	10-11
Favelloni	VV	38.682	16.028	10	10-11
Garopoli	RC	38.526	16.145	10	10-11
Gerocarne	VV	38.587	16.219	10	10-11
Giffone	RC	38.438	16.149	10	10-11
Gioia Tauro	RC	38.426	15.899	10	10-11
Mantineo	VV	38.683	16.057	10	10-11
Melicuccà	VV	38.536	16.158	10	10-11
Messignadi	RC	38.297	15.997	10	10-11
Monsoreto	VV	38.515	16.164	10	10-11
Pannaconi	VV	38.692	16.041	10	10-11
Paradisoni	VV	38.701	16.045	10	10-11
Paravati	VV	38.591	16.06	10	10-11
San Cono	VV	38.683	16.013	10	10-11
San Costantino	VV	38.705	16.002	10	10-11
San Marco	VV	38.675	16.01	10	10-11
Serrata	RC	38.512	16.101	10	10-11
Stelletanone	RC	38.485	16.084	10	10-11
Tritanti	RC	38.448	16.101	10	10-11
Cosoleto Vecchio	RC	38.284	15.925	10	10-11
Delianuova	RC	38.236	15.918	10	10-11
Iatrinoli	RC	38.353	16.007	10	10-11
Lubrichi	RC	38.27	15.95	10	10-11
Molochio	RC	38.308	16.032	10	10-11
Oppido Mamertina	RC	38.291	15.985	10	10-11
Palmi	RC	38.358	15.849	10	10-11
Paracorio	RC	38.234	15.92	10	10-11
Rizziconi	RC	38.411	15.959	10	10-11
Rosarno	RC	38.487	15.976	10	10-11
San Martino	RC	38.361	15.975	10	10-11
Santa Cristina d'Aspromonte	RC	38.255	15.97	10	10-11
Sant'Anna	RC	38.322	15.887	10	10-11
Sant'Elia	RC	38.339	15.846	10	10-11
Santo Stefano in Aspromonte	RC	38.168	15.789	10	10-11
Scido	RC	38.245	15.933	10	10-11
Seminara	RC	38.335	15.872	10	10-11

Sitizano	RC	38.281	15.939	10	10-11
Terranova Sappo Minulio	RC	38.321	16.007	10	10-11
Tresilico	RC	38.299	15.983	10	10-11
Varapodio	RC	38.315	15.984	10	10-11
Radicena	RC	38.355	16.017	10	10-11
Calabrò	VV	38.613	16.076	10	10-11
Caroni	VV	38.567	15.96	10	10-11
Comerconi	VV	38.583	15.933	10	10-11
Diminniti	RC	38.173	15.696	10	10-11
Ferruzzano	RC	38.039	16.087	10	10-11
Filandari	VV	38.615	16.031	10	10-11
Francica	VV	38.616	16.099	10	10-11
Galatoni	RC	38.339	16.037	10	10-11
Garavati	VV	38.593	16	10	10-11
Limbadi	VV	38.555	15.966	10	10-11
Mandaradoni	VV	38.574	15.965	10	10-11
Mandaradoni	VV	38.683	15.985	10	10-11
Molochiello	RC	38.31	16.028	10	10-11
Motta Filocastro	VV	38.571	15.975	10	10-11
Mutari	VV	38.625	16.14	10	10-11
Orsigliadi	VV	38.6	16.003	10	10-11
Rombiolo	VV	38.596	16.005	10	10-11
Sambatello	RC	38.178	15.692	10	10-11
San Calogero	VV	38.573	16.024	10	10-11
San Costantino Calabro	VV	38.631	16.073	10	10-11
San Fili	RC	38.456	16.034	10	10-11
San Giovanni	VV	38.584	16.084	10	10-11
San Giovanni di Sambatello	RC	38.169	15.689	10	10-11
San Nicola de' Legistis	VV	38.561	15.992	10	10-11
Santa Giorgia	RC	38.253	15.936	10	10-11
Sant'Alessio in Aspromonte	RC	38.172	15.758	10	10-11
Scaliti	VV	38.614	16.042	10	10-11
Scrofario	RC	38.335	16.018	10	10-11
Zurgonadio	RC	38.298	15.979	10	10-11
Pongadi	VV	38.615	16.136	10	10-11
San Giorgio Morgeto	RC	38.386	16.107	9-10	9-10
Castellace	RC	38.315	15.94	9-10	9-10
Monterosso Calabro	VV	38.717	16.289	9-10	9-10
Nasiti	RC	38.112	15.696	9-10	9-10
Africo [vecchio]	RC	38.065	15.98	9-10	9-10
Amendolea [vecchia]	RC	37.988	15.892	9-10	9-10
Anoia (Inferiore)	RC	38.435	16.08	9-10	9-10
Anoia Superiore	RC	38.432	16.097	9-10	9-10
Acquaro	VV	38.555	16.189	9-10	9-10
Bracciara	VV	38.565	16.168	9-10	9-10
Cannitello	RC	38.234	15.657	9-10	9-10

Ciano	VV	38.576	16.213	9-10	9-10
Dasà	VV	38.564	16.196	9-10	9-10
Ferrito	RC	38.234	15.66	9-10	9-10
Limpidi	VV	38.541	16.174	9-10	9-10
Maropati	RC	38.441	16.097	9-10	9-10
Miglianò	VV	38.591	16.197	9-10	9-10
Pezzo Inferiore	RC	38.231	15.638	9-10	9-10
Piale	RC	38.224	15.648	9-10	9-10
Porticato	RC	38.234	15.649	9-10	9-10
Potami	VV	38.579	16.207	9-10	9-10
Pronia	VV	38.578	16.189	9-10	9-10
Rosalì	RC	38.198	15.68	9-10	9-10
San Domenico	RC	38.203	15.676	9-10	9-10
Simiatoni	VV	38.558	16.179	9-10	9-10
Comparni	VV	38.568	16.056	9-10	9-10
Cristò	RC	38.389	16.008	9-10	9-10
Feroleto della Chiesa	RC	38.465	16.064	9-10	9-10
Melicuccà	RC	38.302	15.881	9-10	9-10
Mesiano	VV	38.624	16.011	9-10	9-10
Nao	VV	38.628	16.062	9-10	9-10
San Pietro	VV	38.573	16.037	9-10	9-10
Sant'Agata	RC	38.091	15.721	9	9
Longobardi	VV	38.702	16.122	9	9
Cessaniti	VV	38.663	16.026	9	9
San Giorgio	RC	38.356	15.853	9	9
Pimene	VV	38.726	16.213	8-9	8-9
Pizzo	VV	38.733	16.159	8-9	8-9
Sant'Onofrio	VV	38.695	16.144	8-9	8-9
Messina	ME	38.185	15.555	8-9	8-9
Serra San Bruno	VV	38.576	16.33	8-9	8-9
Reggio di Calabria	RC	38.108	15.647	8-9	8-9
Alafito	VV	38.672	15.919	8-9	8-9
Arasì	RC	38.139	15.737	8-9	8-9
Barbalaconi	VV	38.634	15.873	8-9	8-9
Brattirò	VV	38.642	15.887	8-9	8-9
Brivadi	VV	38.636	15.856	8-9	8-9
Carciadi	VV	38.628	15.908	8-9	8-9
Caria	VV	38.646	15.905	8-9	8-9
Ciaramiti	VV	38.65	15.862	8-9	8-9
Croce Valanidi	RC	38.055	15.677	8-9	8-9
Daffinà	VV	38.68	15.951	8-9	8-9
Daffinacello	VV	38.677	15.944	8-9	8-9
Drapia	VV	38.664	15.911	8-9	8-9
Fitili	VV	38.675	15.931	8-9	8-9
Gasponi	VV	38.661	15.904	8-9	8-9
Gioiosa Ionica	RC	38.332	16.302	8-9	8-9

Lampazzone	VV	38.631	15.875	8-9	8-9
Orsigliadi	VV	38.629	15.861	8-9	8-9
Panaia	VV	38.623	15.892	8-9	8-9
Parghelia	VV	38.681	15.923	8-9	8-9
Podargoni	RC	38.162	15.781	8-9	8-9
Ricadi	VV	38.626	15.867	8-9	8-9
San Giovanni	VV	38.675	15.973	8-9	8-9
San Nicolò	VV	38.633	15.851	8-9	8-9
Santa Domenica	VV	38.663	15.866	8-9	8-9
Siderno Superiore	RC	38.289	16.269	8-9	8-9
Spilinga	VV	38.627	15.905	8-9	8-9
Terreti	RC	38.119	15.711	8-9	8-9
Tropea	VV	38.675	15.899	8-9	8-9
Zaccanopoli	VV	38.664	15.929	8-9	8-9
Zambrone	VV	38.699	15.991	8-9	8-9
Zammarò	VV	38.651	16.107	8-9	8-9
Bagaladi	RC	38.026	15.821	8-9	8-9
Bova	RC	37.994	15.932	8-9	8-9
Condofuri	RC	38.005	15.858	8-9	8-9
Gallicianò	RC	38.016	15.886	8-9	8-9
Motta San Giovanni	RC	38.002	15.694	8-9	8-9
Pellaro	RC	38.025	15.656	8-9	8-9
Pentedattilo	RC	37.953	15.762	8-9	8-9
Roccaforte del Greco	RC	38.045	15.9	8-9	8-9
Roghudi Vecchio	RC	38.049	15.916	8-9	8-9
San Lorenzo	RC	38.01	15.834	8-9	8-9
Laureana di Borrello	RC	38.491	16.083	8-9	8-9
Rometta	ME	38.172	15.414	8-9	8-9
Scilla	RC	38.253	15.717	8-9	8-9
Acciarello	RC	38.212	15.638	8-9	8-9
Calimera	VV	38.556	16.018	8-9	8-9
Campo Calabro	RC	38.213	15.659	8-9	8-9
Catona	RC	38.185	15.643	8-9	8-9
Certosa di Santo Stefano del Bosco	VV	38.564	16.319	8-9	8-9
Coccorino	VV	38.604	15.872	8-9	8-9
Fiumara (San Nicola)	RC	38.211	15.693	8-9	8-9
Fontanelle	RC	38.175	15.643	8-9	8-9
Joppolo	VV	38.585	15.896	8-9	8-9
Musalà	RC	38.214	15.671	8-9	8-9
Salice Calabro	RC	38.197	15.659	8-9	8-9
San Roberto	RC	38.211	15.736	8-9	8-9
Arzona	VV	38.622	16.046	8-9	8-9
Badia	VV	38.564	15.956	8-9	8-9
Bruzzano Vecchio	RC	38.021	16.077	8-9	8-9
Calanna	RC	38.183	15.724	8-9	8-9
Caroniti	VV	38.593	15.905	8-9	8-9

Gallico	RC	38.168	15.657	8-9	8-9
Laganadi	RC	38.173	15.741	8-9	8-9
Moladi	VV	38.59	16.002	8-9	8-9
Nicotera	VV	38.551	15.938	8-9	8-9
Papaglionti	VV	38.645	16.016	8-9	8-9
Pernocarello	VV	38.613	16.007	8-9	8-9
Pernocari	VV	38.61	16.006	8-9	8-9
Pizzinni	VV	38.626	16.048	8-9	8-9
Preitoni	VV	38.576	15.922	8-9	8-9
Villa San Giuseppe	RC	38.187	15.671	8-9	8-9
Nicastrello	VV	38.681	16.289	8	8
San Nicola da Crissa	VV	38.663	16.285	8	8
Vallelonga	VV	38.646	16.294	8	8
Spadola	VV	38.603	16.337	8	8
Torre Faro	ME	38.266	15.646	8	8
Zungri	VV	38.654	15.984	8	8
Castelmonardo	VV	38.77	16.303	7-8	7-8
Bianco [vecchio]	RC	38.095	16.118	7-8	7-8
Natile Vecchio	RC	38.188	16.051	7-8	7-8
Ardore	RC	38.191	16.168	7-8	7-8
Benestare	RC	38.184	16.139	7-8	7-8
Bovalino Superiore	RC	38.17	16.156	7-8	7-8
Careri	RC	38.177	16.115	7-8	7-8
Cirella	RC	38.232	16.099	7-8	7-8
Grotteria	RC	38.364	16.265	7-8	7-8
Mammola	RC	38.362	16.24	7-8	7-8
Camini	RC	38.432	16.483	7-8	7-8
Caraffa del Bianco	RC	38.092	16.087	7-8	7-8
Ciminà	RC	38.245	16.141	7-8	7-8
Gerace	RC	38.271	16.22	7-8	7-8
Martone	RC	38.354	16.288	7-8	7-8
Riace	RC	38.418	16.482	7-8	7-8
Roccella Jonica	RC	38.324	16.405	7-8	7-8
Samo	RC	38.073	16.058	7-8	7-8
San Giovanni di Gerace	RC	38.364	16.279	7-8	7-8
San Luca	RC	38.146	16.064	7-8	7-8
Sant'Agata del Bianco	RC	38.091	16.083	7-8	7-8
Sant'Ilario dello Ionio	RC	38.218	16.195	7-8	7-8
Stignano	RC	38.417	16.471	7-8	7-8
Casignana	RC	38.101	16.089	7-8	7-8
Santa Caterina dello Ionio	CZ	38.534	16.521	7-8	7-8
Stilo	RC	38.477	16.468	7-8	7-8
Antonimina	RC	38.272	16.15	7-8	7-8
Cannavò	RC	38.099	15.69	7-8	7-8
Cerasi	RC	38.159	15.751	7-8	7-8
Platì	RC	38.221	16.044	7-8	7-8

Trizzino	RC	38.122	15.709	7-8	7-8
Montebello Ionico	RC	37.982	15.758	7-8	7-8
Pentimele	RC	38.139	15.659	7-8	7-8
Castroreale	ME	38.099	15.211	7-8	7-8
Casalnuovo	RC	38.055	15.993	7-8	7-8
Palizzi	RC	37.966	15.986	7-8	7-8
Potenzoni	VV	38.689	16.003	7-8	7-8
San Leo Vecchio	VV	38.711	16.02	7-8	7-8
Sciconi	VV	38.691	16.031	7-8	7-8
Staiti	RC	37.999	16.034	7-8	7-8
Lipari	ME	38.467	14.955	7-8	7-8
Jonadi	VV	38.627	16.055	7-8	7-8
Presinaci	VV	38.607	16.018	7-8	7-8
Stromboli (San Vincenzo)	ME	38.806	15.235	7-8	7-8
Francavilla Angitola	VV	38.777	16.271	7	7
Capistrano	VV	38.692	16.289	7	7
Maierato	VV	38.706	16.191	7	7
Montesanto	VV	38.708	16.238	7	7
Vibo Valentia	VV	38.673	16.103	7	7
Condojanni	RC	38.208	16.196	7	7
Simbario	VV	38.611	16.335	7	7
Davoli	CZ	38.649	16.485	7	7
Gagliato	CZ	38.676	16.462	7	7
San Nicola	RC	38.202	16.145	7	7
San Sostene	CZ	38.636	16.487	7	7
Satriano	CZ	38.667	16.482	7	7
Portigliola	RC	38.228	16.202	7	7
Agnana Calabra	RC	38.302	16.224	7	7
Canolo	RC	38.314	16.2	7	7
San Luca	RC	38.009	15.75	7	7
Vinco	RC	38.108	15.723	7	7
Melito di Porto Salvo	RC	37.92	15.784	7	7
San Martino	ME	38.207	15.39	7	7
Pietrapennata	RC	37.984	16.008	7	7
Motticella	RC	38.025	16.055	7	7
Patti	ME	38.138	14.966	7	7
Poliolo	VV	38.753	16.31	6-7	6-7
Bombile	RC	38.205	16.173	6-7	6-7
Jacurso	CZ	38.846	16.38	6-7	6-7
Maida	CZ	38.858	16.365	6-7	6-7
Montesoro	VV	38.816	16.292	6-7	6-7
Acconia	CZ	38.837	16.267	6-7	6-7
Centrache	CZ	38.729	16.43	6-7	6-7
Chiaravalle Centrale	CZ	38.68	16.412	6-7	6-7
Curinga	CZ	38.826	16.313	6-7	6-7
Olivadi	CZ	38.725	16.424	6-7	6-7

Palermiti	CZ	38.75	16.454	6-7	6-7
Bivongi	RC	38.482	16.453	6-7	6-7
Brognaturo	VV	38.602	16.342	6-7	6-7
Cardinale	CZ	38.642	16.387	6-7	6-7
Fabrizia	VV	38.486	16.299	6-7	6-7
Girifalco	CZ	38.822	16.425	6-7	6-7
Placanica	RC	38.414	16.451	6-7	6-7
San Pietro a Maida	CZ	38.846	16.345	6-7	6-7
Squillace	CZ	38.781	16.519	6-7	6-7
Stalettì	CZ	38.764	16.54	6-7	6-7
Torre di Ruggiero	CZ	38.651	16.372	6-7	6-7
Vallefiorita	CZ	38.775	16.461	6-7	6-7
Vena di Maida	CZ	38.888	16.407	6-7	6-7
Aiello Calabro	CS	39.117	16.166	6-7	6-7
San Lucido	CS	39.307	16.049	6-7	6-7
Guardavalle	CZ	38.505	16.505	6-7	6-7
Bovetto	RC	38.06	15.674	6-7	6-7
Canale	RC	38.176	16.128	6-7	6-7
Pizzoni	VV	38.623	16.252	6-7	6-7
San Basilio	VV	38.623	16.25	6-7	6-7
Santa Barbara	VV	38.639	16.209	6-7	6-7
Sant'Angelo	VV	38.611	16.169	6-7	6-7
Sorianello	VV	38.592	16.233	6-7	6-7
Soriano Calabro	VV	38.598	16.23	6-7	6-7
Vazzano	VV	38.632	16.247	6-7	6-7
Roccavaldina	ME	38.182	15.373	6-7	6-7
San Pier Niceto	ME	38.158	15.352	6-7	6-7
Valdina	ME	38.193	15.371	6-7	6-7
Venetico	ME	38.193	15.381	6-7	6-7
Crotone	KR	39.081	17.128	6-7	6-7
Linguaglossa	CT	37.842	15.139	6-7	6-7
Mili San Pietro	ME	38.126	15.488	6-7	6-7
Randazzo	CT	37.877	14.948	6-7	6-7
Bivona	VV	38.709	16.103	D	D
Tindari	ME	38.141	15.045	D	D
Borgia	CZ	38.825	16.51	6	6
Caulonia	RC	38.381	16.409	6	6
Amaroni	CZ	38.792	16.447	6	6
Gasperina	CZ	38.739	16.508	6	6
Montauro	CZ	38.747	16.512	6	6
Le Castella	KR	38.908	17.022	6	6
Pozzo di Gotto	ME	38.152	15.232	6	6
Barcellona Pozzo di Gotto	ME	38.146	15.215	6	6
Calvaruso	ME	38.222	15.453	6	6
Condrò	ME	38.173	15.328	6	6
Milazzo	ME	38.224	15.24	6	6

Monforte San Giorgio	ME	38.155	15.382	6	6
Santa Lucia del Mela	ME	38.14	15.281	6	6
Scaletta Superiore	ME	38.051	15.466	SD	SD
Trecroci	VV	38.755	16.315	5-6	5-6
Catanzaro	CZ	38.905	16.594	5-6	5-6
Catanzaro Lido	CZ	38.822	16.613	5-6	5-6
Gagliano	CZ	38.92	16.562	5-6	5-6
Pazzano	RC	38.475	16.452	5	5
Cortale	CZ	38.838	16.412	5	5
Isca sullo Ionio	CZ	38.6	16.52	5	5
Simeri	CZ	38.932	16.662	5	5
Soverato Superiore	CZ	38.688	16.53	5	5
Soveria Simeri	CZ	38.946	16.679	5	5
Cenadi	CZ	38.719	16.415	5	5
Petrizzi	CZ	38.701	16.474	5	5
Albi	CZ	39.024	16.597	5	5
Argusto	CZ	38.679	16.437	5	5
Badolato	CZ	38.568	16.524	5	5
Caraffa di Catanzaro	CZ	38.88	16.486	5	5
Fossato Serralta	CZ	38.995	16.58	5	5
Magisano	CZ	39.013	16.628	5	5
Maranise	CZ	39.012	16.577	5	5
Montepaone	CZ	38.722	16.497	5	5
Noce	CZ	39.017	16.573	5	5
Pentone	CZ	38.986	16.583	5	5
Perito	CS	39.273	16.33	5	5
Petilia Policastro	KR	39.112	16.789	5	5
San Giovanni	CZ	39.018	16.594	5	5
San Mauro Marchesato	KR	39.103	16.925	5	5
San Pietro	CZ	39.012	16.612	5	5
San Vito sullo Ionio	CZ	38.71	16.408	5	5
Santa Severina	KR	39.147	16.913	5	5
Sant'Andrea Apostolo dello Ionio	CZ	38.622	16.528	5	5
Savuci	CZ	39.009	16.582	5	5
Sellia	CZ	38.981	16.629	5	5
Sorbo San Basile	CZ	39.019	16.569	5	5
Taverna	CZ	39.02	16.582	5	5
Monasterace	RC	38.453	16.551	5	5
Cropani	CZ	38.967	16.782	5	5
Marcedusa	CZ	39.027	16.836	5	5
Simeri Crichi (Crichi)	CZ	38.954	16.639	5	5
Zagarise	CZ	38.999	16.663	5	5
Andali	CZ	39.013	16.77	5	5
Apriglianello	KR	39.086	17.052	5	5
Arietta	CZ	39.052	16.789	5	5
Belcastro	CZ	39.017	16.785	5	5

Fuscaldo	CS	39.415	16.03	5	5
Paola	CS	39.36	16.041	5	5
Papanice	KR	39.071	17.03	5	5
Petronà	CZ	39.043	16.758	5	5
Vincolise	CZ	39.018	16.612	5	5
Cerva	CZ	39.022	16.745	5	5
Cuturella	CZ	38.987	16.778	5	5
Mesoraca	KR	39.077	16.789	5	5
Sersale	CZ	39.011	16.728	5	5
Scalea	CS	39.814	15.792	5	5
Scandale	KR	39.121	16.96	5	5
Altolia	ME	38.075	15.446	5	5
Augusta	SR	37.231	15.221	5	5
Giampilieri Superiore	ME	38.069	15.47	5	5
San Filippo Superiore	ME	38.166	15.5	5	5
Feroleto Antico	CZ	38.962	16.388	4-5	4-5
Pianopoli	CZ	38.954	16.389	4-5	4-5
Siracusa	SR	37.073	15.286	4-5	4-5
Catania	CT	37.502	15.087	4-5	4-5
Cutro	KR	39.033	16.982	4	4
Cotronei	KR	39.159	16.778	4	4
Cosenza	CS	39.303	16.252	F	F
Altilia	KR	39.182	16.882	F	F
Rossano	CS	39.574	16.635	F	F
Agrigento	AG	37.312	13.578	F	F
Agropoli	SA	40.35	14.99	F	F
Gallipoli	LE	40.055	17.988	F	F
Mineo	CT	37.266	14.691	F	F
Modica	RG	36.858	14.761	F	F
Monopoli	BA	40.951	17.296	F	F
Sciacca	AG	37.508	13.083	F	F
Palermo	PA	38.115	13.362	3	3
Santa Sofia d'Epiro	CS	39.546	16.329	SF	SF
Napoli	NA	40.849	14.25	SF	SF
Palinuro	SA	40.033	15.288	SF	SF
Vietri di Potenza	PZ	40.599	15.509	SF	SF
Vietri sul Mare	SA	40.67	14.729	SF	SF

Table 2. MACROSEISMIC FIELD – 6 February 1783

MDPs 67

Locality	Province	Lat.	Long.	Intensity [EMS-98]	Intensity [MCS]
Acquaro	RC	38.268	15.899	10*	10-11*
Bagnara Calabra	RC	38.286	15.805	10*	10-11*
Cinquefrondi	RC	38.417	16.095	10*	10-11*
Cittanova	RC	38.353	16.081	10*	10-11*
Drosi	RC	38.426	15.956	10*	10-11*
Galatro	RC	38.46	16.109	10*	10-11*
Melicucco	RC	38.433	16.06	10*	10-11*
Plaesano	RC	38.473	16.077	10*	10-11*
San Pietro di Caridà (Caridà)	RC	38.523	16.135	10*	10-11*
San Procopio	RC	38.281	15.891	10*	10-11*
Sant'Eufemia d'Aspromonte	RC	38.263	15.857	10*	10-11*
Sinopoli (Superiore)	RC	38.264	15.878	10*	10-11*
Sinopoli Inferiore	RC	38.261	15.886	10*	10-11*
Sinopoli Vecchio	RC	38.281	15.908	10*	10-11*
Polistena	RC	38.406	16.076	10*	10-11*
Iatrinoli	RC	38.353	16.007	10*	10-11*
Cosoleto Vecchio	RC	38.284	15.925	10*	10-11*
Delianuova	RC	38.236	15.918	10*	10-11*
Lubrichi	RC	38.27	15.95	10*	10-11*
Molochio	RC	38.308	16.032	10*	10-11*
Oppido Mamertina	RC	38.291	15.985	10*	10-11*
Palmi	RC	38.358	15.849	10*	10-11*
Paracorio	RC	38.234	15.92	10*	10-11*
Rizziconi	RC	38.411	15.959	10*	10-11*
Rosarno	RC	38.487	15.976	10*	10-11*
San Martino	RC	38.361	15.975	10*	10-11*
Santa Cristina d'Aspromonte	RC	38.255	15.97	10*	10-11*
Sant'Anna	RC	38.322	15.887	10*	10-11*
Sant'Elia	RC	38.339	15.846	10*	10-11*
Santo Stefano in Aspromonte	RC	38.168	15.789	10*	10-11*
Scido	RC	38.245	15.933	10*	10-11*
Seminara	RC	38.335	15.872	10*	10-11*
Sitizano	RC	38.281	15.939	10*	10-11*
Terranova Sappo Minulio	RC	38.321	16.007	10*	10-11*
Tresilico	RC	38.299	15.983	10*	10-11*
Varapodio	RC	38.315	15.984	10*	10-11*
Radicena	RC	38.355	16.017	10*	10-11*
San Giorgio Morgeto	RC	38.386	16.107	9-10*	9-10*
Castellace	RC	38.315	15.94	9-10*	9-10*
Messina	ME	38.185	15.555	9-10*	9-10*
Anoia (Inferiore)	RC	38.435	16.08	9-10*	9-10*

Anoia Superiore	RC	38.432	16.097	9-10*	9-10*
Sant'Agata	RC	38.091	15.721	9*	9*
San Giorgio	RC	38.356	15.853	9*	9*
Reggio di Calabria	RC	38.108	15.647	8-9*	8-9*
Laureana di Borrello	RC	38.491	16.083	8-9*	8-9*
Rometta	ME	38.172	15.414	8-9*	8-9*
Scilla	RC	38.253	15.717	8-9*	8-9*
Torre Faro	ME	38.266	15.646	8*	8*
Ardore	RC	38.191	16.168	7-8*	7-8*
Grotteria	RC	38.364	16.265	7-8*	7-8*
Mammola	RC	38.362	16.24	7-8*	7-8*
Castroreale	ME	38.099	15.211	7-8*	7-8*
Lipari	ME	38.467	14.955	7-8*	7-8*
Vibo Valentia	VV	38.673	16.103	7*	7*
San Martino	ME	38.207	15.39	7*	7*
Bombile	RC	38.205	16.173	6-7	6-7
Roccavaldina	ME	38.182	15.373	6-7	6-7
San Pier Niceto	ME	38.158	15.352	6-7	6-7
Valdina	ME	38.193	15.371	6-7	6-7
Venetico	ME	38.193	15.381	6-7	6-7
Pozzo di Gotto	ME	38.152	15.232	6-7	6-7
Bivona	VV	38.709	16.103	D	D
Caulonia	RC	38.381	16.409	6	6
Catanzaro	CZ	38.905	16.594	5-6	5-6
Catanzaro Lido	CZ	38.822	16.613	5-6	5-6
Siracusa	SR	37.073	15.286	4-5	4-5

Table 3. MACROSEISMIC FIELD – 7 February 1783

MDPs 327

Locality	Province	Lat.	Long.	Intensity [EMS-98]	Intensity [MCS]
Pizzoni	VV	38.623	16.252	10	10-11
San Basilio	VV	38.623	16.25	10	10-11
Santa Barbara	VV	38.639	16.209	10	10-11
Sant'Angelo	VV	38.611	16.169	10	10-11
Sorianello	VV	38.592	16.233	10	10-11
Soriano Calabro	VV	38.598	16.23	10	10-11
Vazzano	VV	38.632	16.247	10	10-11
Panaia	VV	38.68	16.234	10*	10-11*
San Giorgio Morgeto	RC	38.386	16.107	10*	10-11*
Sant'Agata	RC	38.091	15.721	10*	10-11*
Armo	RC	38.07	15.715	10*	10-11*
Cardeto	RC	38.084	15.768	10*	10-11*
Filogaso	VV	38.681	16.228	10*	10-11*
Fossato Ionico	RC	38.013	15.766	10*	10-11*
Mezzocasale	VV	38.646	16.106	10*	10-11*
Mosorrofa	RC	38.098	15.724	10*	10-11*
Ortì Superiore	RC	38.15	15.724	10*	10-11*
Pavigliana	RC	38.104	15.714	10*	10-11*
Perlupo	RC	38.132	15.723	10*	10-11*
Piscopio	VV	38.661	16.113	10*	10-11*
San Gregorio d'Ippona	VV	38.643	16.105	10*	10-11*
San Pietro di Bivona	VV	38.703	16.111	10*	10-11*
Schindilifà	RC	38.164	15.76	10*	10-11*
Stefanaconi	VV	38.673	16.122	10*	10-11*
Straorino	RC	38.132	15.747	10*	10-11*
Triparni	VV	38.681	16.067	10*	10-11*
Vena Media	VV	38.669	16.057	10*	10-11*
Vena Superiore	VV	38.66	16.057	10*	10-11*
Mileto [vecchio]	VV	38.593	16.08	10*	10-11*
Acquaro	RC	38.268	15.899	10*	10-11*
Bagnara Calabra	RC	38.286	15.805	10*	10-11*
Cinquefrondi	RC	38.417	16.095	10*	10-11*
Cittanova	RC	38.353	16.081	10*	10-11*
Drosi	RC	38.426	15.956	10*	10-11*
Galatro	RC	38.46	16.109	10*	10-11*
Melicucco	RC	38.433	16.06	10*	10-11*
Plaesano	RC	38.473	16.077	10*	10-11*
Polistena	RC	38.406	16.076	10*	10-11*
San Pietro di Caridà (Caridà)	RC	38.523	16.135	10*	10-11*
San Procopio	RC	38.281	15.891	10*	10-11*
Sant'Eufemia d'Aspromonte	RC	38.263	15.857	10*	10-11*

Sinopoli (Superiore)	RC	38.264	15.878	10*	10-11*
Sinopoli Inferiore	RC	38.261	15.886	10*	10-11*
Sinopoli Vecchio	RC	38.281	15.908	10*	10-11*
Arena	VV	38.562	16.209	10*	10-11*
Bellantone	RC	38.497	16.091	10*	10-11*
Borrello	RC	38.513	16.069	10*	10-11*
Briatico Vecchio	VV	38.707	16.023	10*	10-11*
Candidoni	RC	38.505	16.086	10*	10-11*
Conidoni	VV	38.698	16.035	10*	10-11*
Daffinà	VV	38.559	16.105	10*	10-11*
Dinami	VV	38.528	16.147	10*	10-11*
Engreste	RC	38.204	15.674	10*	10-11*
Favelloni	VV	38.682	16.028	10*	10-11*
Garopoli	RC	38.526	16.145	10*	10-11*
Gerocarne	VV	38.587	16.219	10*	10-11*
Giffone	RC	38.438	16.149	10*	10-11*
Gioia Tauro	RC	38.426	15.899	10*	10-11*
Mantineo	VV	38.683	16.057	10*	10-11*
Melicuccà	VV	38.536	16.158	10*	10-11*
Messignadi	RC	38.297	15.997	10*	10-11*
Monsoreto	VV	38.515	16.164	10*	10-11*
Pannaconi	VV	38.692	16.041	10*	10-11*
Paradisoni	VV	38.701	16.045	10*	10-11*
Paravati	VV	38.591	16.06	10*	10-11*
San Cono	VV	38.683	16.013	10*	10-11*
San Costantino	VV	38.705	16.002	10*	10-11*
San Marco	VV	38.675	16.01	10*	10-11*
Serrata	RC	38.512	16.101	10*	10-11*
Stelletanone	RC	38.485	16.084	10*	10-11*
Tritanti	RC	38.448	16.101	10*	10-11*
Castellace	RC	38.315	15.94	9-10*	9-10*
Monterosso Calabro	VV	38.717	16.289	9-10*	9-10*
Messina	ME	38.185	15.555	9-10*	9-10*
Nasiti	RC	38.112	15.696	9-10*	9-10*
Africo [vecchio]	RC	38.065	15.98	9-10*	9-10*
Amendolea [vecchia]	RC	37.988	15.892	9-10*	9-10*
Anoia (Inferiore)	RC	38.435	16.08	9-10*	9-10*
Anoia Superiore	RC	38.432	16.097	9-10*	9-10*
Acquaro	VV	38.555	16.189	9-10*	9-10*
Bracciara	VV	38.565	16.168	9-10*	9-10*
Cannitello	RC	38.234	15.657	9-10*	9-10*
Ciano	VV	38.576	16.213	9-10*	9-10*
Dasà	VV	38.564	16.196	9-10*	9-10*
Ferrito	RC	38.234	15.66	9-10*	9-10*
Limpidi	VV	38.541	16.174	9-10*	9-10*
Maropati	RC	38.441	16.097	9-10*	9-10*

Miglianò	VV	38.591	16.197	9-10*	9-10*
Pezzo Inferiore	RC	38.231	15.638	9-10*	9-10*
Piale	RC	38.224	15.648	9-10*	9-10*
Porticato	RC	38.234	15.649	9-10*	9-10*
Potami	VV	38.579	16.207	9-10*	9-10*
Pronia	VV	38.578	16.189	9-10*	9-10*
Rosalì	RC	38.198	15.68	9-10*	9-10*
San Domenico	RC	38.203	15.676	9-10*	9-10*
Simiatoni	VV	38.558	16.179	9-10*	9-10*
Longobardi	VV	38.702	16.122	9*	9*
Laureana di Borrello	RC	38.491	16.083	9*	9*
Cessaniti	VV	38.663	16.026	9*	9*
Brancaleone Superiore	RC	37.981	16.081	8-9	8-9
Pimene	VV	38.726	16.213	8-9*	8-9*
Pizzo	VV	38.733	16.159	8-9*	8-9*
Sant'Onofrio	VV	38.695	16.144	8-9*	8-9*
Spadola	VV	38.603	16.337	8-9*	8-9*
Bianco [vecchio]	RC	38.095	16.118	8-9*	8-9*
Serra San Bruno	VV	38.576	16.33	8-9*	8-9*
Reggio di Calabria	RC	38.108	15.647	8-9*	8-9*
Alafito	VV	38.672	15.919	8-9*	8-9*
Arasì	RC	38.139	15.737	8-9*	8-9*
Barbalaconi	VV	38.634	15.873	8-9*	8-9*
Brattirò	VV	38.642	15.887	8-9*	8-9*
Brivadi	VV	38.636	15.856	8-9*	8-9*
Carciadi	VV	38.628	15.908	8-9*	8-9*
Caria	VV	38.646	15.905	8-9*	8-9*
Ciaramiti	VV	38.65	15.862	8-9*	8-9*
Croce Valanidi	RC	38.055	15.677	8-9*	8-9*
Daffinà	VV	38.68	15.951	8-9*	8-9*
Daffinacello	VV	38.677	15.944	8-9*	8-9*
Drapia	VV	38.664	15.911	8-9*	8-9*
Fitili	VV	38.675	15.931	8-9*	8-9*
Gasponi	VV	38.661	15.904	8-9*	8-9*
Gioiosa Ionica	RC	38.332	16.302	8-9*	8-9*
Lampazzone	VV	38.631	15.875	8-9*	8-9*
Orsigliadi	VV	38.629	15.861	8-9*	8-9*
Panaia	VV	38.623	15.892	8-9*	8-9*
Parghelia	VV	38.681	15.923	8-9*	8-9*
Podargoni	RC	38.162	15.781	8-9*	8-9*
Ricadi	VV	38.626	15.867	8-9*	8-9*
San Giovanni	VV	38.675	15.973	8-9*	8-9*
San Nicolò	VV	38.633	15.851	8-9*	8-9*
Santa Domenica	VV	38.663	15.866	8-9*	8-9*
Siderno Superiore	RC	38.289	16.269	8-9*	8-9*
Spilinga	VV	38.627	15.905	8-9*	8-9*

Terreti	RC	38.119	15.711	8-9*	8-9*
Tropea	VV	38.675	15.899	8-9*	8-9*
Zaccanopoli	VV	38.664	15.929	8-9*	8-9*
Zambrone	VV	38.699	15.991	8-9*	8-9*
Zammarò	VV	38.651	16.107	8-9*	8-9*
Bagaladi	RC	38.026	15.821	8-9*	8-9*
Bova	RC	37.994	15.932	8-9*	8-9*
Condofuri	RC	38.005	15.858	8-9*	8-9*
Gallicianò	RC	38.016	15.886	8-9*	8-9*
Motta San Giovanni	RC	38.002	15.694	8-9*	8-9*
Pellaro	RC	38.025	15.656	8-9*	8-9*
Pentedattilo	RC	37.953	15.762	8-9*	8-9*
Roccaforte del Greco	RC	38.045	15.9	8-9*	8-9*
Roghudi Vecchio	RC	38.049	15.916	8-9*	8-9*
San Lorenzo	RC	38.01	15.834	8-9*	8-9*
Rometta	ME	38.172	15.414	8-9*	8-9*
Scilla	RC	38.253	15.717	8-9*	8-9*
Acciarello	RC	38.212	15.638	8-9*	8-9*
Calimera	VV	38.556	16.018	8-9*	8-9*
Campo Calabro	RC	38.213	15.659	8-9*	8-9*
Catona	RC	38.185	15.643	8-9*	8-9*
Certosa di Santo Stefano del Bosco	VV	38.564	16.319	8-9*	8-9*
Coccorino	VV	38.604	15.872	8-9*	8-9*
Fiumara (San Nicola)	RC	38.211	15.693	8-9*	8-9*
Fontanelle	RC	38.175	15.643	8-9*	8-9*
Joppolo	VV	38.585	15.896	8-9*	8-9*
Musalà	RC	38.214	15.671	8-9*	8-9*
Salice Calabro	RC	38.197	15.659	8-9*	8-9*
San Roberto	RC	38.211	15.736	8-9*	8-9*
Nicastrello	VV	38.681	16.289	8*	8*
San Nicola da Crissa	VV	38.663	16.285	8*	8*
Vallelonga	VV	38.646	16.294	8*	8*
Natile Vecchio	RC	38.188	16.051	8*	8*
Ardore	RC	38.191	16.168	8*	8*
Benestare	RC	38.184	16.139	8*	8*
Bovalino Superiore	RC	38.17	16.156	8*	8*
Careri	RC	38.177	16.115	8*	8*
Cirella	RC	38.232	16.099	8*	8*
Castelmonardo	VV	38.77	16.303	7-8*	7-8*
Grotteria	RC	38.364	16.265	7-8*	7-8*
Mammola	RC	38.362	16.24	7-8*	7-8*
Camini	RC	38.432	16.483	7-8*	7-8*
Caraffa del Bianco	RC	38.092	16.087	7-8*	7-8*
Ciminà	RC	38.245	16.141	7-8*	7-8*
Gerace	RC	38.271	16.22	7-8*	7-8*
Martone	RC	38.354	16.288	7-8*	7-8*

Riace	RC	38.418	16.482	7-8*	7-8*
Roccella Jonica	RC	38.324	16.405	7-8*	7-8*
Samo	RC	38.073	16.058	7-8*	7-8*
San Giovanni di Gerace	RC	38.364	16.279	7-8*	7-8*
San Luca	RC	38.146	16.064	7-8*	7-8*
Sant'Agata del Bianco	RC	38.091	16.083	7-8*	7-8*
Sant'Ilario dello Ionio	RC	38.218	16.195	7-8*	7-8*
Stignano	RC	38.417	16.471	7-8*	7-8*
Condojanni	RC	38.208	16.196	7-8*	7-8*
Simbario	VV	38.611	16.335	7-8*	7-8*
Casignana	RC	38.101	16.089	7-8*	7-8*
Santa Caterina dello Ionio	CZ	38.534	16.521	7-8*	7-8*
Stilo	RC	38.477	16.468	7-8*	7-8*
Antonimina	RC	38.272	16.15	7-8*	7-8*
Cannavò	RC	38.099	15.69	7-8*	7-8*
Cerasi	RC	38.159	15.751	7-8*	7-8*
Platì	RC	38.221	16.044	7-8*	7-8*
Trizzino	RC	38.122	15.709	7-8*	7-8*
Montebello Ionico	RC	37.982	15.758	7-8*	7-8*
Pentimele	RC	38.139	15.659	7-8*	7-8*
Castroreale	ME	38.099	15.211	7-8*	7-8*
Casalnuovo	RC	38.055	15.993	7-8*	7-8*
Palizzi	RC	37.966	15.986	7-8*	7-8*
Potenzoni	VV	38.689	16.003	7-8*	7-8*
San Leo Vecchio	VV	38.711	16.02	7-8*	7-8*
Sciconi	VV	38.691	16.031	7-8*	7-8*
Staiti	RC	37.999	16.034	7-8*	7-8*
Bombile	RC	38.205	16.173	7	7
Francavilla Angitola	VV	38.777	16.271	7*	7*
Capistrano	VV	38.692	16.289	7*	7*
Maierato	VV	38.706	16.191	7*	7*
Montesanto	VV	38.708	16.238	7*	7*
Vibo Valentia	VV	38.673	16.103	7*	7*
Davoli	CZ	38.649	16.485	7*	7*
Gagliato	CZ	38.676	16.462	7*	7*
San Nicola	RC	38.202	16.145	7*	7*
San Sostene	CZ	38.636	16.487	7*	7*
Satriano	CZ	38.667	16.482	7*	7*
Portigliola	RC	38.228	16.202	7*	7*
Agnana Calabra	RC	38.302	16.224	7*	7*
Canolo	RC	38.314	16.2	7*	7*
San Luca	RC	38.009	15.75	7*	7*
Vinco	RC	38.108	15.723	7*	7*
Melito di Porto Salvo	RC	37.92	15.784	7*	7*
San Martino	ME	38.207	15.39	7*	7*
Pozzo di Gotto	ME	38.152	15.232	7*	7*

Pietrapennata	RC	37.984	16.008	7*	7*
Poliolo	VV	38.753	16.31	6-7	6-7
Jacurso	CZ	38.846	16.38	6-7	6-7
Maida	CZ	38.858	16.365	6-7	6-7
Montesoro	VV	38.816	16.292	6-7	6-7
Acconia	CZ	38.837	16.267	6-7	6-7
Centrache	CZ	38.729	16.43	6-7	6-7
Chiaravalle Centrale	CZ	38.68	16.412	6-7	6-7
Curinga	CZ	38.826	16.313	6-7	6-7
Olivadi	CZ	38.725	16.424	6-7	6-7
Palermiti	CZ	38.75	16.454	6-7	6-7
Bivongi	RC	38.482	16.453	6-7	6-7
Brognaturo	VV	38.602	16.342	6-7	6-7
Cardinale	CZ	38.642	16.387	6-7	6-7
Fabrizia	VV	38.486	16.299	6-7	6-7
Girifalco	CZ	38.822	16.425	6-7	6-7
Placanica	RC	38.414	16.451	6-7	6-7
San Pietro a Maida	CZ	38.846	16.345	6-7	6-7
Squillace	CZ	38.781	16.519	6-7	6-7
Stalettì	CZ	38.764	16.54	6-7	6-7
Torre di Ruggiero	CZ	38.651	16.372	6-7	6-7
Vallefiorita	CZ	38.775	16.461	6-7	6-7
Vena di Maida	CZ	38.888	16.407	6-7	6-7
Aiello Calabro	CS	39.117	16.166	6-7	6-7
San Lucido	CS	39.307	16.049	6-7	6-7
Guardavalle	CZ	38.505	16.505	6-7	6-7
Bovetto	RC	38.06	15.674	6-7	6-7
Canale	RC	38.176	16.128	6-7	6-7
Roccavaldina	ME	38.182	15.373	6-7	6-7
San Pier Niceto	ME	38.158	15.352	6-7	6-7
Valdina	ME	38.193	15.371	6-7	6-7
Venetico	ME	38.193	15.381	6-7	6-7
Bivona	VV	38.709	16.103	D	D
Borgia	CZ	38.825	16.51	6	6
Caulonia	RC	38.381	16.409	6	6
Amaroni	CZ	38.792	16.447	6	6
Gasperina	CZ	38.739	16.508	6	6
Montauro	CZ	38.747	16.512	6	6
Le Castella	KR	38.908	17.022	6	6
Trecroci	VV	38.755	16.315	5-6	5-6
Catanzaro	CZ	38.905	16.594	5-6	5-6
Catanzaro Lido	CZ	38.822	16.613	5-6	5-6
Gagliano	CZ	38.92	16.562	5-6	5-6
Pazzano	RC	38.475	16.452	5	5
Cortale	CZ	38.838	16.412	5	5
Isca sullo Ionio	CZ	38.6	16.52	5	5

Simeri	CZ	38.932	16.662	5	5
Soverato Superiore	CZ	38.688	16.53	5	5
Soveria Simeri	CZ	38.946	16.679	5	5
Cenadi	CZ	38.719	16.415	5	5
Petrizzi	CZ	38.701	16.474	5	5
Albi	CZ	39.024	16.597	5	5
Argusto	CZ	38.679	16.437	5	5
Badolato	CZ	38.568	16.524	5	5
Caraffa di Catanzaro	CZ	38.88	16.486	5	5
Fossato Serralta	CZ	38.995	16.58	5	5
Magisano	CZ	39.013	16.628	5	5
Maranise	CZ	39.012	16.577	5	5
Montepaone	CZ	38.722	16.497	5	5
Noce	CZ	39.017	16.573	5	5
Pentone	CZ	38.986	16.583	5	5
Perito	CS	39.273	16.33	5	5
Petilia Policastro	KR	39.112	16.789	5	5
San Giovanni	CZ	39.018	16.594	5	5
San Mauro Marchesato	KR	39.103	16.925	5	5
San Pietro	CZ	39.012	16.612	5	5
San Vito sullo Ionio	CZ	38.71	16.408	5	5
Santa Severina	KR	39.147	16.913	5	5
Sant'Andrea Apostolo dello Ionio	CZ	38.622	16.528	5	5
Savuci	CZ	39.009	16.582	5	5
Sellia	CZ	38.981	16.629	5	5
Sorbo San Basile	CZ	39.019	16.569	5	5
Taverna	CZ	39.02	16.582	5	5
Monasterace	RC	38.453	16.551	5	5
Cropani	CZ	38.967	16.782	5	5
Marcedusa	CZ	39.027	16.836	5	5
Simeri Crichi (Crichi)	CZ	38.954	16.639	5	5
Zagarise	CZ	38.999	16.663	5	5
Andali	CZ	39.013	16.77	5	5
Apriglianello	KR	39.086	17.052	5	5
Arietta	CZ	39.052	16.789	5	5
Belcastro	CZ	39.017	16.785	5	5
Fuscaldo	CS	39.415	16.03	5	5
Paola	CS	39.36	16.041	5	5
Papanice	KR	39.071	17.03	5	5
Petronà	CZ	39.043	16.758	5	5
Vincolise	CZ	39.018	16.612	5	5
Cerva	CZ	39.022	16.745	5	5
Cuturella	CZ	38.987	16.778	5	5
Mesoraca	KR	39.077	16.789	5	5
Sersale	CZ	39.011	16.728	5	5
Scalea	CS	39.814	15.792	5	5

Scandale	KR	39.121	16.96	5	5
Feroleto Antico	CZ	38.962	16.388	4-5	4-5
Pianopoli	CZ	38.954	16.389	4-5	4-5
Cutro	KR	39.033	16.982	4	4
Cotronei	KR	39.159	16.778	4	4
Cosenza	CS	39.303	16.252	F	F
Altilia	KR	39.182	16.882	F	F
Rossano	CS	39.574	16.635	F	F
Santa Sofia d'Epiro	CS	39.546	16.329	SF	SF
Cassano allo Ionio	CS	39.784	16.318	NC	NC

Table 4. MACROSEISMIC FIELD – 1 March 1783

MDPs 22

Locality	Province	Lat.	Long.	Intensity [EMS-98]	Intensity [MCS]
Panaia	VV	38.68	16.234	10*	10-11*
Mileto [vecchio]	VV	38.593	16.08	10*	10-11*
Messina	ME	38.185	15.555	9-10*	9-10*
Nicastrello	VV	38.681	16.289	9-10*	9-10*
San Nicola da Crissa	VV	38.663	16.285	9-10*	9-10*
Vallelonga	VV	38.646	16.294	9-10*	9-10*
Poliolo	VV	38.753	16.31	9	9
Trecroci	VV	38.755	16.315	9	9
Castelmonardo	VV	38.77	16.303	8-9*	8-9*
Reggio di Calabria	RC	38.108	15.647	8-9*	8-9*
Francavilla Angitola	VV	38.777	16.271	8*	8*
Capistrano	VV	38.692	16.289	7-8*	7-8*
Maierato	VV	38.706	16.191	7-8*	7-8*
Montesanto	VV	38.708	16.238	7-8*	7-8*
Vibo Valentia	VV	38.673	16.103	7-8*	7-8*
Cosenza	CS	39.303	16.252	7-8	7-8
Catanzaro	CZ	38.905	16.594	5-6	5-6
Catanzaro Lido	CZ	38.822	16.613	5-6	5-6
Tiriolo	CZ	38.947	16.509	5	5
Scalea	CS	39.814	15.792	5	5
Rossano	CS	39.574	16.635	F	F
Santa Sofia d'Epiro	CS	39.546	16.329	F	F

Table 5. MACROSEISMIC FIELD – 28 March 1783

MDPs 339

Locality	Province	Lat.	Long.	Intensity [EMS-98]	Intensity [MCS]
Jacurso	CZ	38.846	16.38	10	10-11
Maida	CZ	38.858	16.365	10	10-11
Montesoro	VV	38.816	16.292	10	10-11
Borgia	CZ	38.825	16.51	10	10-11
Cortale	CZ	38.838	16.412	10	10-11
San Floro	CZ	38.837	16.519	10	10-11
Poliolo	VV	38.753	16.31	10*	10-11*
Trecroci	VV	38.755	16.315	10*	10-11*
Panaia	VV	38.68	16.234	10*	10-11*
Castelmonardo	VV	38.77	16.303	10*	10-11*
Francavilla Angitola	VV	38.777	16.271	10*	10-11*
Capistrano	VV	38.692	16.289	10*	10-11*
Maierato	VV	38.706	16.191	10*	10-11*
Montesanto	VV	38.708	16.238	10*	10-11*
San Giorgio Morgeto	RC	38.386	16.107	10*	10-11*
Sant'Agata	RC	38.091	15.721	10*	10-11*
Armo	RC	38.07	15.715	10*	10-11*
Cardeto	RC	38.084	15.768	10*	10-11*
Filogaso	VV	38.681	16.228	10*	10-11*
Fossato Ionico	RC	38.013	15.766	10*	10-11*
Mezzocasale	VV	38.646	16.106	10*	10-11*
Mosorrofa	RC	38.098	15.724	10*	10-11*
Ortì Superiore	RC	38.15	15.724	10*	10-11*
Pavigliana	RC	38.104	15.714	10*	10-11*
Perlupo	RC	38.132	15.723	10*	10-11*
Piscopio	VV	38.661	16.113	10*	10-11*
San Gregorio d'Ippona	VV	38.643	16.105	10*	10-11*
San Pietro di Bivona	VV	38.703	16.111	10*	10-11*
Schindilifà	RC	38.164	15.76	10*	10-11*
Stefanaconi	VV	38.673	16.122	10*	10-11*
Straorino	RC	38.132	15.747	10*	10-11*
Triparni	VV	38.681	16.067	10*	10-11*
Vena Media	VV	38.669	16.057	10*	10-11*
Vena Superiore	VV	38.66	16.057	10*	10-11*
Castellace	RC	38.315	15.94	10*	10-11*
Monterosso Calabro	VV	38.717	16.289	10*	10-11*
Pimene	VV	38.726	16.213	10*	10-11*
Pizzo	VV	38.733	16.159	10*	10-11*
Sant'Onofrio	VV	38.695	16.144	10*	10-11*
Acconia	CZ	38.837	16.267	9-10	9-10

Centrache	CZ	38.729	16.43	9-10	9-10
Chiaravalle Centrale	CZ	38.68	16.412	9-10	9-10
Curinga	CZ	38.826	16.313	9-10	9-10
Olivadi	CZ	38.725	16.424	9-10	9-10
Palermiti	CZ	38.75	16.454	9-10	9-10
Isca sullo Ionio	CZ	38.6	16.52	9-10	9-10
Simeri	CZ	38.932	16.662	9-10	9-10
Soverato Superiore	CZ	38.688	16.53	9-10	9-10
Soveria Simeri	CZ	38.946	16.679	9-10	9-10
Marcellinara	CZ	38.928	16.494	9-10	9-10
Settingiano	CZ	38.913	16.514	9-10	9-10
Messina	ME	38.185	15.555	9-10*	9-10*
Nicastrello	VV	38.681	16.289	9-10*	9-10*
San Nicola da Crissa	VV	38.663	16.285	9-10*	9-10*
Vallelonga	VV	38.646	16.294	9-10*	9-10*
Nasiti	RC	38.112	15.696	9-10*	9-10*
Spadola	VV	38.603	16.337	9-10*	9-10*
Bianco [vecchio]	RC	38.095	16.118	9-10*	9-10*
Natile Vecchio	RC	38.188	16.051	9-10*	9-10*
Cenadi	CZ	38.719	16.415	9	9
Petrizzi	CZ	38.701	16.474	9	9
Longobardi	VV	38.702	16.122	9*	9*
Serra San Bruno	VV	38.576	16.33	9*	9*
Altavilla	CS	39.333	16.311	9	9
Tiriolo	CZ	38.947	16.509	8-9	8-9
Bivongi	RC	38.482	16.453	8-9	8-9
Brognaturo	VV	38.602	16.342	8-9	8-9
Cardinale	CZ	38.642	16.387	8-9	8-9
Fabrizia	VV	38.486	16.299	8-9	8-9
Girifalco	CZ	38.822	16.425	8-9	8-9
Placanica	RC	38.414	16.451	8-9	8-9
San Pietro a Maida	CZ	38.846	16.345	8-9	8-9
Squillace	CZ	38.781	16.519	8-9	8-9
Stalettì	CZ	38.764	16.54	8-9	8-9
Torre di Ruggiero	CZ	38.651	16.372	8-9	8-9
Vallefiorita	CZ	38.775	16.461	8-9	8-9
Vena di Maida	CZ	38.888	16.407	8-9	8-9
Caulonia	RC	38.381	16.409	8-9	8-9
Amaroni	CZ	38.792	16.447	8-9	8-9
Gasperina	CZ	38.739	16.508	8-9	8-9
Montauro	CZ	38.747	16.512	8-9	8-9
Albi	CZ	39.024	16.597	8-9	8-9
Argusto	CZ	38.679	16.437	8-9	8-9
Badolato	CZ	38.568	16.524	8-9	8-9
Caraffa di Catanzaro	CZ	38.88	16.486	8-9	8-9
Fossato Serralta	CZ	38.995	16.58	8-9	8-9

Magisano	CZ	39.013	16.628	8-9	8-9
Maranise	CZ	39.012	16.577	8-9	8-9
Montepaone	CZ	38.722	16.497	8-9	8-9
Noce	CZ	39.017	16.573	8-9	8-9
Pentone	CZ	38.986	16.583	8-9	8-9
Perito	CS	39.273	16.33	8-9	8-9
Petilia Policastro	KR	39.112	16.789	8-9	8-9
San Giovanni	CZ	39.018	16.594	8-9	8-9
San Mauro Marchesato	KR	39.103	16.925	8-9	8-9
San Pietro	CZ	39.012	16.612	8-9	8-9
San Vito sullo Ionio	CZ	38.71	16.408	8-9	8-9
Santa Severina	KR	39.147	16.913	8-9	8-9
Sant'Andrea Apostolo dello Ionio	CZ	38.622	16.528	8-9	8-9
Savuci	CZ	39.009	16.582	8-9	8-9
Sellia	CZ	38.981	16.629	8-9	8-9
Sorbo San Basile	CZ	39.019	16.569	8-9	8-9
Taverna	CZ	39.02	16.582	8-9	8-9
Feroleto Antico	CZ	38.962	16.388	8-9	8-9
Pianopoli	CZ	38.954	16.389	8-9	8-9
Cutro	KR	39.033	16.982	8-9	8-9
Amato	CZ	38.942	16.463	8-9	8-9
Castagna	CZ	39.053	16.436	8-9	8-9
Celico	CS	39.309	16.34	8-9	8-9
Gimigliano	CZ	38.973	16.527	8-9	8-9
Miglierina	CZ	38.947	16.472	8-9	8-9
San Pietro Apostolo	CZ	39.003	16.467	8-9	8-9
Santo Stefano di Rogliano	CS	39.193	16.324	8-9	8-9
Reggio di Calabria	RC	38.108	15.647	8-9*	8-9*
Vibo Valentia	VV	38.673	16.103	8-9*	8-9*
Alafito	VV	38.672	15.919	8-9*	8-9*
Arasì	RC	38.139	15.737	8-9*	8-9*
Barbalaconi	VV	38.634	15.873	8-9*	8-9*
Brattirò	VV	38.642	15.887	8-9*	8-9*
Brivadi	VV	38.636	15.856	8-9*	8-9*
Carciadi	VV	38.628	15.908	8-9*	8-9*
Caria	VV	38.646	15.905	8-9*	8-9*
Ciaramiti	VV	38.65	15.862	8-9*	8-9*
Croce Valanidi	RC	38.055	15.677	8-9*	8-9*
Daffinà	VV	38.68	15.951	8-9*	8-9*
Daffinacello	VV	38.677	15.944	8-9*	8-9*
Drapia	VV	38.664	15.911	8-9*	8-9*
Fitili	VV	38.675	15.931	8-9*	8-9*
Gasponi	VV	38.661	15.904	8-9*	8-9*
Gioiosa Ionica	RC	38.332	16.302	8-9*	8-9*
Lampazzone	VV	38.631	15.875	8-9*	8-9*
Orsigliadi	VV	38.629	15.861	8-9*	8-9*

Panaia	VV	38.623	15.892	8-9*	8-9*
Parghelia	VV	38.681	15.923	8-9*	8-9*
Podargoni	RC	38.162	15.781	8-9*	8-9*
Ricadi	VV	38.626	15.867	8-9*	8-9*
San Giovanni	VV	38.675	15.973	8-9*	8-9*
San Nicolò	VV	38.633	15.851	8-9*	8-9*
Santa Domenica	VV	38.663	15.866	8-9*	8-9*
Siderno Superiore	RC	38.289	16.269	8-9*	8-9*
Spilinga	VV	38.627	15.905	8-9*	8-9*
Terreti	RC	38.119	15.711	8-9*	8-9*
Tropea	VV	38.675	15.899	8-9*	8-9*
Zaccanopoli	VV	38.664	15.929	8-9*	8-9*
Zambrone	VV	38.699	15.991	8-9*	8-9*
Zammarò	VV	38.651	16.107	8-9*	8-9*
Ardore	RC	38.191	16.168	8-9*	8-9*
Benestare	RC	38.184	16.139	8-9*	8-9*
Bovalino Superiore	RC	38.17	16.156	8-9*	8-9*
Careri	RC	38.177	16.115	8-9*	8-9*
Cirella	RC	38.232	16.099	8-9*	8-9*
Grotteria	RC	38.364	16.265	8-9*	8-9*
Mammola	RC	38.362	16.24	8-9*	8-9*
Camini	RC	38.432	16.483	8-9*	8-9*
Caraffa del Bianco	RC	38.092	16.087	8-9*	8-9*
Ciminà	RC	38.245	16.141	8-9*	8-9*
Gerace	RC	38.271	16.22	8-9*	8-9*
Martone	RC	38.354	16.288	8-9*	8-9*
Riace	RC	38.418	16.482	8-9*	8-9*
Roccella Jonica	RC	38.324	16.405	8-9*	8-9*
Samo	RC	38.073	16.058	8-9*	8-9*
San Giovanni di Gerace	RC	38.364	16.279	8-9*	8-9*
San Luca	RC	38.146	16.064	8-9*	8-9*
Sant'Agata del Bianco	RC	38.091	16.083	8-9*	8-9*
Sant'Ilario dello Ionio	RC	38.218	16.195	8-9*	8-9*
Stignano	RC	38.417	16.471	8-9*	8-9*
Condojanni	RC	38.208	16.196	8-9*	8-9*
Simbario	VV	38.611	16.335	8-9*	8-9*
Davoli	CZ	38.649	16.485	8-9*	8-9*
Gagliato	CZ	38.676	16.462	8-9*	8-9*
San Nicola	RC	38.202	16.145	8-9*	8-9*
San Sostene	CZ	38.636	16.487	8-9*	8-9*
Satriano	CZ	38.667	16.482	8-9*	8-9*
Monasterace	RC	38.453	16.551	8	8
Roccelletta	CZ	38.81	16.601	8	8
Casignana	RC	38.101	16.089	8*	8*
Santa Caterina dello Ionio	CZ	38.534	16.521	8*	8*
Stilo	RC	38.477	16.468	8*	8*

Catanzaro	CZ	38.905	16.594	7-8	7-8
Catanzaro Lido	CZ	38.822	16.613	7-8	7-8
Aiello Calabro	CS	39.117	16.166	7-8	7-8
San Lucido	CS	39.307	16.049	7-8	7-8
Gagliano	CZ	38.92	16.562	7-8	7-8
Cropani	CZ	38.967	16.782	7-8	7-8
Marcedusa	CZ	39.027	16.836	7-8	7-8
Simeri Crichi (Crichi)	CZ	38.954	16.639	7-8	7-8
Zagarise	CZ	38.999	16.663	7-8	7-8
Accaria	CZ	38.98	16.365	7-8	7-8
Altilia	CS	39.129	16.252	7-8	7-8
Angoli	CZ	38.971	16.436	7-8	7-8
Aprigliano	CS	39.24	16.342	7-8	7-8
Borgo Partenope	CS	39.27	16.304	7-8	7-8
Cerisano	CS	39.276	16.175	7-8	7-8
Donnici Inferiore	CS	39.251	16.29	7-8	7-8
Donnici Superiore	CS	39.252	16.301	7-8	7-8
Grimaldi	CS	39.142	16.235	7-8	7-8
Lamezia Terme (Nicastro)	CZ	38.974	16.318	7-8	7-8
Lappano	CS	39.319	16.312	7-8	7-8
Laurignano	CS	39.277	16.241	7-8	7-8
Macchia Albanese	CS	39.58	16.381	7-8	7-8
Malito	CS	39.154	16.248	7-8	7-8
Mangone	CS	39.203	16.334	7-8	7-8
Montalto Uffugo	CS	39.405	16.158	7-8	7-8
Motta	CS	39.31	16.286	7-8	7-8
Mottafollone	CS	39.648	16.064	7-8	7-8
Nocera Terinese	CZ	39.036	16.16	7-8	7-8
Piane Crati	CS	39.233	16.325	7-8	7-8
Rende	CS	39.331	16.183	7-8	7-8
Roccabernarda	KR	39.133	16.868	7-8	7-8
Roggiano Gravina	CS	39.615	16.157	7-8	7-8
Rose	CS	39.399	16.288	7-8	7-8
San Benedetto in Guarano	CS	39.339	16.302	7-8	7-8
San Fili	CS	39.338	16.144	7-8	7-8
San Pietro in Amantea	CS	39.136	16.112	7-8	7-8
San Pietro in Guarano	CS	39.342	16.311	7-8	7-8
San Sisto dei Valdesi	CS	39.377	16.15	7-8	7-8
Sant'Eufemia	CZ	38.92	16.254	7-8	7-8
Sant'Ippolito	CS	39.266	16.295	7-8	7-8
Scala Coeli	CS	39.445	16.89	7-8	7-8
Serra Pedace	CS	39.277	16.346	7-8	7-8
Serrastretta	CZ	39.013	16.416	7-8	7-8
Spezzano della Sila	CS	39.299	16.34	7-8	7-8
Torano Castello	CS	39.504	16.147	7-8	7-8
Zumpano	CS	39.31	16.291	7-8	7-8

Cosenza	CS	39.303	16.252	7-8*	7-8*
Bombile	RC	38.205	16.173	7-8*	7-8*
Pazzano	RC	38.475	16.452	7-8*	7-8*
Antonimina	RC	38.272	16.15	7-8*	7-8*
Cannavò	RC	38.099	15.69	7-8*	7-8*
Cerasi	RC	38.159	15.751	7-8*	7-8*
Platì	RC	38.221	16.044	7-8*	7-8*
Trizzino	RC	38.122	15.709	7-8*	7-8*
Portigliola	RC	38.228	16.202	7-8*	7-8*
Guardavalle	CZ	38.505	16.505	7	7
Le Castella	KR	38.908	17.022	7	7
Andali	CZ	39.013	16.77	7	7
Apriglianello	KR	39.086	17.052	7	7
Arietta	CZ	39.052	16.789	7	7
Belcastro	CZ	39.017	16.785	7	7
Fuscaldo	CS	39.415	16.03	7	7
Paola	CS	39.36	16.041	7	7
Papanice	KR	39.071	17.03	7	7
Petronà	CZ	39.043	16.758	7	7
Vincolise	CZ	39.018	16.612	7	7
Migliuso	CZ	38.954	16.433	7	7
Amantea	CS	39.132	16.081	7	7
Carlopoli	CZ	39.055	16.456	7	7
Carolei	CS	39.253	16.218	7	7
Casole Bruzio	CS	39.281	16.331	7	7
Castiglione Cosentino	CS	39.351	16.288	7	7
Castiglione Marittimo	CZ	38.981	16.159	7	7
Cicala	CZ	39.021	16.486	7	7
Crosia	CS	39.566	16.773	7	7
Dipignano	CS	39.237	16.252	7	7
Fagnano Castello	CS	39.564	16.054	7	7
Falerna	CZ	39.002	16.173	7	7
Figline Vegliaturo	CS	39.225	16.331	7	7
Ievoli	CZ	38.972	16.404	7	7
Longobardi	CS	39.206	16.076	7	7
Longobucco	CS	39.449	16.611	7	7
Magli	CS	39.278	16.312	7	7
Marano Marchesato	CS	39.313	16.172	7	7
Martirano	CZ	39.08	16.248	7	7
Pietrafitta	CS	39.26	16.34	7	7
Platania	CZ	39.005	16.32	7	7
Pulsano	CS	39.253	16.238	7	7
Rota Greca	CS	39.467	16.113	7	7
Rovito	CS	39.308	16.321	7	7
Sambiase	CZ	38.966	16.282	7	7
San Benedetto Ullano	CS	39.426	16.123	7	7

San Mango d'Aquino	CZ	39.058	16.191	7	7
San Marco Argentano	CS	39.556	16.119	7	7
San Sosti	CS	39.66	16.028	7	7
Sant'Agata di Esaro	CS	39.619	15.983	7	7
Serra d'Aiello	CS	39.089	16.129	7	7
Terrati	CS	39.134	16.142	7	7
Terravecchia	CS	39.465	16.946	7	7
Tessano	CS	39.256	16.241	7	7
Trenta	CS	39.283	16.321	7	7
Vaccarizzo	CS	39.41	16.135	7	7
Zangarona	CZ	38.97	16.344	7	7
Agnana Calabra	RC	38.302	16.224	7*	7*
Canolo	RC	38.314	16.2	7*	7*
San Luca	RC	38.009	15.75	7*	7*
Vinco	RC	38.108	15.723	7*	7*
Bovetto	RC	38.06	15.674	6-7	6-7
Canale	RC	38.176	16.128	6-7	6-7
Cerva	CZ	39.022	16.745	6-7	6-7
Cuturella	CZ	38.987	16.778	6-7	6-7
Mesoraca	KR	39.077	16.789	6-7	6-7
Sersale	CZ	39.011	16.728	6-7	6-7
Belmonte Calabro	CS	39.16	16.079	6-7	6-7
Belsito	CS	39.174	16.287	6-7	6-7
Bisignano	CS	39.513	16.285	6-7	6-7
Bocchigliero	CS	39.418	16.751	6-7	6-7
Carpanzano	CS	39.147	16.303	6-7	6-7
Castrolibero	CS	39.307	16.194	6-7	6-7
Fiumefreddo Bruzio	CS	39.235	16.066	6-7	6-7
Flavetto	CS	39.311	16.319	6-7	6-7
Gizzeria	CZ	38.981	16.206	6-7	6-7
Ioggi	CS	39.576	16.08	6-7	6-7
Pedace	CS	39.274	16.34	6-7	6-7
Rogliano	CS	39.178	16.323	6-7	6-7
Rovella	CS	39.303	16.288	6-7	6-7
Savuto	CS	39.071	16.164	6-7	6-7
Fondaco Vecchio	CZ	38.813	16.234	D	D
Altilia	KR	39.182	16.882	6	6
Sartano	CS	39.51	16.178	6	6
Diamante	CS	39.678	15.82	SD	SD
Laghitello	CS	39.167	16.153	SD	SD
Lago	CS	39.169	16.147	SD	SD
Falconara Albanese	CS	39.275	16.091	SD	SD
Scalea	CS	39.814	15.792	5	5
Scandale	KR	39.121	16.96	5	5
Africo [vecchio]	RC	38.065	15.98	5*	5*
Amendolea [vecchia]	RC	37.988	15.892	5*	5*

Bagaladi	RC	38.026	15.821	5*	5*
Bova	RC	37.994	15.932	5*	5*
Condofuri	RC	38.005	15.858	5*	5*
Gallicianò	RC	38.016	15.886	5*	5*
Motta San Giovanni	RC	38.002	15.694	5*	5*
Pellaro	RC	38.025	15.656	5*	5*
Pentedattilo	RC	37.953	15.762	5*	5*
Roccaforte del Greco	RC	38.045	15.9	5*	5*
Roghudi Vecchio	RC	38.049	15.916	5*	5*
San Lorenzo	RC	38.01	15.834	5*	5*
Montebello Ionico	RC	37.982	15.758	5*	5*
Pentimele	RC	38.139	15.659	5*	5*
Melito di Porto Salvo	RC	37.92	15.784	5*	5*
Cotronei	KR	39.159	16.778	4	4
Isola di Capo Rizzuto	KR	38.959	17.096	4	4
Rossano	CS	39.574	16.635	F	F
Santa Sofia d'Epiro	CS	39.546	16.329	F	F
Napoli	NA	40.849	14.25	F	F
Bari	BA	41.129	16.869	SF	SF
Otranto	LE	40.144	18.491	SF	SF
Salerno	SA	40.68	14.76	SF	SF
Cetraro	CS	39.516	15.941	NC	NC
Marzi	CS	39.171	16.306	NC	NC

Table 6. MACROSEISMIC FIELD – Uncertain date

MDPs 8

Locality	Province	Lat.	Long.	Intensity [EMS-98]	Intensity [MCS]
Porto Salvo	VV	38.706	16.08	9-10*	9-10*
Rocca Angitola	VV	38.748	16.223	8-9*	8-9*
Vatoni	RC	38.378	16.014	8-9*	8-9*
Campoli Vipere	RC	38.449	16.393	6-7*	6-7*
Palinudo	CS	39.114	16.422	6-7*	6-7*
Conflenti (Conflenti Inferiore)	CZ	39.071	16.286	NC	NC
Conflenti Superiore	CZ	39.067	16.293	NC	NC
Morano Calabro	CS	39.844	16.136	NC	NC

Table 7. New localities

Locality	Municipality	Province	Lat.	Long.	Other toponyms
Bari	Bari	BA	41.129	16.869	
Porto Salvo	Vibo Valentia	VV	38.706	16.08	P. Salvo
Rocca Angitola	Maierato	VV	38.748	16.223	Rocca
Vatoni	Taurianova	RC	38.378	16.014	Vatome
Campoli Vipere	Caulonia	RC	38.449	16.393	Campoli
Palinudo	Bianchi	CS	39.114	16.422	Paliduro
Sant'Elia	Palmi	RC	38.339	15.846	
San Giorgio	Palmi	RC	38.356	15.853	
Monsoreto	Dinami	VV	38.515	16.164	
Vietri di Potenza	Vietri di Potenza	PZ	40.599	15.509	
Agrigento	Agrigento	AG	37.312	13.578	Girgenti
Sciacca	Sciacca	AG	37.508	13.083	
Cristò	Taurianova	RC	38.389	16.008	

Appendix C

The macroseismic observation relating to the localities are reported in an external supplementary file.